AFCRL-68-0133
MARCH 1968
ENVIRONMENTAL RESEARCH PAPERS, NO. 283

AIR FORCE CAMBRIDGE RESEARCH LABORATORIES
L. G. HANSCOM FIELD, BEDFORD, MASSACHUSETTS

Playa Surface Morphology: Miscellaneous Investigations

Editor
JAMES T. NEAL, CAPT, USAF

Contributors
D. CARPENTER
R.Z. GORE
D.B. KRINSLEY
W.S. MOTTS
J.T. NEAL
G.E. STOERTZ
C.C. WOO

OFFICE OF AEROSPACE RESEARCH
United States Air Force

AFCRL-68-0133
MARCH 1968
ENVIRONMENTAL RESEARCH PAPERS, NO. 283

TERRESTRIAL SCIENCES LABORATORY PROJECT 8623

AIR FORCE CAMBRIDGE RESEARCH LABORATORIES
L. G. HANSCOM FIELD, BEDFORD, MASSACHUSETTS

Playa Surface Morphology: Miscellaneous Investigations

Editor
JAMES T. NEAL, CAPT, USAF

Contributors
D. CARPENTER
R.Z. GORE
D.B. KRINSLEY
W.S. MOTTS
J.T. NEAL
G.E. STOERTZ
C.C. WOO

This research has been sponsored in part by Air Force Weapons Laboratory Kirtland AFB, New Mexico, and Air Force Flight Test Center, Edwards AFB, California.

OFFICE OF AEROSPACE RESEARCH
United States Air Force

Abstract

Numerous environmental processes affect the development and stability of playa (lakebed) surfaces. Of special significance are hydrologic processes that control the amount and flow of both surface and ground water, and climatic variations which in turn influence the hydrology. This report, in six parts, examines some aspects of the playa surface environment. Chapter 1 is an introduction. Chapter 2 describes microrelief changes that developed at Harper Playa, California, following flooding of the playa in 1965-66. Chapter 3 documents a subsurface hydrologic investigation at Rogers Playa, California. The investigation revealed that the piezometric surface has lowered into sand layers beneath the surface, and it may explain why giant desiccation fissures have formed in the surface clays. Chapter 4 describes an investigation of seven Australian playas and suggests that Australia did not undergo a pluvial period like that of the western United States. Chapter 5 describes three kavirs (playas) in northern Iran and indicates that former lakes did exist there, but not to the same extent as in the western United States. Chapter 6 examines the possibilities of observing playa surface changes from satellites, using the present remote sensor technology. It also states that Gemini color photography and high resolution vidicon (TV) imagery are currently useful.

Contents

PLAYA SURFACE MORPHOLOGY: MISCELLANEOUS INVESTIGATIONS

I. Introduction

James T. Neal, Capt, USAF
Air Force Cambridge Research Laboratories
Bedford, Massachusetts

Playas (dry or intermittent lakes) have been used for a variety of military and civil purposes for many years. These large and extremely flat expanses of barren desert are unique landforms that have desirable military attributes, especially for the testing of vehicles and aircraft, and for emergency landing grounds. Civil exploitation, such as the extraction of mineral products, has in general been concerned more with economic than geomorphologic considerations. In recent years the significance of playas in hydrologic studies has become apparent because they frequently indicate the amount of ground-water discharge. In spite of their wide usage, playas have been one of the least understood of terrestrial landforms.

In 1962 the Air Force Cambridge Research Laboratories initiated a research program aimed at explaining the geology of playas. At that time, a general study of playas in the western United States was undertaken to gain an improved understanding of the geologic, mineralogic, and hydrologic environment of playas. See Neal (1965). In 1965 the study was expanded by United States Geological Survey geologists to include other desert regions including Mexico, Iran, Chile,

---

(Received for publication 1 February 1968)

and Australia, so that geologic correlations could be drawn and comparisons made with playas in the United States.

During the course of the investigations numerous research problem areas have become significant and have provided the motivation for additional study. Giant desiccation fissures as much as 1 meter wide, 5 meters deep, and 100 meters and more in length that opened on Rogers Playa (at Edwards Air Force Base, California) over the past fifteen years, now occupy nearly 20 percent of the lakebed area. They create a traffic hazard and have caused considerable concern at the base. Pronounced surface microrelief changes over relatively short intervals of time have been noted on other playas and demonstrate the fact that playas cannot be regarded as stable features of the earth's landscape; that is, they are "dynamic" landforms which change character with time. The changes noted are caused in part by variations in the amount and flow of both surface and ground water. In many cases the effects are cumulative and may represent long-term changes caused by climatic variation.

In order to exploit fully the unique natural advantages that playas provide, it is necessary to develop basic geologic information, so that both short- and long-term predictions can be made regarding their future stability. The studies documented in this report attempt to fill some current voids in such knowledge. Special emphasis is placed on those aspects dealing with the development of geomorphic features, and with changes in surface properties with time.

Chapter 2 describes an essentially complete change in surface microrelief conditions in the sediments of Harper Playa, California, that markedly changed the strength of the crust. The changes took place following flooding of the playa during the winter of 1965-66.

Chapter 3 examines the subsurface geology and hydrology at Rogers Playa, California, in an attempt to explain the extensive large-scale fissuring of the lakebed that has occurred over the past several years. A drilling and sediment analysis program is described.

Chapter 4 describes the environment and developmental history of Australian playas. It demonstrates the influence of past climates on surface characteristics that exist at present.

Chapter 5 considers the past climatic influence on several playas in Iran and demonstrates that although their surface features are in many respects similar to those of playas in the United States, their geologic history is not.

Chapter 6 is concerned with man's ability to observe and record the geomorphologic changes that occur on playas, and specifically examines the possibilities for monitoring surface changes by using the new remote sensing techniques available on several satellite systems.

The research described in this report has been conducted under Office of Aerospace Research (OAR) Project 8623, Geologic Properties, and has received additional support from the Air Force Weapons Laboratory, Kirtland Air Force Base, New Mexico, and from the Air Force Flight Test Center, Edwards Air Force Base, California. The Air Force Weapons Laboratory, the lead laboratory for United States Air Force civil engineering research, has sponsored this research in order to gain further understanding of the problems presented by playas.

References

Neal, J. T. (Ed.) (1965) Geology, Mineralogy, and Hydrology of U. S. Playas, AFCRL Environmental Research Paper No. 96, 176 p.

Contents

II. Playa Surface Changes at Harper Lake, California: 1962-1967

James T. Neal, Capt, USAF
Air Force Cambridge Research Laboratories
Bedford, Massachusetts

Abstract

Pronounced surface changes occurred at Harper Lake (playa), California, following extensive flooding during the winter of 1965-66. The predominant surface prior to the flooding was soft, dry, and friable silty clay, but the reconstitution of this material, combined with the dissolution of salt, resulted in a hard, dry crust. The reconstituted surface shows a substantial increase in strength, although some areas that had changed were showing strength degradation in late 1967, concurrent with an increase in salt accumulation. The observations show that playa surfaces with relatively low salt contents are highly subject to change. The amount of capillary discharge taking place appears to influence the permanency of change that occurs. Variation in detrital mineral composition appears relatively less important in controlling the playa surface development than soluble salt content. However, a higher granular content of detrital components tends to favor salt accumulation.

1. INTRODUCTION

Harper Lake (the geographic name) is a playa located 56 km east-northeast of Edwards Air Force Base in the western Mojave Desert, California. Figure 1 is an aerial view of the playa, which has been marked on aviators' maps as an emergency landing ground for aircraft unable to land at Edwards, or elsewhere. Harper Playa was studied and mapped in 1962 as part of a general study of playas (Neal, 1963). When the playa was revisited in 1966, it was noted that marked changes had occurred in the nature of the surface soils and associated microrelief. The principal change was the conversion of extensive areas of soft, dry, friable playa surface to a hard, dry crust. In 1967 part of the newly-formed hard crust had reverted to the soft condition that existed in 1962. Similar changes have been observed elsewhere (Neal and Motts, 1967), but those at Harper Playa are most distinctive and widespread.

Harper Playa has complex geologic characteristics, an important one being that the playa surface is composed of several contrasting soil and microrelief forms. Additionally, the hydrologic regime has been altered by intensive pumping for agriculture south of the playa, which has caused water-table drawdown that in turn ultimately affects capillary discharge through the playa surface. For these reaons it is desirable to learn more about the geologic environment and the factors responsible for geomorphic change.

This report summarizes information gained during the 1962 and 1966 mapping of the playa, and from subsequent field and laboratory tests that examined the properties of the sediments. The surface mapping was conducted by automobile traversing, generally at 500-m intervals, across the playa. Locations of all data points are shown on Figure 6.

2. PHYSICAL SETTING

2.1 Physical Geography

Harper Playa, 21 km northeast of Kramer Junction, California, is situated in the western portion of the Mojave block, a regional geologic structural unit bounded by the San Andreas and Garlock faults as shown by the map in Figure 2. The valley is located in a subtle structural trough created by secondary faulting related to the San Andreas movement. The valley and the region west and south for 15 to 25 km are of generally low relief in which a few ridges and hills rise gently, but without definite pattern, 150 to 450 m above a broad alluvial plain.

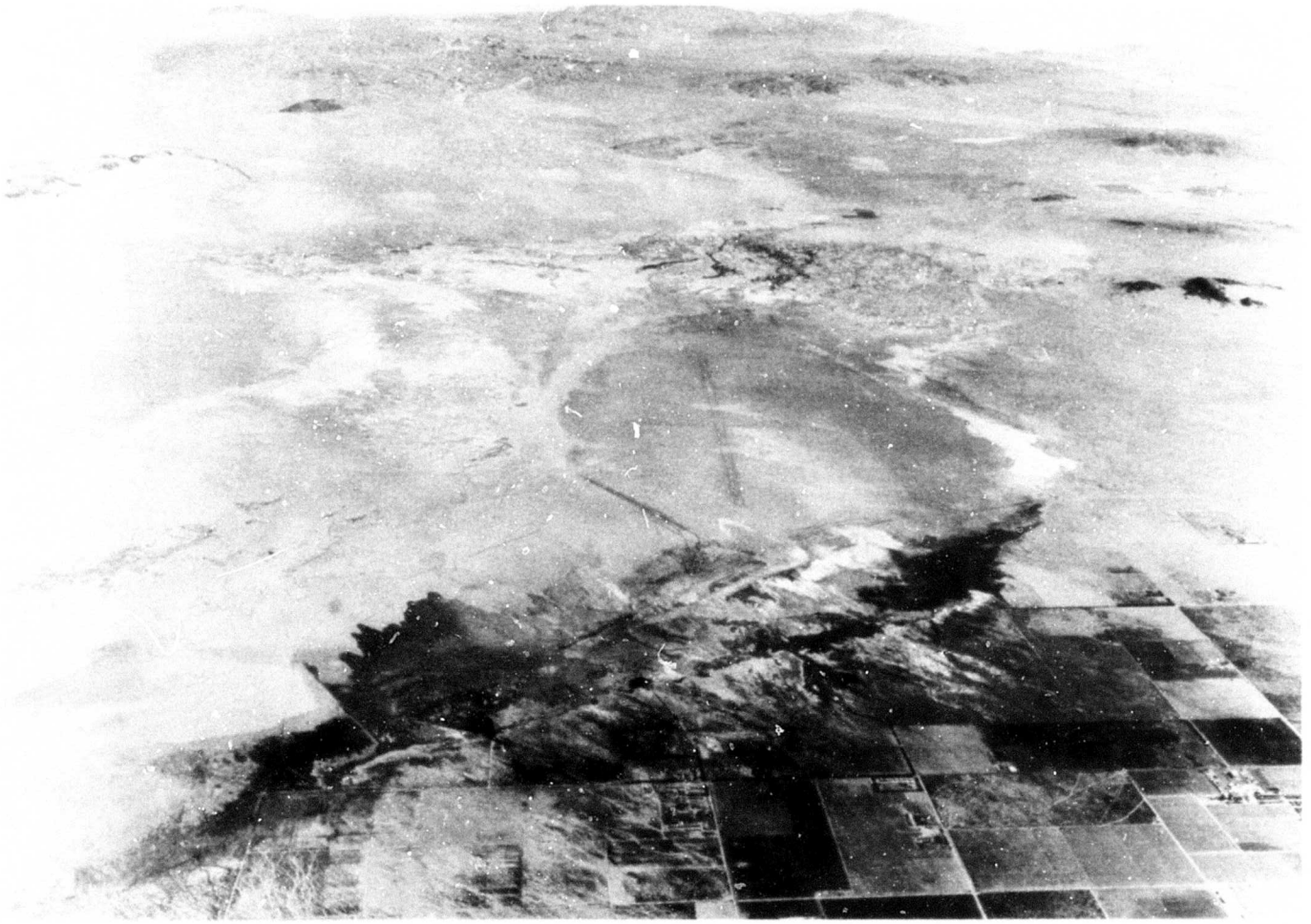

Figure 1. Aerial View, Looking East, of the Playa in Harper Valley, California. Dark areas in center foreground are moist zones that resulted from irrigation runoff. The northern vegetated dune area (left) has similar reflectance to the barren playa, but hard clay zones appear lighter. The hard clay area on the southern edge (right center) also appears lighter than the adjacent soft, dry, friable surfaces that were predominant. November 1962, USAF.

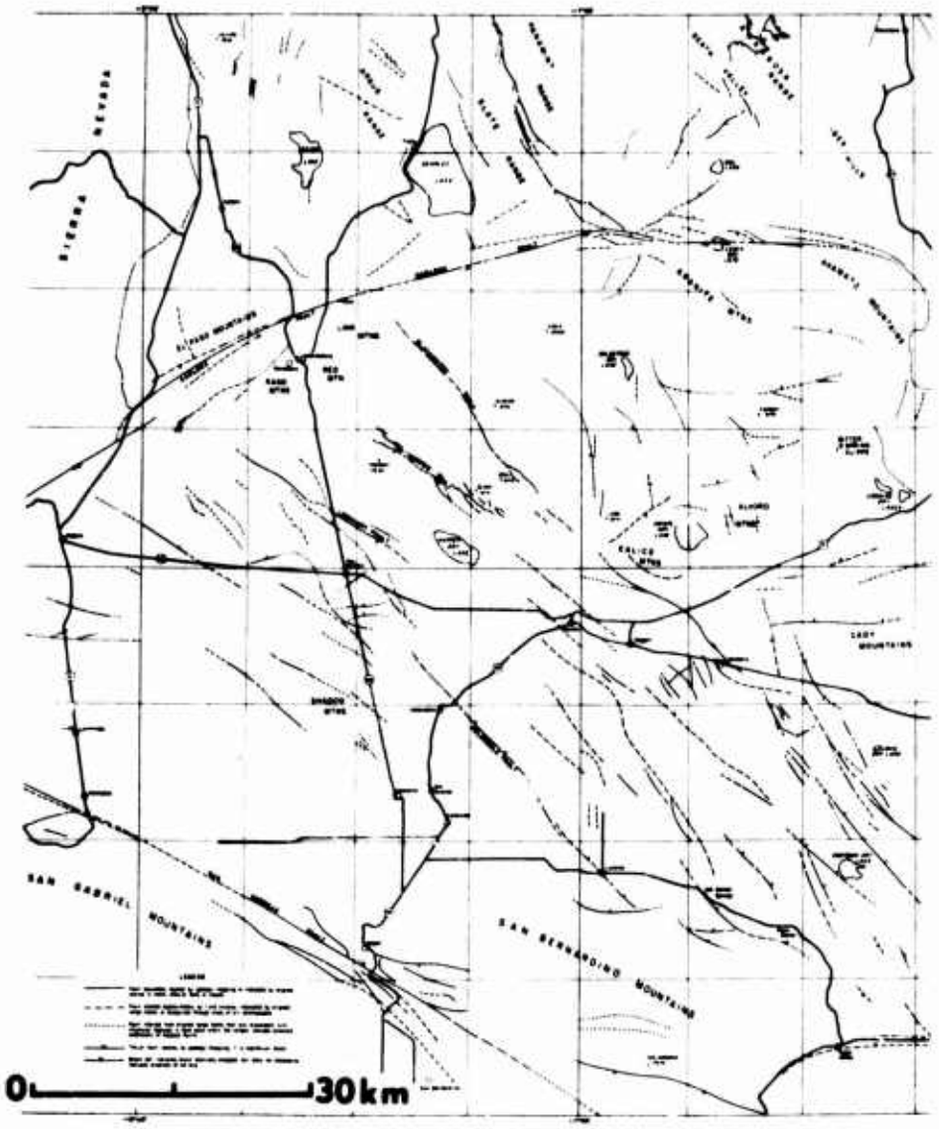

Figure 2. Location Map of Harper Playa (Center) Showing Known and Inferred Faults (Solid and Dashed Lines Respectively); from Hewett (1955).

Alluvial slopes rise gradually in all directions from the playa as shown in Figure 1. The north and east slopes are slightly steeper, reaching 400-m-high basalt-capped mountains within a few kilometers, as shown in Figure 3. Lower slopes are pediments with an alluvial cover. The alluvium increases in thickness approaching the playa; in the trough the sediments are as much as 370 m thick.

Figure 3. Northern Limit of the Barren Portion of the Playa. Vehicle rests on hard, dry clay; beyond lie soft, dry, friable surfaces with saline encrustations and sporadic small dune areas, interrupted by small barren patches of dry clay. Black Mountain rises in the background following the gradual ascent up the alluvial slopes.

Creosote bush is the characteristic plant found on the alluvial slopes; around the north side of the playa salt grass extends over a considerable area. At the southeast end of the valley, rabbit brush grows abundantly beyond the salt grass area and extends half a mile beyond the barren playa. Mesquite trees line many stream channels entering the playa from the east.

The north side of the playa is covered with sand dunes stabilized with vegetation, locally reaching heights of 5 m, although most are 2 m or less. The barren playa exhibits zones of both hard, dry clay crusts and soft, dry, friable surfaces.

The barren playa surface occupies about 30 sq km and is 617 m in elevation. Annual precipitation is 125 mm or less. August temperatures frequently reach 45°C, and January temperatures may fall to -10°C.

2.2 General Geology

During the Paleozoic thick geosynclinal sediments were deposited in the Cordilleran Geosyncline, extending as far as the western Mojave Desert. Few exposures are present because subsequent Tertiary erosion removed much of the material. Major pre-Tertiary structure trends generally north; Hewett (1955) suggests that 25,000 to 30,000 ft of sediments were laid down in the Paleozoic.

Palezoic and Mesozoic sediments of this region are greatly deformed and where they are in contact with igneous intrusives, the intrusion and deformation appear to be contemporaneous. Quartz monzonites have been mapped several miles west of the playa, along with other undivided pre-Cretaceous metamorphic rocks. While ages of the intrusives are not available, the deformation and intrusion are probably related to the Laramide orogeny.

Faulting delineated the Mojave block during Tertiary times. Eocene and Oligocene sediments are absent in the block but are present to the north, so it is concluded that the Mojave block started to rise in early Eocene, or possibly late Cretaceous, and continued to rise until middle Miocene. The pre-Tertiary rocks

within the block were continuously eroded; 10,000 to 15,000 ft of rock were removed. The basins were then formed in the block between middle Miocene and middle Pliocene (Hewett, 1955).

Hewett (1955) aptly summarizes the following period from middle Pliocene to middle Pleistocene: "(it) was characterized by erosion during which large areas of soft rocks were reduced to low relief, and the hard rocks were sustained in hills and a few mountain ridges; during this period, the products of erosion seem largely to have been removed from the block."

"About middle Pleistocene time, renewed movement on old faults interrupted the existing streams, accentuated the relief of many mountains, especially in the eastern part, and produced many of the existing depressions with their dry and saline playas. Probably middle Pleistocene time marks the beginning of subsidence of the western part of the block, accompanied or followed by the nearly horizontal movement along both the Garlock and San Andreas faults, which are indicated by the offset stream courses."

Although there is no direct evidence of a former Pleistocene lake in the valley, a number of features suggest its existence. The divide east of Hinkley separating Harper Valley from the Mojave River is low enough so that discharge from the river into the valley was likely. Existence of the playa itself suggests a former lake; shells have been reported from depths of several hundred feet in blue clay sediments. Great sediment thicknesses and elevated strand lines are suggestive of older Pleistocene lakes in the Mojave Desert. Harper Lake is presumably the present remnant of larger Pleistocene Lake Harper. Hubbs and Miller (1948) report that Lake Thompson overflowed into Lake Kane, but not into Harper Valley.

During the Pleistocene, basalt flows covered much of the landscape. Black Mountain north of the playa consists of horizontal flows resting on the partly eroded Miocene sediments. The basalts dip steeply southward where they are broken by the Harper Valley Fault.

Harper Valley is bordered by faults on the north and south as can be seen in Figure 1, and may be considered a down-faulted structural basin. There is a general parallelism of the faults with the San Andreas fault; these faults were probably formed during periods of great horizontal pressure accompanying vertical movement when the Mojave block was rising, that is, during Eocene, Oligocene, and lower Miocene. The faults show evidence of movement in late Quaternary time as well (Hewett, 1955). There may also be some faulting more recent than the lava flows. Gravity data south of the playa have shown anomalous gravity lows with steep gradients (Mabey, 1960). This anomaly has been interpreted as indicating a fault that is probably continuous with the Lockhart fault,

and which also may be related to the Helendale fault. See Figure 1. These data along with indirect surface evidence of Dibblee (in Mabey, 1960) suggest an essentially continuous fault zone south and west of the playa.

Gravity data by Mabey also show a "low" at the northwest end of Harper Lake, indicating that the playa is somewhat offset from the thickest section of Cenozoic sediments in the valley fill. Drilling has shown that the upper surface of the basement complex is generally within 370 m of the surface.

Recent activity is negligible: wind-blown sand covers the southeast end of Black Mountain in the form of "climbing" dunes; the northeast portion of the playa itself is also covered with small dunes. Small dune areas are also present south of the playa. Gradual erosion and sedimentation are occurring in the alluvial slopes and on the playa.

2.3 Hydrology and Drainage

The drainage basin of Harper Playa is not large when compared with many other playas, and the surrounding mountains are neither high nor widespread. Therefore, the quantity of water entering the basin cannot be great unless ground water is contributed from an adjoining basin. There is some likelihood that ground water may enter the basin from the Mojave River Basin, and possibly from other adjoining basins (Thompson, 1929).

Most of the rain that infrequently falls on the alluvial slopes adjacent to the playa is usually absorbed quickly and enters the basin as ground water. Water which does reach the playa enters through several small channels along the northern border, the eastern and south-eastern end, and from springs and irrigation runoff along the southern border. See Figure 1. Drainage then moves toward the lowest portions of the playa. Figure 1 shows water stains which reflect the drainage movement on the playa. Because of the extreme flatness and lack of relief on the playa water 10 cm deep can spread over distances of several kilometers. The annual evaporation rate of 200 cm is extremely high, and surface water does not persist for long, especially during summer months. The winter rains that flooded the playa in 1965-66 fell during the minimum annual evaporation period; consequently the effect on resedimenting the surficial materials was considerable and long-lasting.

Ground water beneath the playa is generally shallow (2 to 6 m), which permits capillary discharge through the surface. Evaporation of this capillary water causes evaporite minerals to form on the surface. Because of the low permeability of the lacustrine sediments, the ground water immediately beneath the playa is termed "perched" and is not to be confused with ground water that is pumped in the agricultural areas near the playa. Depth to water levels increases away

from the playa; within 3 to 5 km the depth to water is nearly always less than 30 meters. Thompson (1929) reported that water was frequently under artesian pressure and mentioned the occurrence of flowing wells. It is not certain whether artesian conditions are present today. Kunkel (1962) suggests that there is movement of ground water from Cuddeback Lake southward into Harper Valley. Extensive irrigation south and west of the playa has created a large pumping depression (Stone, 1957; Kunkel, 1962).

3. SURFICIAL SEDIMENTS AND MICRORELIEF

3.1 General Properties

The soils of Harper Playa are former lake sediments of Pleistocene Lake Harper, and material which has subsequently been deposited from alluvium in the valley. Additionally, capillary discharge of ground water has deposited varying amounts of evaporite minerals at the surface. Although there is not a well developed soil profile as such, a marked zonation exists where saline ground water deposits the evaporites.

The predominant color of Harper Lake soils is characteristically light tan on the dry surface; below the surface the soils become darker brown with increasing moisture and plasticity. Where salt encrustations occur the color is white to brownish gray, depending on the amount of salt. Below about 4 m is blue-gray clay, which is probably undisturbed and unoxidized Pleistocene lake sediments.

Surface soils on the barren part of the playa are diverse in character. They may be grouped into two major textural categories, and into those transitional between the two. The two major types are hard, dry crusts and soft, dry, friable surfaces ("self-rising ground" of previous authors). The latter surface discharges greater amounts of ground water through capillarity and evaporation. Both surfaces are predominantly silty clay, although higher silt contents seem to effect increased ground water discharge. Comparative photographs of the two contrasting surfaces are shown in Figures 4 and 5 and representative strength values are given in Table 1. Physical and mineralogic properties of these two contrasting types of playa surfaces are discussed by Langer and Kerr (1966).

Transitional phases occur in several locations where relatively hard crusts appear similar in microrelief to the soft, dry, friable surfaces. These places seem to reflect flooding and subsequent drying of the soft, friable surfaces. The northern part of the barren playa is characteristically sandy, as is much of the southern part. The sand is frequently encountered beneath silty clay surface

Figure 4. Soft, Dry, Friable Surface in October 1962 at Location of Sample S-5 and S-8. Compare with Figure 5. This was the predominant surface condition on the playa from 1962 to 1965.

Figure 5. Hard, Dry Crust in November 1966 at the Same Location as Figure 4. Note increase in strength. This was the predominant surface condition on the playa in November 1966.

Table 1. Comparative Penetrometer and Surface Hardness Observations*

STATION LOCATION (see Fig. 6)	DATE OF MEASUREMENT OR OBSERVATION				REMARKS
	28 October 1962	8 November 1966	2 March 1967	14 September 1967	
P-1	NMp surface soft and friable (see Fig. 13)	0" - 35 psi 3 - 170 6 - 90 (see Fig. 14) 12 - 80	NM; surface hard; see data for P-2	0" - 0 psi 3 - 15 6 - 50 (see Fig. 15) 12 - 85	Data demonstrate change from soft (1962-63) to hard (1966) surface, and return to soft condition (Sept. 67) (sample S-1)
P-2	NM; condition comparable to P-1	NM; condition comparable to P-1	0" - 20 psi 3 - 60 6 - 65 12 - 100	0 - 0 3 - 50 6 - 60 12 - 80	Decreased strength shown in Sept. 67 measurement - consistent with observation at P-1
P-3	NM	NM	NM	0 - 0 3 - 5 6 - 20 12 - 50 18 - 75	Sticky - wet surface; compare with P-4 (see Fig. 10)
P-4	NM	NM	NM	0 - 10 3 - 35 6 - 55 12 - 80 18 - 85	Soft, dry, friable surface, compare with P-3 (see Fig. 10) Note strength increase in upper six inches
P-5	NM; soft, dry, friable surface	0 - 45 3 - 175 6 - 300	0 - 35 3 - 140 6 - 270	0 - 85 3 - 240 6 - 300	March 1967 data shows decreased strength followed by increase in Sept. 1967
P-6	0 - 0 3 - 0 6 - 125 9 - 300 (see Fig. 4)	0 - 95 3 - 150 (see Fig. 5) 6 - 300	0 - 65 3 - 120 6 - 300	0 - 135 3 - 255 6 - 300	Pronounced change from 1962-66: conversion of soft surface to hard crust (sample S-4)
P-7	0 - 15 3 - 90 (meas. 15Jan63) 6 - 225 9 - 300	NM; hard, dry crust	0 - 95 3 - 125 6 - 250 9 - 300	0 - 155 3 - 245 6 - 250+	Substantial strength increase in 1966 and 1967 over 1962 - conversion of soft surface to hard crust
P-8	NM; soft, dry, friable surface	NM; hard, dry crust	0 - 105 3 - 150 6 - 250+	0 - 195 3 - 245 6 - 275	" " "
P-9	0 - 0 3 - 0 6 - 100 9 - 210	NM, soft, dry friable surface	0 - 30 3 - 30 6 - 35 12 - 240	0 - 40 3 - 55 6 - 55 12 - 260	Overall strength relatively unchanged from 1962; compare with P-8 - this station not flooded during 1965-66 winter
P-10	" " (see Fig. 12)	0 - 20 3 - 65 (soft, dry, 6 - 65 friable) 12 - 250	0 - 10 3 - 10 6 - 20 12 - 250	0 - 15 3 - 15 6 - 25 12 - 225	Strength relatively unchanged from 1962 (Fig. 12) but slight decrease in 1967 over 1966 (sample S-7)

*Numerical values given are average of 3 measurements and express relative differences in pounds/sq. in. Depth of measurement given in inches (left side of columns); NM = not measured with penetrometer

layers. Central areas of the playa are predominantly silty clays. The material is usually uniform in appearance at depth, but grain size analyses show considerable variation.

The northern one-third of the playa is a complex association of sand dunes, vegetation mounds, and alluvium in which hard, dry clay areas occur, along with soft, dry, friable surfaces. See Figure 3. Salt grass growths in soft, salt-stained soil may be seen in juxtaposition with zones of dry clay. The vegetation may be partly responsible for the salt efflorescence by permitting increased capillary discharge and transpiration of ground water. This vegetated segment of Harper Lake showed little apparent change from 1962 to 1967.

3.2 October 1962 Surface Condition

Hard, dry clay was present on the southern periphery and on the area adjacent to the northern dune area. See Figure 7. In these areas mudcrack polygons were typically well defined, flat, and of small to medium size. The polygons were raised in places and they also appeared as transitional phases with soft, friable surfaces. Portions of the southern dry clay area were noted to be moist at the surface. Such moisture is usually derived from irrigation runoff and should not be confused with capillary water. See Figures 10 and 11.

Soft, dry, friable surfaces were generally present in central portions of the playa (Figures 4 and 7) and displayed a diversity of forms. Salt stains and thin salt crusts were common in the eastern half of the playa. This surface was "lumpy" in places and had an irregular appearance, but elsewhere it was relatively smooth and even. The variations appeared to be caused in part by standing water following rainfall, which caused the surface to be levelled. This dry, puffy clay-silt has low bulk density, and exhibited little strength to depths of 10 to 20 centimeters. Below this depth the soil was moist and highly plastic and had even less strength.

3.3 November 1966 Surface Condition

During the 1965-66 winter extensive flooding covered much of Harper Lake with standing water. Upon drying in the spring of 1966 the surface of the barren playa was principally a hard, dry crust, with only a few isolated "islands" of the soft, dry, friable surface which had been predominant in 1962-1965. Compare Figures 7 and 8. The "islands" had apparently not been flooded, as tire tracks made in 1962 were still plainly visible in 1966 (Figure 12). A comparison of strength values (Table 1) reveals significant changes. Comparative photographs taken in 1962 (Figures 4 and 13) and 1966 (Figures 5 and 14) at identical locations show dramatically the increase in strength where soft surfaces were flooded and then dried to form hard crusts.

Shallow pits were observed in 1962 near the center of the playa as shown by Figure 16. They were generally about 10 cm deep, 30 cm in diameter, and occupied an area of about 1 sq km. Re-examination of this area in 1966 revealed that the pits were completely filled as shown in Figure 17. The pits may have formed initially from slumping due to escaping gas during a time when the playa was under water (Neal, 1966). The complete obliteration of these pits that occurred between 1962 and 1966 shows that they are highly ephemeral.

3.4 March 1967 Surface Condition

Although the playa was not remapped in March 1967, penetrometer measurements and strength observations were recorded. The surface condition was in general similar to the surface condition in November 1966, but subtle variations were recorded on the cone penetrometer. See Table 1. Several stations (P-5-9) show an apparent decrease from the November 1966 and September 1967 measurements. This difference was noticed mainly in the hard clay crusts and may be caused by increased moisture and humidity during the winter months.

3.5 September 1967 Surface Condition

In September 1967 the western part of the playa was again becoming soft, as it was during the initial 1962 surface mapping. See Figures 7 to 9. Comparative strength measurements (Table 1) of stations P-1 and 2 (Figure 6) and Figures 13 to 15 show the conversion of a soft surface (1962) to a hard crust (1966) and the reversion to a soft surface in September, 1967.

The eastern part of the playa had surface conditions essentially similar to those of 1966 and March, 1967. Compare Figure 9 with Figures 7 and 8. Increases in surface strength were noted and therefore do not suggest trends toward strength degradation. See Table 1.

4. MINERALOGY OF HARPER PLAYA SEDIMENTS *

The following data and summary are based on the analysis of eight surface samples collected around and along a traverse line which is approximately parallel with the major axis of Harper Lake. See Figure 6 and Table 2.

---

*Mineral analyses conducted by Richard Z. Gore, Department of Geology, Boston University, Boston, Massachusetts.

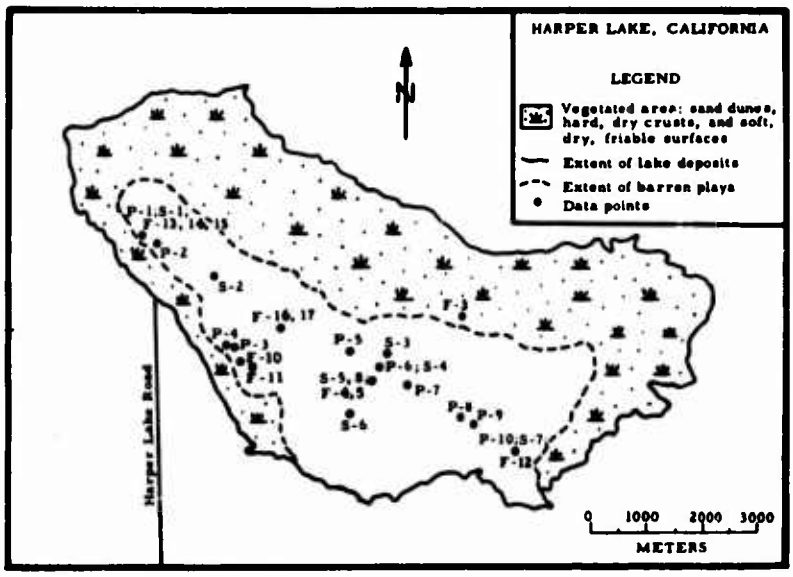

Figure 6. Location Map of Samples (S-1, etc.), Ground Photographs (F-2 = Figure 2, etc.) and Penetrometer Data (P-1 of Table 1, etc.)

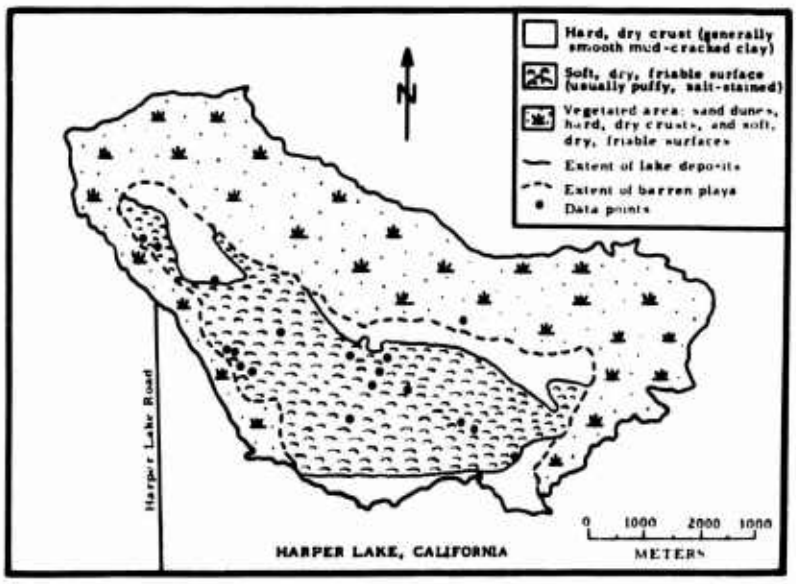

Figure 7. Map of Playa Surface Conditions, October 1962

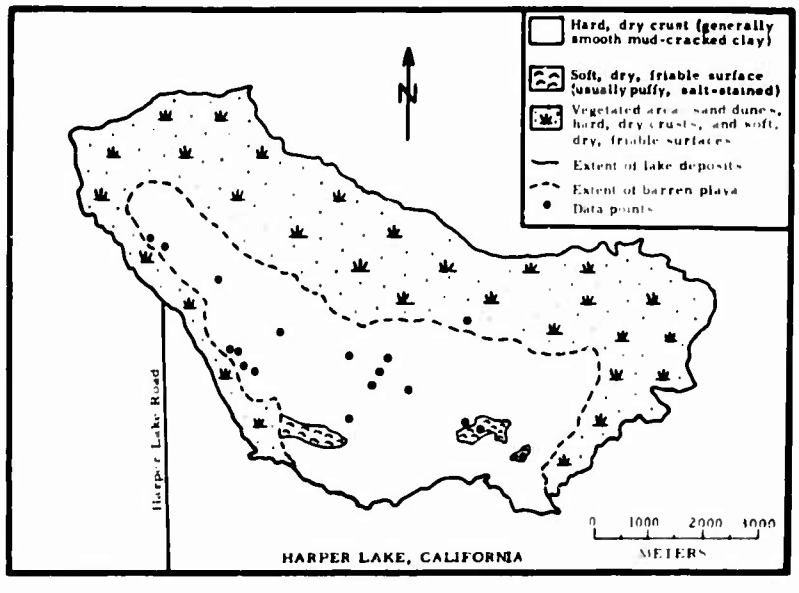

Figure 8. Map of Playa Surface Conditions, November 1966

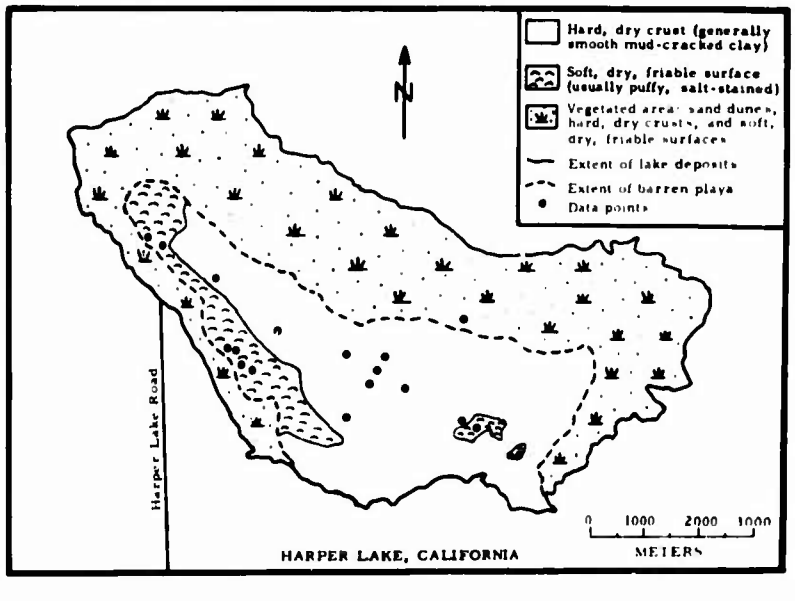

Figure 9. Map of Playa Surface Conditions, September 1967

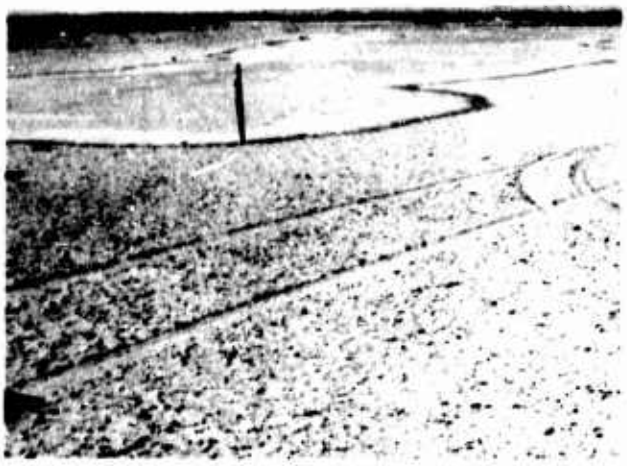

Figure 10. Moist Surface (at Stake) Resulting from Irrigation Runoff. Note wheel ruts in soft, dry, friable surface. Surface is smooth and mud-cracked and may represent strength degradation of a hard, dry crust.

Figure 11. Moist Surface (Dark Area) on Hard, Dry Crust. Vehicle leaves no wheel rut. (Compare with Figure 10.)

Figure 12. Comparison of Tire Ruts Made in November 1966 (Left) and October 1962 (Right) in a Soft, Dry Friable Surface. It appears that this area was not flooded in contrast to most of the barren playa, and consequently was virtually unchanged.

Figure 13. Soft, Dry, Friable Surface in October 1962 Near Western Edge of Playa. Salt stains were prevalent on the surface. Note wheel ruts.

Figure 14. Hard, Dry Crust in November 1966 at Same Location as Figure 13. Surface was flooded the previous winter. Note virtual absence of wheel ruts. Vestiges of tracks from previous rutting in 1962 are visible, however.

Figure 15. Soft, Dry, Friable Surface in September 1967, Identical Location as Figures 13 and 14. Reversion to 1962 strength is evident (See Table 1), but surface is not nearly as rough.

Figure 16. Shallow Depressions That Occupied a Relatively Large Portion of the Playa in October 1962

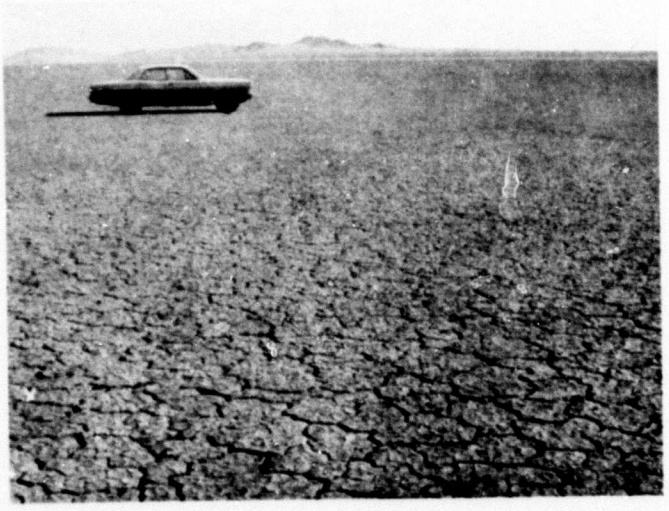

Figure 17. Identical Location as Figure 16, November 1966. Depressions had been completely filled following flooding of the playa during the 1965-66 winter.

Table 2. Mineralogic Samples

Sample No. (See Figure 6)	Date Collected	Surface Condition at Time of Collection	Remarks
S-1	Nov. 1966	Hard, dry crust (Figure 14)	Surface soft, dry, friable in 1962
S-2	Nov. 1966	Hard, dry crust	Surface soft, dry, friable in 1962
S-3	Nov. 1966	Hard, dry crust	Surface soft, dry, friable in 1962
S-4	Nov. 1966	Hard, dry crust	Surface soft, dry, friable in 1962
S-5*	Nov. 1966	Hard, dry crust (Figure 5)	Surface soft, dry, friable in 1962
S-6	Nov. 1966	Hard, dry crust	Surface soft, dry, friable in 1962
S-7	Nov. 1966	Soft, dry, friable surface (Figure 12)	Surface unchanged from 1962
S-8*	Oct. 1962	Soft, dry, friable surface (Figure 4)	Hard, dry crust in 1966-67

* Same location

4.1 Size Analysis

Results of pipette analyses are given in Figures 18 and 19, and in Table 3. There is a significantly smaller amount of $< 2\ \mu$ material in S-1 and S-2. Although both locations had a hard, dry crust at the time of sample collection, the S-1 location showed a reversion to puffy conditions in September 1967 (Figures 13 to 15), whereas S-2 did not. Because of the higher granular component, and because surface changes are taking place nearby (Figure 9), it is thought that the S-2 location is also susceptible to change. These observations are in keeping with the conclusion of Langer and Kerr (1966) that puffy surfaces have higher granular components.

4.2 Detrital Components

The coarser sand ($> 149\ \mu$) fraction of all the Harper Lake samples has a similar mineralogic composition. The major constituents are plagioclase (albite-oligoclase), quartz and microcline, with microcline less abundant. Other minerals always present, but generally in small amounts ($< 5\%$), are magnetite, hornblende, and muscovite. Minerals common in minor amounts but not always present are biotite, dolomite(?), olivine (?), and garnet (?).

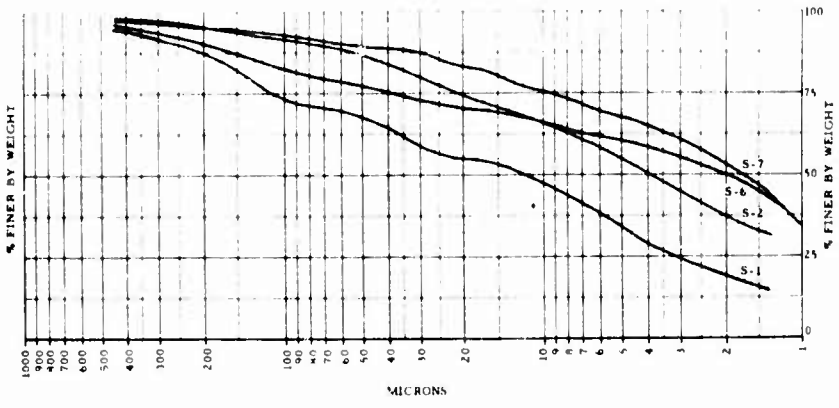

Figure 18. Graph of Size Analyses, Samples S-1, S-2, S-6 and S-7

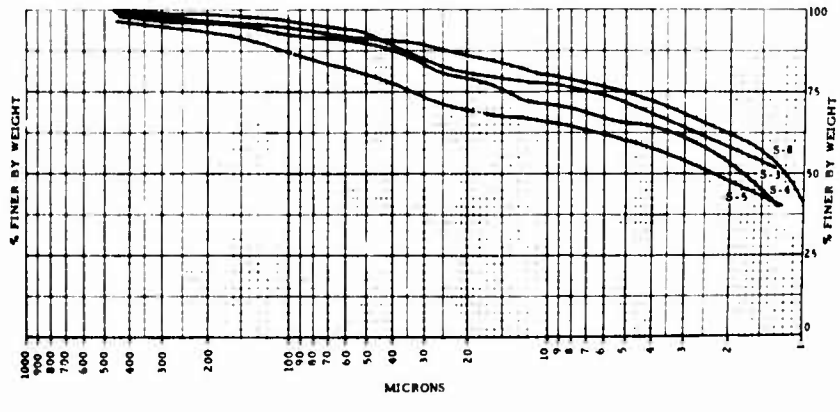

Figure 19. Graph of Size Analyses, Samples S-3, S-4, S-5 and S-8

The quartz occurs as subangular to subrounded grains with some of the larger grains containing euhedral crystals of magnetite. The plagioclase is fresh and shows no obvious alteration. Most of the grains appear to be cleavage fragments which have been abraded to subangular and subrounded shapes. The microcline grains generally show signs of alteration and are more rounded than the plagioclase. The biotite, magnetite and hornblende show minor aleration and are generally subangular in shape. The composition of the finer sand and coarse silt fraction is similar to the coarse sand fraction with one exception -- the micas (mainly muscovite) are much more abundant than they are in the coarser material. This concentration of the micas in the finer fractions is common because the perfect basal cleavage of these minerals allows them to be divided into very thin plates which are easily broken.

Table 3. Particle Size Distribution of Harper Lake Sediments**

Sample	< 1.5 μ	1.5-5 μ	5-10 μ	10-20 μ	20-40 μ	40-80 μ	> 80 μ	< 5 μ	> 5 μ	% Salt
S-1	15.5*	18.5	13.5	7.5	9	7.2	28.8	34 †	66 ‡	2.5
S-2	32.5	22.5	11	8	9.8	6.8	10	55	45	2.9
S-3	53.5	18.0	6	3.5	8	6.5	4.5	71.5	28.5	<2
S-4	45	19	7.2	7.8	9	4	8.5	64	36	<2
S-5	43	17	6	3	8.5	7	15.5	60	40	2.3
S-6	45	15.5	5.5	4.5	5	5.5	19	60.5	39.5	2.3
S-7	47	20.5	8.5	7.0	5.8	3.2	8	67.5	32.5	18.8
S-8	57	17.8	5.2	6	4.5	2.8	6.8	74.8	25.2	10.1

* % of total clastics

† < 5 μ represents total clay

‡ > 5 μ represents total "granular" components

** Particle size nomenclature:

Size, μ		
< 1	-	colloids, clay
1-5	-	coarse clay
5-10	-	fine silt
10-20	-	medium silt
20-40	-	coarse silt
40-80	-	fine sand
> 80	-	medium sand and coarser

X-ray patterns were not made on the 5 μ to 37 μ material but microscopic examination suggests it is similar in composition and distribution to the > 37 μ fraction.

4.3 Clay Components

The clay fraction (< 2 μ) of all samples was examined by X-ray diffraction. Three patterns were run for each sample: (1) water-sedimented, air dried; (2) treated with ethylene glycol; and (3) heated to 550°C. These tests revealed that illite and montmorillonite are the major components of the clay fraction in all samples. All samples indicate the presence of small amounts of mixed layer montmorillonite-illite. Other clay minerals are discussed in following paragraphs.

Illite is recognized by d-spacings of 10.0, 5.0 3.3, and 2.0Å. These spacings are not shifted by treatment with ethylene glycol, although the amplitude and shape of the 10Å peak does change. Güven (1965) states that the increase in symmetry and amplitude of this peak indicates that the illite layers are associated with expandable layers. This change is clearly seen in the patterns of samples S-3, S-4, S-5, S-6, and S-7. See Figures 20 and 21. Samples S-1 and S-2, taken near the western edge of the playa, show a smaller change upon treatment which may indicate a smaller amount of associated expandable layers. Upon heating to 550°C the 10Å peak of illite increases in amplitude and symmetry, because of the collapse of the expandable layer components to 10Å. See Figures 24 and 25.

In the air dried specimens montmorillonite shows a broad diffuse peak of 2 to 3Å width centered near 14Å. The degree of hydration and the nature of the exchangeable cation may shift this peak between 12.6 and 16.9Å. See Figure 20, S-4 and S-5, and Figure 21, S-1 and S-2. Treatment with ethylene glycol results in a pronounced increase in the 14Å spacing to between 17Å and 18Å. Compare Figures 20 and 21 with Figures 22 and 23. The 14Å peak collapses completely to 10Å on heating to 550°C. See Figures 24 and 25.

Chlorite has a 14Å peak which is not affected by ethylene glycol treatment and shifts only slightly when heated. The 14Å peak disappeared from all specimens after heating, indicating that chlorite is not present in detectable quantities.

Vermiculite is characterized by a peak at 14.2Å. Treatment with ethylene glycol does not produce any large change in the position of the 14.2Å peak. Güven (1965) pointed to small peaks in the 14Å area of ethylene glycol-treated specimens as being Mg vermiculite. Such peaks are clearly seen in some patterns. Vermiculite can be verified by studying samples saturated with Mg++. The broad peak centered between 14Å and 15Å, seen in air dried samples, gives rise after saturation with Mg++ and treatment with ethylene glycol to reflections at 18Å. This 18Å peak is indicative of montmorillonite. If vermiculite is present, a 14.2Å

peak should also be present and would generally be of greater intensity than any peak in a similar position on specimens that are treated with ethylene glycol alone.

In Figure 23, S-2, as in many of the samples treated with ethylene glycol, a 14.2Å peak may be present and is accompanied by a 7.1Å peak. This typical pattern could suggest the presence of montmorillonite, illite and vermiculite. However, if the 14Å peak is simply a weak reflection from a mixed layer clay, this pattern could indicate that montmorillonite, illite and kaolinite are the chief clay minerals. If vermiculite is present, saturation with Mg^{++} followed by treatment with ethylene glycol should isolate and intensify the 14Å peak. If vermiculite is absent the 14Å peak seen in Figure 23, S-2 and S-3 should shift or disappear.

The Mg^{++} saturated sample treated with ethylene glycol in Figure 26 does not show any definite peak at 14.2Å and the peak or plateau discussed above has shifted to 13.1Å, and the 7.1Å is not present in detectable quantities and the 7.1Å peak, which is normally very weak in vermiculite, is probably due to kaolinite.

The asymmetry of both the illite 10.15Å reflection on the low angle side and the montmorillonite on the high angle side accompanied by many weak reflections in the low angle range of the X-ray diffraction pattern suggest the presence of mixed layer illite- montmorillonite.

It is not possible to determine precisely the origin of the clay mineral suite seen in the Harper Lake samples but the general lack of alteration in the coarser clastics, especially mafics, suggests an allogenic rather than authigenic history for the principal clay minerals. All the X-ray patterns of samples (S-3, S-4, S-5, S-6, S-7, and S-8) showed a fairly strong reflection at 5.6Å. This spacing is common to some zeolite minerals, for example, analcite, and may indicate their presence. No obvious correlation of clay mineralogy with crustal types is evident.

4.4 Soluble Components

Halite is the only common soluble salt and ranges from less than 2% to 18.8% by weight in the samples tested. A small, questionable 3.15Å peak appeared in the X-ray pattern of salt extracted from S-7; this is the major sylvite peak. Calcite is present but it may all be detrital. It is present in all of the samples and produces strong X-ray reflections in both the unoriented whole sample and in the sedimented clay fraction.

Table 3 lists the total soluble salt content of the samples. All of the locations sampled in November 1966 had soft, puffy surfaces in 1962, but, except for S-7, had all converted to hard, dry crusts in November 1966 following the evaporation of rains that flooded the playa the previous winter. Salt contents are similar in samples S-1 to S-6; however, in S-7, which did not convert, a significantly higher

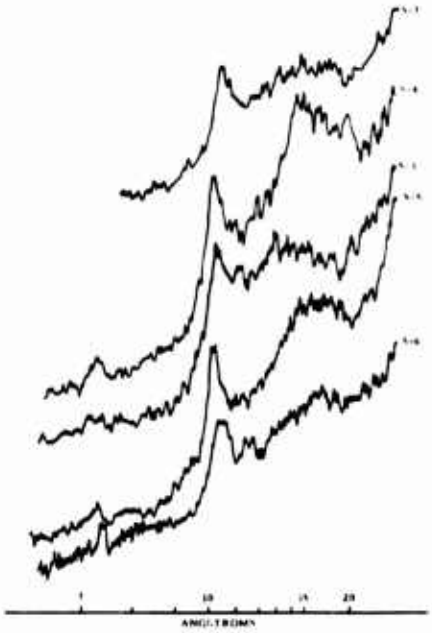

Figure 20. X-Ray Diffraction Patterns of Air-Dried Oriented Clays

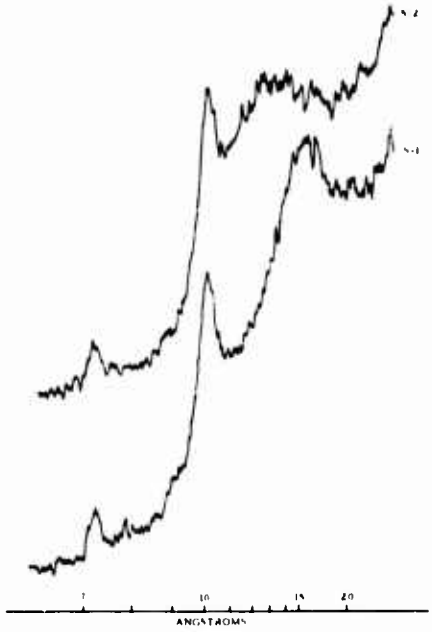

Figure 21. X-Ray Diffraction Patterns of Air-Dried Oriented Clays

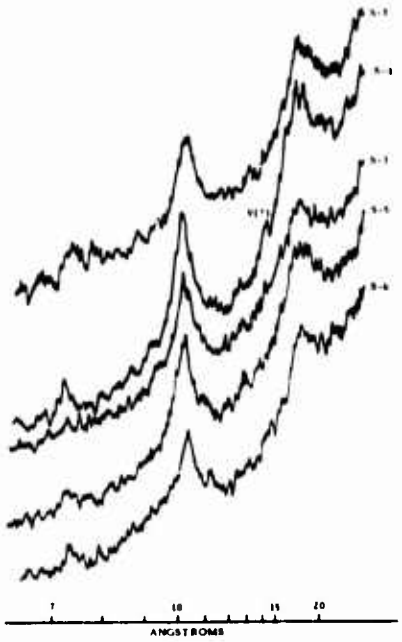

Figure 22. X-Ray Diffraction Patterns of Clays Treated with Ethylene Glycol

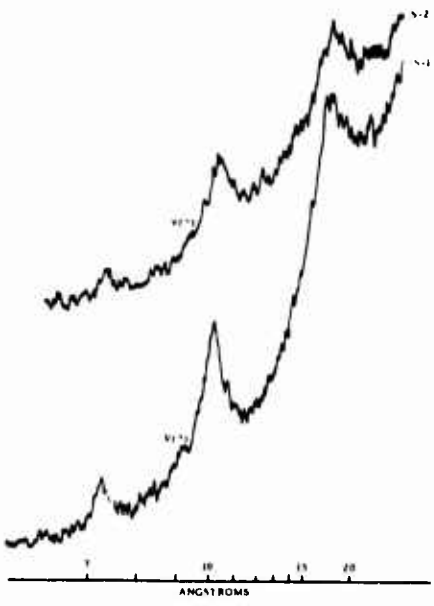

Figure 23. X-Ray Diffraction Patterns of Clays Treated with Ethylene Glycol

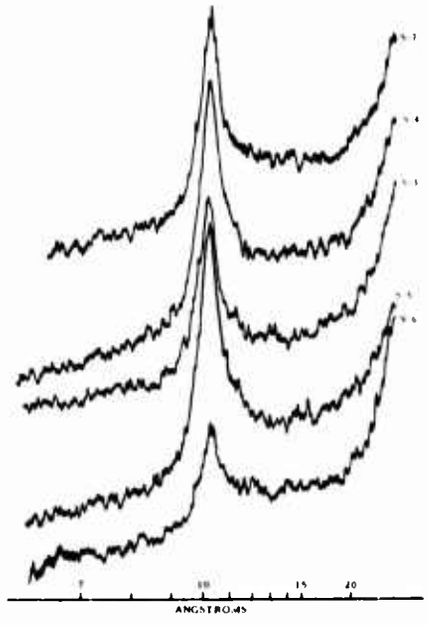

Figure 24. X-Ray Diffraction Patterns of Clays Heated to 550°C

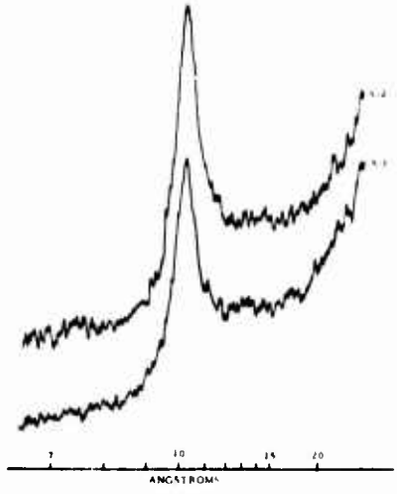

Figure 25. X-Ray Diffraction Patterns of Clays Heated to 550°C

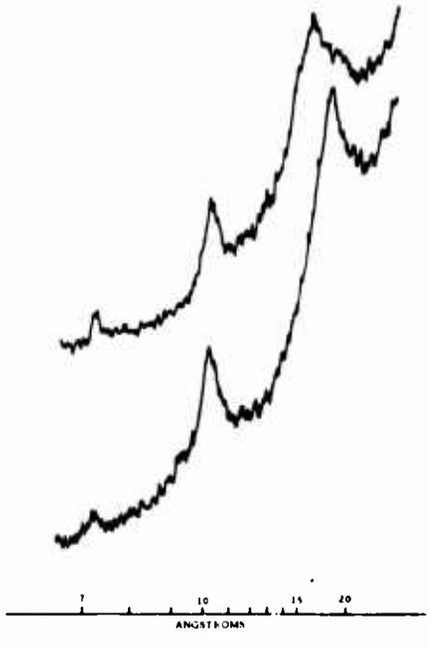

Figure 26. X-Ray Diffraction Patterns of Sample S-2, Upper Saturated with Mg++, Bottom Saturated with Mg++ and Then with Ethylene Glycol

amount of salt is shown. The S-8 sample taken in 1962 also shows a significantly higher salt content than the 1966 sample taken from the same location. It is noteworthy that in 1962 the surface was puffy as shown in Figure 4, but in 1966 it was hard as shown in Figure 5. The S-1 location showed a reversion to puffy conditions in September 1967, whereas the other locations with a similar salt content (S-2 through S-6) did not.

The salt content of S-1 had increased to 7.7% in September 1967, in comparison to 2.5% in the November 1966 sample. The salt content of S-4 in September 1967 showed no change from the $< 2\%$ amount of November 1966. These comparative measurements show the effect of salt content on strength degradation. They may also reveal relative differences in the amount of capillary discharge. The change noted at S-1 in September 1967 occurred after the period of highest capillary discharge that occurs during the hot summer months. Surface changes had not been noticed in March, 1967.

The foregoing observations show the partial dependence of puffy ground development on salt content, but they also raise the question of where the salt goes during such surface changes. As the salt in moderately puffy surfaces (not thick brine-associated deposits) is generally concentrated in the upper 10 to 20 cm, it is apparently almost completely dissolved during extensive flooding, and then deposited elsewhere if the water is blown around or off the playa. Sheetwash is known to behave in this manner on playas and is thus an important agent in effecting surface changes. Dried salt flakes are also known to be easily removed by wind alone, after saline water evaporates and leaves a surface residue.

The foregoing observations raise the additional question of what effect the lowering of regional water tables will have on further change in the newly formed hard, dry crusts. When capillarity is greatly diminished by lowering of ground-water levels, soft surfaces, once formed, can be relatively stable, but once they change, the change becomes permanent. This has happened at Rosamond Lake, California, where surfaces that were once puffy and that discharged ground water are now permanently hard. It is known that regional ground-water levels in Harper Valley have fallen greatly. The effect on the playa is inevitable, although it may be slow because of low permeability and dewatering rates in lacustrine sediments. The amount of capillary decline in the Harper Lake playa sediments is not certain, but in several 1962 test wells emplaced in soft, puffy surfaces, the sediments were reasonably dry to depths as great as 3 meters. This depth exceeds what is usually found beneath puffy surfaces. The subsurface moisture and lack of increase in measured salt contents at the sample S-4 location suggest that this area of the playa may remain relatively stable.

5. SUMMARY AND CONCLUSIONS

Pronounced surface changes occurred at Harper Lake (playa) following flooding which covered most of the playa during the 1965-1966 winter. Extensive areas that had soft, dry, friable surfaces in 1962 were converted to a hard, dry crust with a substantial increase in the bearing capacity of the surface. In some places the hard crust is again reverting to a soft surface. The reconstitution of a soft, puffy surface into a hard crust appears to be concomitant with the dissolution of surface evaporite minerals, principally halite. Mineralogy of these surfaces shows little variance with either time or crustal type. There is evidence that crusts with a higher granular component favor development of puffy surfaces. Strength degradation is correlative with the soluble salt content of the sediments.

The types of surfaces present on the barren playa do not alone indicate how much ground-water discharge is occurring through the surface. It is apparent from penetrometer data that only the upper 20 cm is affected in strength variation and that some hard crusts that were formerly puffy must continue to discharge ground water from the capillary fringe, which was little affected during flooding. However, some puffy crusts that were converted may undergo relatively permanent change because of capillary decline related to regional lowering of groundwater levels. That is, these were relict surfaces at the time of flooding.

The observations at Harper Lake also demonstrate that playas are "dynamic" landforms; that is, they change with time (Neal and Motts, 1967). For playas having relatively low salt contents such as Harper Lake, hard or soft surfaces may be highly ephemeral.

The changes at Harper Lake took place in a relatively short period of time and some changes may be relatively long-lasting. These and future observations may be useful in determining the amount of time that is necessary for the various types of playa crusts to develop. Further observation should be made of Harper Lake to determine the relative permanency of the changes that have occurred. Penetrometer measurements should be made and can reveal subtle changes that might not otherwise be noticed. Observations and measurements should be correlated with meteorologic events such as rain, flooding, and so on, and with man's activities such as further drawdown of regional water tables.

Acknowledgments

The assistance of Dr. T. P. Rooney in supervising the mineral analysis is gratefully acknowledged. The editorial advice of Dr. T. P. Rooney, Lt. R. S. Williams, Jr., Dr. W. S. Motts, Prof. P. F. Kerr and Mr. D. Krinsley is greatly appreciated.

References

Gliven, N. and Kerr, P. F. (1966) Selected Great Basin Playa clays, Am. Mineralogist 51:1056-1067.

Hewett, D. F. (1955) Structural Features of the Mojave Desert Region, Geol. Soc. Amer. Spec. Paper 62, p. 377.

Hubbs, C. L. and Miller, R. R. (1948) The zoological evidence: correlation between fish distribution and hydrographic history in the desert basins of western United States; in Part II, The Great Basin, Univ. of Utah Bull. 38(No. 20), 166 p.

Kunkel, F. (1962) Reconnaissance of Ground Water in the Western Part of the Mojave Desert Region, California, U. S. Geological Survey Atlas HA-31.

Langer, A. M. and Kerr, P. F. (1966) Mojave Playa crusts: physical properties and mineral content, J. Sed. Petrology 36(No. 2):377-396.

Mabey, D. R. (1960) Gravity Survey of the Western Mojave Desert, California, U. S. Geol. Survey Prof. Paper 316-D, pp. 51-72.

Neal, J. T. (1963) Geology of Selected Playas, Project Water Hole, Open-file Report, Terrestrial Sciences Laboratory, AFCRL, Bedford, Mass, 235 p.

Neal, J. T. (1966) Lake Mead Pits, Geotimes 10(No. 6):2.

Neal, J. T. and Motts, W. S. (1967) Recent geomorphic changes in playas of western U.S. J. Geol. 75(No. 5):511-525.

Stone, R. S. (1957) Ground Water Reconnaissance in the Western part of the Mojave Desert, California, with Particular Respect to the Boron Content of Well Water, U.S. Geological Survey Open File Report, 102 p.

Thompson, D. G. (1929) The Mojave Desert Region, California, U.S. Geological Survey Water Supply Paper 578, 759 p.

Contents

III. Report of Test Drilling on Rogers, Coyote, Rosamond, and Panamint Playas in 1966

Ward S. Motts and David Carpenter
University of Massachusetts
Amherst, Massachusetts

Abstract

Continuous cores were obtained during test drilling on Rosamond, Rogers, Coyote, North Panamint, and South Panamint Playas. Four major types of fine-grained playa and lacustrine deposits underlie Rogers and Rosamond Playas to maximum depths of 75 and 200 feet respectively. These types are an upper silty clay unit, a lower highly plastic clay unit, varve-like alternations of silt or sand and clay, and lenses of silt and sand interbedded in the silts and clays. Thick and areally extensive sands and gravels, deposited from alluvial fans, underlie these four fine-grained units. Sediments from Rosamond Playa generally contain more clay and were deposited in deeper water than sediments from Rogers Playa. Underlying both Rogers and Rosamond Playas, piezometric surfaces are lowest in the central axial parts of the playas where silts and clays are thickest. Soil-moisture analyses from Rogers and Rosamond Playas reveal that their clays and silts are undergoing desiccation which has resulted in the continued formation of giant desiccation fissures through 1968. The fine-grained sediments of Rogers are desiccating relatively rapidly because of a lowering of the piezometric surface within the deep-seated blanket of sands and gravels.

A test hole drilled near the center of Coyote Playa penetrated 204 feet of clay, interbedded with minor amounts of sand and silt, which in turn is underlain by thick sand and gravel containing water under artesian pressure. The position of the artesian head 20 feet above the playa surface, and the abrupt down-hole increase of soil moisture from the surface indicate that ground water is discharging from the surface of Coyote Playa by capillarity. Three test holes in North Panamint Playa penetrated predominantly clays and silts interbedded with unsaturated lenses of sand and silt; whereas, three test holes in South Panamint Playa penetrated predominantly sand and silt saturated at shallow depth and interbedded with minor amounts of silt and clay.

Prepared under Contract AF19(628)-2486 with partial funding from Air Force Weapons Laboratory and Air Force Flight Test Center.

1. INTRODUCTION

1.1 Purpose

During the summer of 1966 a drilling program was conducted on Rogers, Rosamond, Coyote, North Panamint, and South Panamint Playas, California. One major purpose of the drilling program was to study the sedimentology and hydrology of the playa sediments. Another was to learn more about the origin of giant desiccation polygons. Because the 1966 drilling program is a continuation of a similar 1965 program, some reference is made in this report to data collected during 1965.

1.2 Methods of Investigation

Cores and sediment samples were taken from test holes: one on Rosamond Playa, six on Rogers Playa, one on Coyote Playa, three on North Panamint Playa, and three on Sourth Panamint Playa. Figure 1 shows the location of the playas. Depths of the test holes ranged from 30 ft to 275 feet. Soil samples were taken at 5-ft to 10-ft intervals for gravimetric analyses, which were made at the sedimentation laboratory at the University of Massachusetts. Detailed size and mineralogical analyses of the test cores are now being made at the laboratory and will be discussed in a future report. Water samples were obtained in the field and analyzed for chemical constituents by the Water Resources Division of the U.S. Geological Survey, Sacramento, California.

2. ROGERS AND ROSAMOND PLAYAS

2.1 Stratigraphy and Sedimentation

Rogers and Rosamond Playas are part of Antelope Valley, which is a large topographic and ground-water basin bounded on the north and northwest by the Tehachapi Mountains, on the south and southeast by the San Gabriel Mountains, and on the east by low hills and divides that separate it from Lower Majave Valley, Harper Valley and Fremont Valley. Antelope Valley is underlain by rock units of three major groups which are separated by unconformities (Dibblee, 1963, p. 141): (1) pre-Tertiary crystalline rocks, (2) Tertiary volcanic pyroclastics and sedimentary rocks, and (3) Quaternary sedimentary deposits. Figure 2 shows the general geology and structure of Antelope Valley in the area of Rogers and Rosamond Playas.

The Quaternary sedimentary deposits of the project area consist of clastic materials ranging in size from large boulders on the alluvial fans to fine-grained

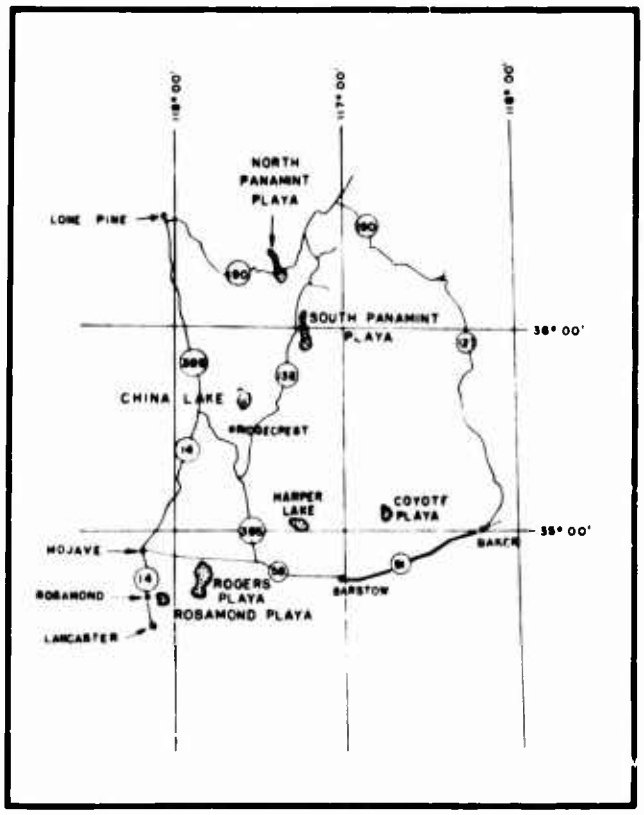

Figure 1. Location Map of Playas Test Drilled in 1966

clay in the playa. For the most part the deposits have been carried by streams draining the adjoining mountains; however, some have been carried by wind. The deposits were laid down in alluvial fans, along stream channels and flood plains, and in lakes formed in pluvial times. The Quaternary sedimentary deposits have been subdivided into Older Alluvium and Younger Alluvium. Older Alluvium ranges in thickness from a few feet to more than 1500 feet (Dutcher and Worts, 1963, p. 77); in places it is cemented into a firm fanglomerate. In places the Older Alluvium has been deformed and dissected. Younger Alluvium consists for the most part of unconsolidated gravels, sands, silts and clays. These materials form recent fan and alluvial deposits, playa and lacustrine deposits, and lake-shore deposits. Fine-grained playa and lacustrine deposits of Younger Alluvium underlie Rogers and Rosamond playas and grade laterally into equivalent coarser lake-shore deposits. Sand and gravel underlie the fine-grained playa and lacustrine deposits. In the following discussion the term playa deposits will describe both sediments that are deposited in a lacustrine environment and those deposited more recently in a playa environment.

The playa deposits may be subdivided into four predominant types: (1) an upper silty clay unit, (2) a lower highly plastic clay unit, (3) varve-like alternations of

Figure 2. General Geology and Structure of Antelope Valley in the Area of Rogers and Rosamond Playas

silt or sand and clay, and (4) lenses of silt and sand interlayered in the fine-grained playa materials. Figures 3 to 8 show stratigraphic relationships of the playa deposits. Their thickness ranges from 0 to more than 200 ft in Rosamond Playa, from 0 to more than 75 ft in the south part of Rogers Playa and from 0 to 45 ft in the north part of Rogers Playa. As shown on Figure 5, two areas of thick clay underlie Rogers Playa, one in the southern, and the other in the northern part of the playa. As shown on Figures 4 and 6, the fine-grained deposits of Rogers Playa also thicken along the geographic axis of the playa, which is generally parallel to section B-B' shown in Figure 5.

The upper silty clay unit is a maximum of 23 ft thick in the southern part and 18 ft in the northern part of Rogers Playa. The thickest part of the silty clay unit of Rogers Playa generally corresponds with the areas of thickest accumulation of fine-grained sediments. Near the center of Rosamond Playa, the silty clay unit thickens to about 20 feet. The silty clay unit of both playas generally has moderate to poor plasticity and is highly calcareous; fragments of calcareous material are common in some places, and desiccation cracks have been found in the more calcareous beds. The silty clay unit has numerous calcite-silt laminations. The silt in the unit is predominantly quartz with minor amounts of feldspar and biotite flakes.

A clay unit underlies the upper silty clay in all parts of Rogers and Rosamond Playas. See Figures 4, 5, 6 and 8. The clay is highly plastic, moderately moist, and extremely fine grained. Size analyses of the clay indicate large amounts of very fine-grained material. Samples from both Rogers and Rosamond Playas show high clay size content that generally comprises most of the total sample. The unit has characteristic color variations. The upper part of the unit is reddish brown in color and grades into an underlying grayish blue. At the boundary of the color change, streaks of gray and brown clay appear to cross bedding planes and commonly occur as swirls and convolute forms.

A thin bed of moist clay occurs within the sand unit that underlies the fine-grained playa deposits. This plastic clay is a few feet thick throughout most of Rogers Playa and occurs from about 2 to 15 ft from the top of the sand. The thin bed of clay grades laterally into silt and sand along the margins of the playa. It forms an excellent stratigraphic marker.

Varve-like alternating beds of silt or sand and clay occur in Rogers and Rosamond Playas. See Figures 5 and 8. The silt and sand beds are about 1/4 in. thick and consist of medium to coarse silt with abundant mica flakes. The clay beds range in thickness from 2 to 6 in. and are moist fine clay and silty clay. The alternating beds of silt or sand and clay grade laterally into silty and clayey sand in the northern part of Rogers Playa. See Figure 4. There are two other types of rhythmical bedding in sediments of Rosamond Playa: (1) Laminations of alternating clay and

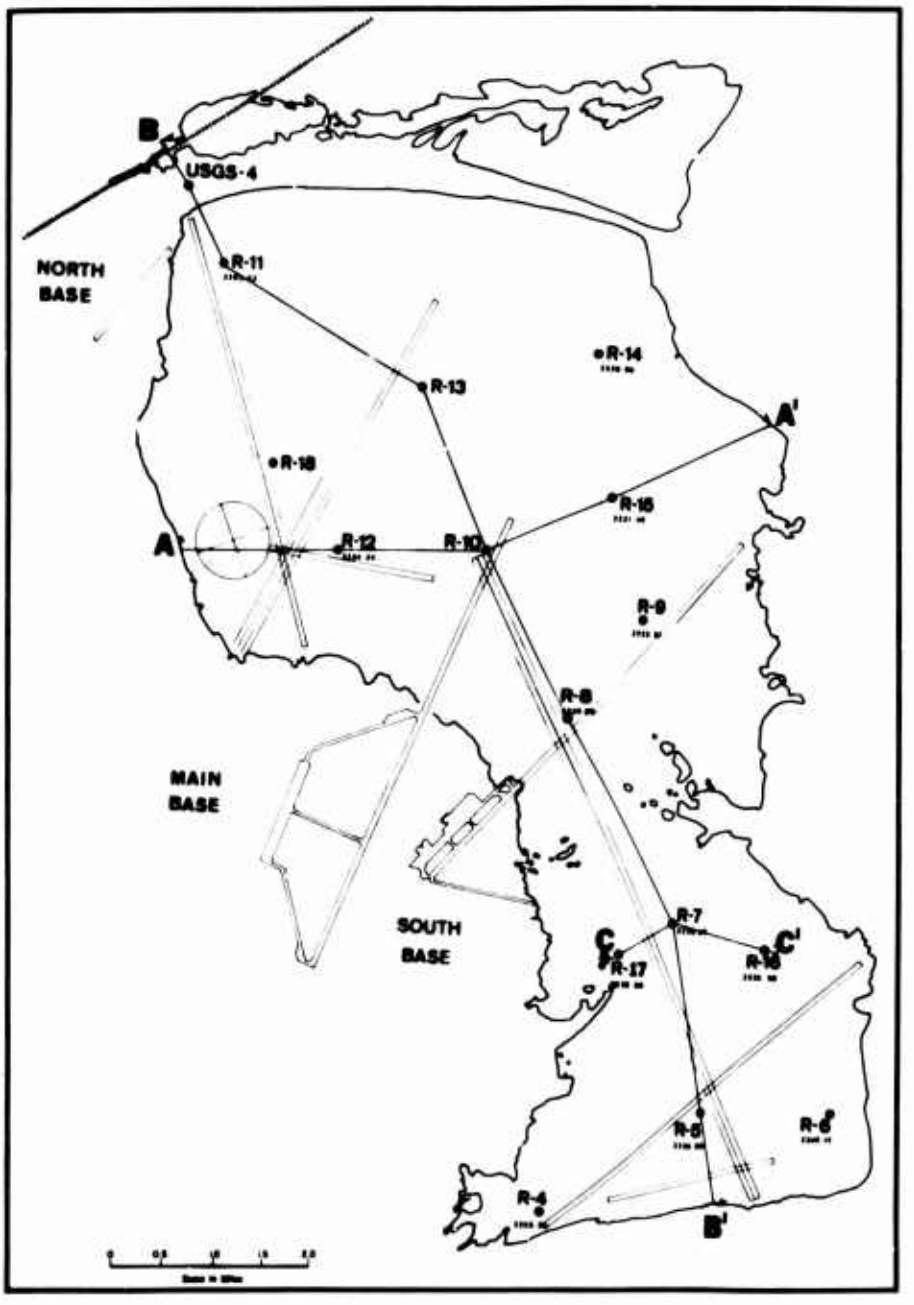

Figure 3. Map of Rogers Playa Showing Lines of Cross Sections and Elevations of Piezometric Surfaces in Test Wells

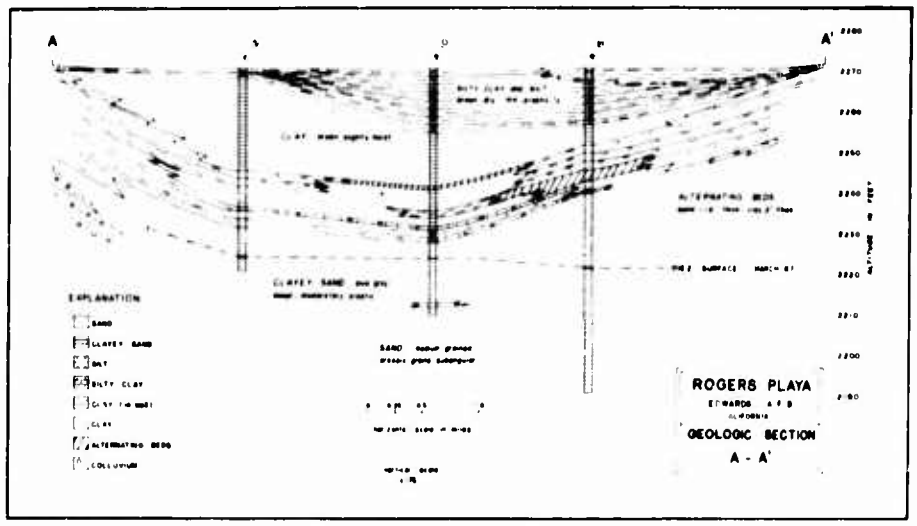

Figure 4. Geologic Section A-A', Rogers Playa

calcite in sediments form couplets that may be varves. These clay-calcite laminations are found in all three test holes in Rosamond Playa. (2) A difference in grain size from coarse to fine silt size form another type of rhythmical couplet. The core from Rosamond 1, drilled in 1965, shows dark gray to black layers from 41 to 43 ft and from 49 to 50 feet. These dark layers have a high organic content which may have originated during a time of intensive biologic activity in the lake.

There is a pronounced difference between the sediments of Rogers Playa and those of Rosamond Playa. The fine-grained sediments of Rosamond Playa contain more clay and were deposited under deeper water conditions than the sediments from Rogers Playa. It is noteworthy that pollen from Rogers cores were abraded, badly oxidized and not identifiable, whereas pollen from Rosamond Test Hole 1 was unaltered and could be identified.

In both Rogers and Rosamond Playas lenses and beds of coarse silt and fine sand are interbedded with the plastic clays and silty clays. These coarser-grained units interfinger with the fine-grained deposits along the margin of the playas. The locations of the coarser units have influenced the development of the giant desiccation polygons discussed in the following section, Hydrology and Soil Moisture. The sands and silts may have been brought into the lake during times of excessive rainfall and flooding. The well-sorted sands in these lenses indicates eolean origin.

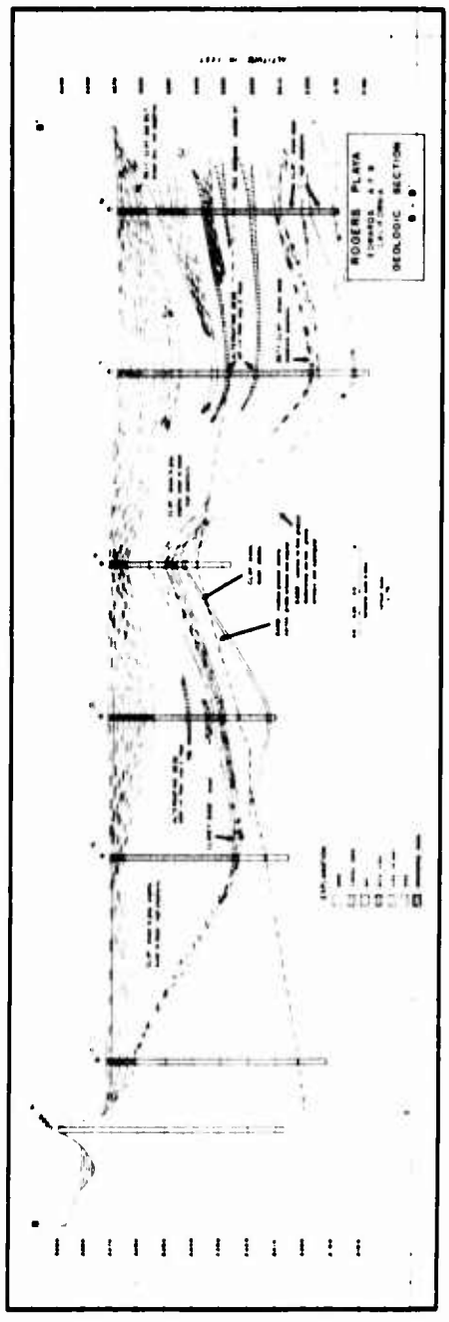

Figure 5. Geologic Section B-B', Rogers Playa

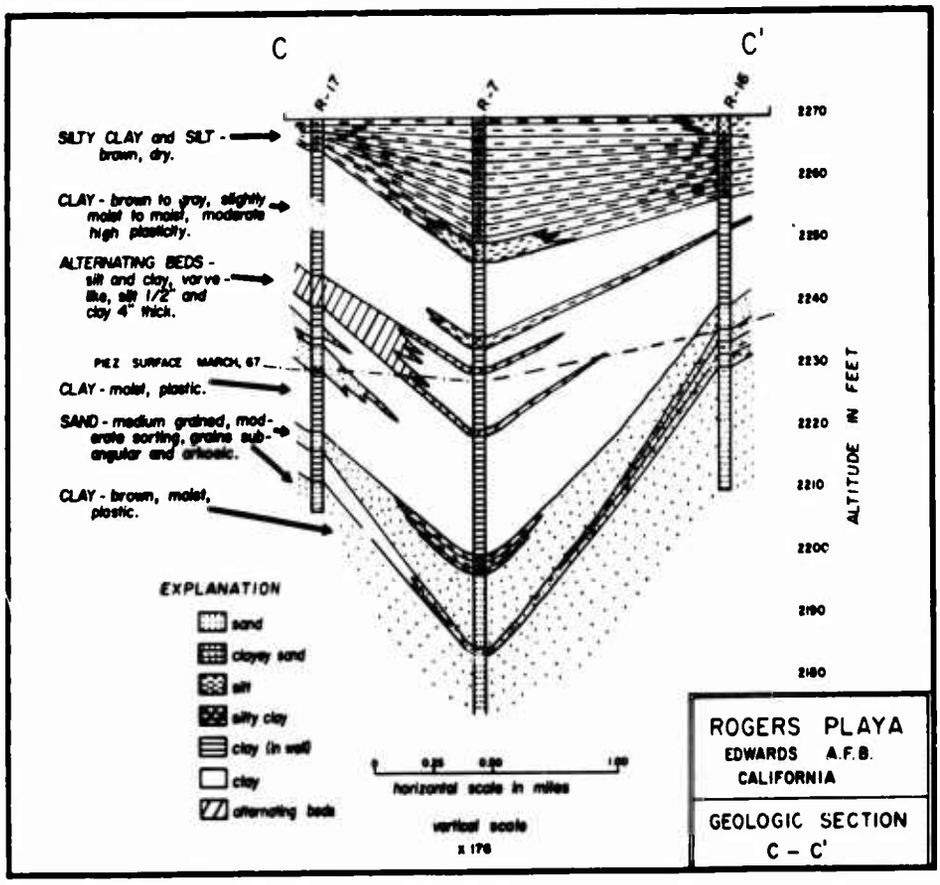

Figure 6. Geologic Section C-C', Rogers Playa

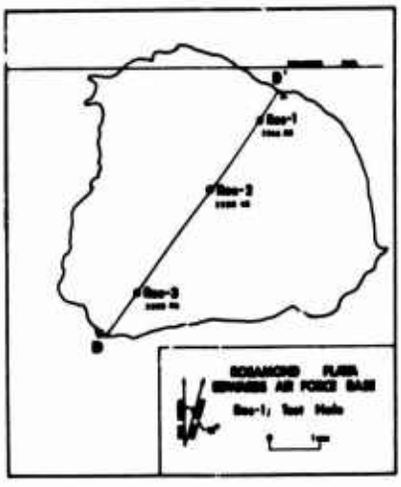

Figure 7. Map of Rosamond Playa Showing Line of Cross Section D-D' and Elevations of Piezometric Surfaces in Test Wells

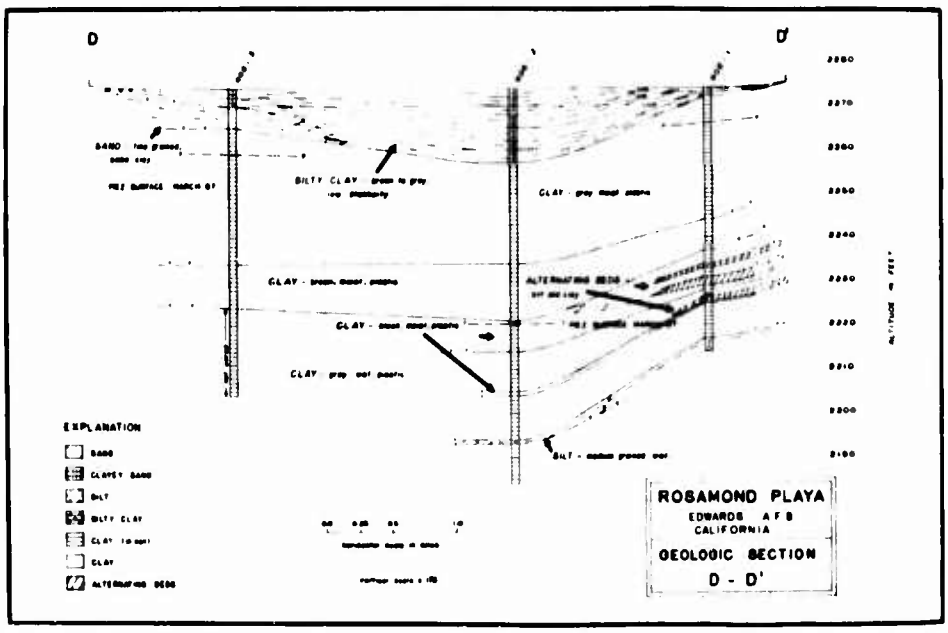

Figure 8. Geologic Section D-D', Rosamond Playa

2.2 Hydrology and Soil Moisture

Dutcher and Worts (1963, p. 117, 118) show that two major aquifers underlie Rogers and Rosamond Playas--the "Principal Water Body" (Shallow Aquifer of this report) and the "Deeper Aquifer." Water in the Shallow Aquifer is largely in the Younger Alluvium which includes playa deposits and associated sand and silt lenses of Rogers and Rosamond Playas. Most water in the Deeper Aquifer is in the Older Alluvium. Throughout the Lancaster Basin, under natural conditions prior to 1940, the head of water in the Deeper Aquifer was higher than the head in the Shallow Aquifer, and generally higher than the playa surfaces. A large amount of discharge occurred through the playa surfaces, and a spring was reported in Rogers Lake (Dutcher and Worts, 1963, p. 141). Because of increased withdrawals from the Deeper Aquifer after 1940, the head of water in this aquifer was depressed below that of the Shallow Aquifer. The reversal of heads caused draining of water from the playa sand lenses into the Deeper Aquifer. Lowering the piezometric heads below the sandy zones has resulted in evaporation of water from the fine-grained clays and silts. This evaporation is the primary cause of the desiccation of the playa sediments and the formation of giant polygons. (Neal and Motts, 1967). The sequential development of giant polygons is shown on Figure 9.

As shown on the test well logs (Appendix A), water was encountered under hydrostatic pressure in each of the test holes. Also, in each hole, the level to which the piezometric head rose was below the surface of the playa. On Rogers Playa the maximum rise of water, 40 ft, occurred at Test Hole 6 and the minimum rise of

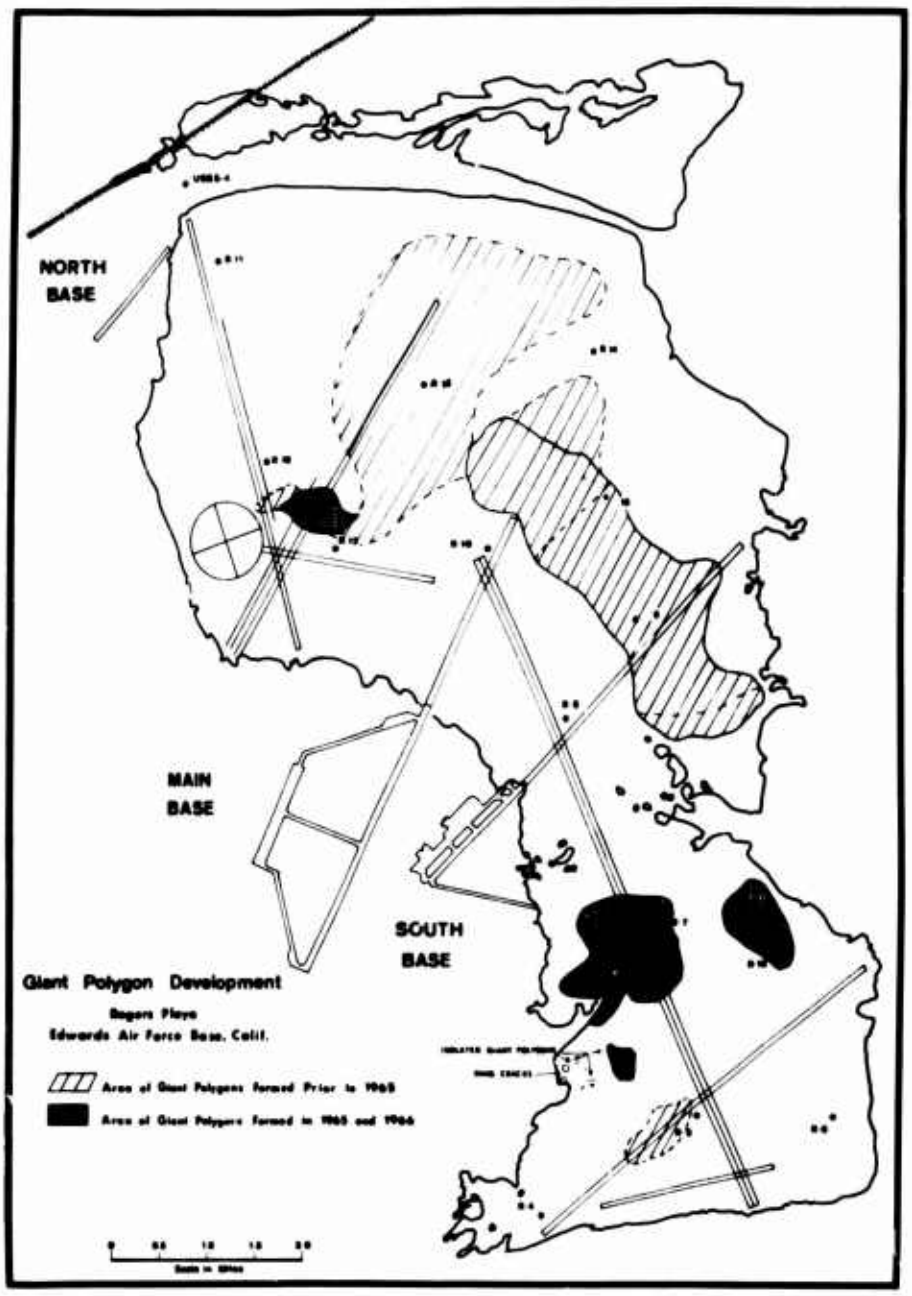

Figure 9. Sequential Development of Giant Desiccation Polygons, Rogers Playa

water, 2 ft, occurred at Test Hole 11. On Rosamond Playa water rose 50 ft at Test Hole 1.

Underlying both Rogers and Rosamond Playas depressed piezometric surfaces extend along sedimentary axes of the thick clay and silts. At Rosamond Playa a higher piezometric surface occurs in sands penetrated by Test Holes 1 and 3; it is 40 to 50 ft above the deeper piezometric surface penetrated by Test Hole 2. The higher piezometric surfaces along the margins of Rosamond Playa are due to saturated sand and silt lenses that interfinger with the playa deposits. On Rogers Playa the depressed piezometric surface occurs along an axis through Test Holes 7 and 5. See Figure 3. As indicated on Figure 6, this generally coincides with the thickest section of fine-grained lacustrine and playa deposits. A sharp rise of soil moisture that occurs in Test Hole 17 on Rogers Playa indicates the presence of a water-bearing zone from 22 to 35 ft. However, drier clays occur at 40-ft depth in Test Hole 17, indicating deep seated desiccation.

The soil moisture contents were determined from gravimetric tests of samples collected in the field and analyzed in the laboratory. From a study of the logs and corresponding moisture contents a few generalizations can now be made. First, soil moisture content is closely related to the texture of the sediments; where the sediments become more silty and sandy the moisture content decreases. This explains abrupt fluctuation of the moisture curves down the hole on most logs. Second, in many of the test holes, for example in Rosamond 2, there is a downward increase of moisture in fine-grained sediments of the same size. Third, in some test holes, for example Rogers 15, 17, and 18, clays above sand zones showed considerable loss of moisture. These relationships in the central and northern part of Rogers Playa indicate desiccation of the playa deposits. It should be noted that throughout this part of Rogers Playa the piezometric surface has lowered within the underlying extensive sand body, allowing subsurface evaporation of the upper fine-grained lacustrine and playa deposits. See Figures 4 and 5. Capillary movement would occur if the sand units in physical contact with the clays were filled with water.

Figure 10 shows the soil moisture limits for test-hole samples from Rogers Playa in 1965 and 1966. Both curves show a gradual increase of soil moisture to depths of 15 to 25 feet. At this depth the 1966 curve shows a larger spread towards the drier side, which indicates that desiccation may have occurred from 1965 to 1966. It is noteworthy that the severe floodings of Rogers during 1965 and 1966 had little effect on the soil moisture curves during 1966. Water stood on the playa surface from mid-November, 1965 through April, 1966. The 1966 curves show no appreciable increase of shallow soil-moisture content, revealing the low permeability of the clays. Surface-water infiltration into the playa clays may be impeded by the upward movement of capillary water.

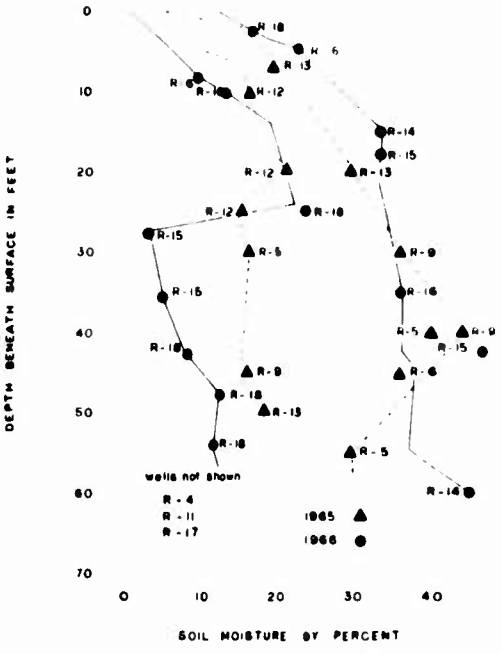

Figure 10. Limits of Soil Moisture Content with Depth for Years 1965 and 1966, Rogers Playa

3. COYOTE PLAYA

The test hole on Coyote Playa was drilled near the center of the playa as shown by Figure 11, and penetrated 204 ft of clay and silty clay interbedded with minor amounts of sand and silt. These fine-grained sediments were deposited under playa and lacustrine conditions and consist predominantly of clay which is highly plastic and moist. Major sand zones in the lacustrine deposits occur from 41 to 44 ft, and from 165 to 170 feet. From 204 to 275 ft the test hole penetrated sands, gravel and fanglomerate of the desert fans and desert flat. Water under artesian pressure was encountered in the sands and gravels, and rose to a height of 20 feet above the playa surface. Water from the test well flowed uniformly at a rate of about 100 gallons per minute, and was slightly saline, but potable.

An abrupt increase of soil moisture content occurs from nearly zero at the surface to 18 percent at a depth of one foot. See Graph 6, Appendix B. With minor fluctuations the moisture content gradually increases from 18 to about 40 percent at a depth of 114 feet. For the most part, the moisture content of Coyote Playa ranges from 20 to 30 percent. The abrupt increase in soil moisture at the surface and the high moisture content down the hole suggests that water is moving upward by capillary movement and is discharging at the surface. The strong artesian head also suggests that water probably moves slowly upward through the lacustrine sediments; the movement is slow because of the plastic, poorly permeable nature of the clays. The surface clays in the vicinity of the test hole have desiccated

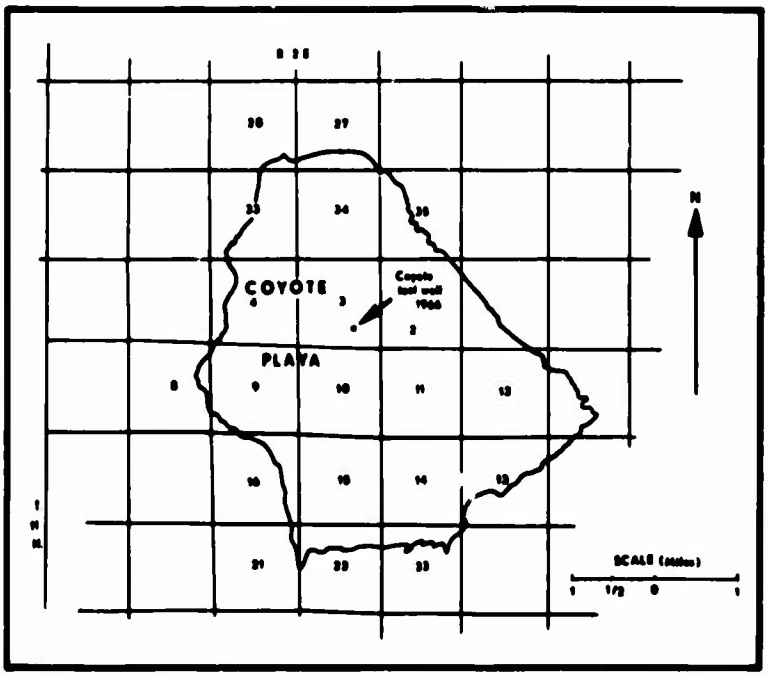

Figure 11. Location of Coyote Playa Test Wells

to form polygons ranging from 6 in. to 1 ft across with a hard surface crust about 1 in. thick. It is noteworthy that self rising ground occurs along the margins of the cracks. The deeper artesian aquifer, rather than surface water, must be the source of the high moisture content of Coyote Playa clays. Field evidence from Rogers and Big Smoky Playas indicates that there is little percolation of surface water downward in plastic clays even where water is present on the playa surface for months. See paragraph 2.2 on Rogers Playa.

4. NORTH PANAMINT PLAYA

Three test holes, Test Hole 1 in the northern part, Test Hole 2 in the central part and Test Hole 3 in the southern part, were drilled on North Panamint Playa. See Figure 12. Test Holes 1 and 2 were both less than 30 ft deep, whereas Test Hole 3 was drilled to a total depth of 162 ft. See Log 10, Appendix A. Test Holes 1 and 2 penetrated predominantly clays and fine-grained silts interbedded with minor sands. Both test holes were terminated at shallow depth because they encountered high porosity fracture zones in the clay. The fracture zones were large since all mud circulation was lost in the holes. These fracture zones may be related to the formation of the giant desiccation polygons, or they may represent a

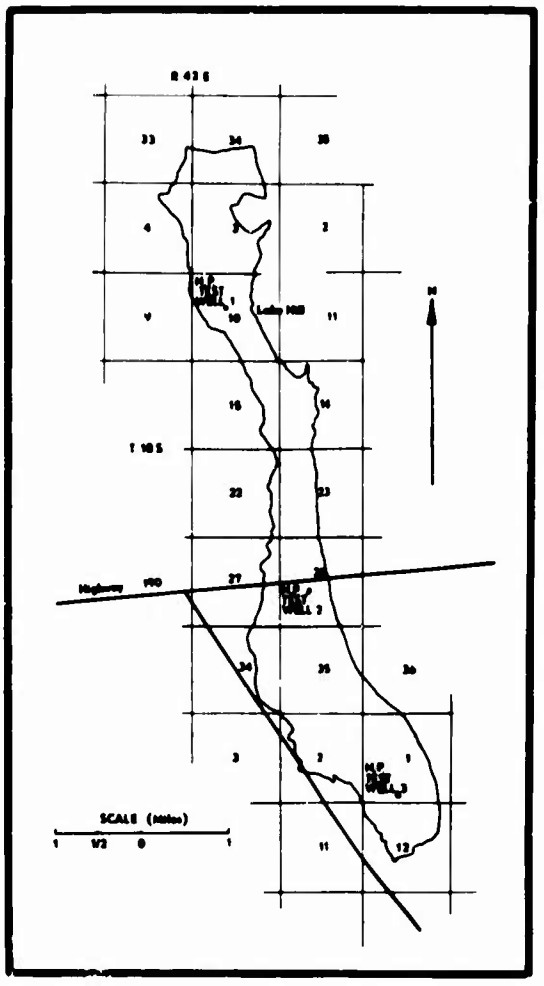

Figure 12. Location of North Panamint Playa Test Wells

fracture zone at depth resulting from playa desiccation. However, there was no evidence of giant polygons at the surface.

Test Hole 3 penetrated predominantly clays and silts interbedded with sands and silts. The major sand and silt zones occur at 45 to 51 ft, 62 to 66 ft, and 122 to 140 feet. The latter zone also contained gravel of pebble size. The fine-grained sediments in Test Hole 3 were deposited in lacustrine and playa environments. The upper 30 ft of materials, which are predominantly silt, may be modern playa deposits, whereas the deeper and more plastic clays probably were deposited in the lacustrine environment of Pleistocene Lake Panamint. The interbedded sands and gravels were deposited by encroachment of the nearby desert flat and alluvial fans. Test Hole 3 was terminated at a depth of 162 ft, where wet sands were encountered. There was standing water in the hole when drilling terminated; however, the water was not present after a few days. The wet sands and silts indicate that the bottom of the hole was near the water table.

Soil moisture contents of Test Holes 1 and 2 (Graph 7, Appendix B) have a gradual increase of moisture to a depth of 25 ft and then minor fluctuations down the hole. This gradual increase of moisture at shallow depths may be characteristic of a desiccating playa. Note the abrupt increase of soil moisture with depth in Coyote Playa which, as good evidence shows, is actively transpiring water. Another noteworthy feature of soil moistures in the fine-grained materials on Test Hole 3 is the abrupt increase of moisture from 35 to 43 feet. This moisture increase occurs immediately above a major sand zone which was not water saturated. See Graph 7, Appendix B. If the sand zone is hydrologically connected to surface exposures of gravel and sands the zone at intervals may become flooded with water from a season of heavy precipitation. The flooding and filling of the sand zone would cause capillary rise of water in adjacent silts and clays which explains their increase in moisture.

5. SOUTH PANAMINT PLAYA

Three test holes were drilled on South Panamint Playa. See Figure 13. Test Hole 1 in the central part of the playa was drilled to a depth of 83 ft; Test Hole 2, about 20 ft from Test Hole 1, was drilled to a depth of 30 ft; and Test Hole 3 in the northern part of the playa was drilled to a depth of 25 feet. All holes penetrated predominantly silt and sand. The log of Test Hole 1 (Log 11, Appendix A) shows silt and sand interbedded with minor amounts of clay. The colors of sediments in this hole are brown and yellow to a depth of 16 ft and grays, blues and greens to a depth of 83 feet. South Panamint, a groundwater discharging playa, is underlain by an abundance of sand and silt, whereas North Panamint, not a groundwater discharging playa, is underlain predominantly by silts and clays. Both playas are in the same topographic valley and have similar lighologic source areas.

Casing was placed in Test Hole 1 at 80 ft, and in the adjacent Test Hole 2 at 20 feet. In Test Hole 1 water occurred about 8 ft below the surface, whereas in Test Hole 2, the shallow well, water was about 4 ft below the surface. This indicates that deeper water under higher hydrostatic head is moving up into the shallow playa sediments. The samples of water from both test holes are being analyzed for chemical content.

The surface at Test Hole 1 was hard, compacted, had polygonal cracks, and superficially resembled some of the hard, dry surfaced playas. However, close inspection of the surface materials showed very large quantities of silt and high moisture contents immediately below the surface. The soil moisture contents of Test Hole 1 generally are less than 25 percent. These relatively low values are

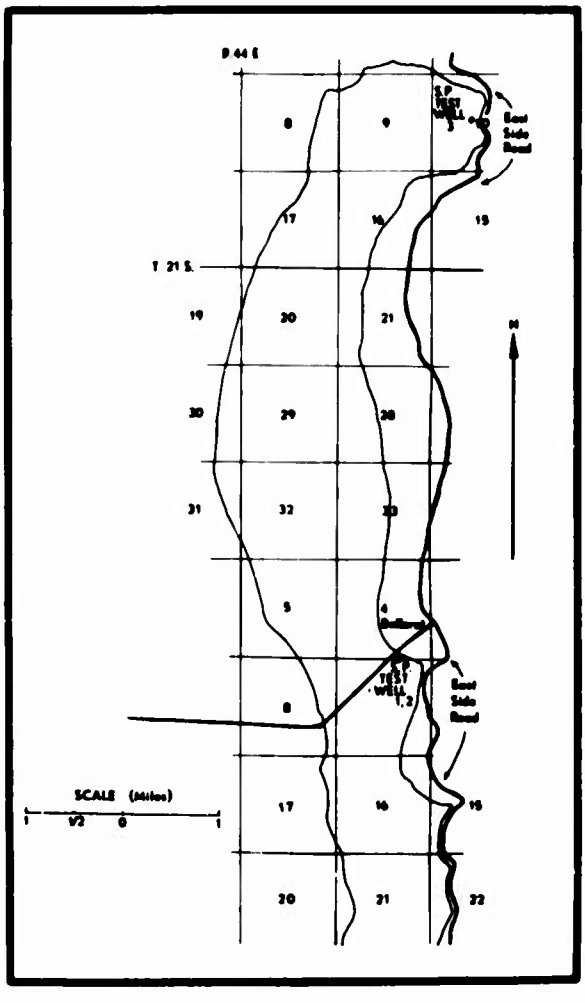

Figure 13. Location of South Panamint Playa Test Wells

probably due to the large amounts of silt and sand in the samples. Test Hole 3 was drilled in the northern part of the playa and near a depression discharging large amounts of ground water. Soft sands and silts were penetrated during drilling and water occurred about 3 ft below the surface. Casing was placed in this hole to a depth of 25 ft, but it soon sank out of sight because of the unstable nature of the deposits.

6. SUMMARY AND CONCLUSIONS

Test drilling reveals that Rogers and Rosamond Playas have thin blankets of silt and clay, interbedded with lenses of coarse silts and sands, that are underlain by thick sands and gravels. Silts and clays deposited in lake and playa environments reach a maximum thickness of 45 feet in northern Rogers, 75 feet in southern Rogers, and 200 feet in Rosamond Playa. The deposits may be divided into four major lithologic types. (1) An upper silty clay unit of moderate plasticity reaches a maximum thickness of about 20 ft in Rogers and Rosamond Playas. (2) A highly plastic clay unit underlies the upper silty clay in all parts of Rogers and Rosamond Playas. (3) A thin bed of plastic clay forms an excellent stratigraphic marker in the basal, thick sands and gravels. (4) Varve-like alternating beds of silt or sand and clay form rhythmical units; the silt and sand beds are about 1/4 in. thick and the clay beds are 2 to 6 in. thick.

Soil-moisture contents from test-hole samples of Rogers and Rosamond Playas indicate the following: (1) Soil moisture content is closely related to the texture of the sediments. The moisture content decreases where sediments become more sandy and silty. (2) In many test holes, soil moisture increases downward in sediments of the same size. (3) In some test holes, clays above sand zones showed a considerable loss of moisture content indicating that the clays are undergoing desiccation resulting in the continued formation of giant desiccation polygons through 1968.

Soil-moisture values of test-hole samples from Rogers Playa taken in 1965 and 1966 show a gradual increase from the surface downward to depths of 15-25 feet. The 1966 curve shows a larger spread at this depth indicating that desiccation may have occurred between 1965 and 1966. The 1966 curves show no appreciable increase of soil-moisture content at shallow depth, although water stood on the playa surface from mid-November, 1965 through April, 1966.

A test hole drilled near the center of Coyote Playa penetrated 204 feet of predominantly clay, underlain by sands, gravel, and fanglomerate containing water that rose under artesian pressure to a height of 20 feet above the playa surface. Three test holes in North Panamint Playa penetrated mostly clays and silts interbedded with sands and silts. Test holes in the middle and northern parts of the playa, at depths of less than 30 feet, penetrated high porosity zones which may be part of a subsurface fracture system formed by giant desiccation polygons. Three holes in South Panamint Playa penetrated silt and sand interbedded with minor amounts of clay, and penetrated a shallow water table. It is noteworthy that South Panamint discharges much ground water and is underlain mostly by coarse silts and sands; whereas, North Panamint Playa discharges little or no ground water, but is underlain mainly by silts and clays.

Acknowledgments

Under the supervision of Ward Motts, David Carpenter and Philip Durgin logged cores from test holes in the field and collected samples for soil moisture analysis. David Carpenter, assisted by David Drake, worked on his master's thesis on Rogers Playa and Philip Durgin, assisted by Paul Raffoul, worked on his master's thesis on North Panamint Playa. The authors are indebted to many people at Edwards Air Force Base, especially Col. Hill and Mr. Joe Reif, whose cooperation helped make this study possible. The authors are also indebted to geologists of the U.S. Geological Survey, especially L. S. Dutcher, F. N. Geissner, and W. R. Moyle, Jr., for their interest and cooperation in this project.

References

Dibblee, T. W., Jr. (1963) Geology of the Willow Springs and Rosamond Quadrangles California, U.S. Geological Survey Bulletin 1089-C, pp. 141-253.

Dutcher, L. C. and Worts, G. F., Jr. (1963) Geology, Hydrology and Water Supply of Edwards Air Force Base, Kern County, California, U.S. Geological Survey, Open File Report, District Office, Sacramento, California.

Hagar, D. J. (1966) Geomorphology of Coyote Valley, San Bernardino County, California, Univ. of Massachusetts, Ph.D. Dissertation, 208 p.

Motts, W. S. (1965) Hydrologic types of playas and closed valleys and some relations of hydrology to playa geology. Chap. 3 in Geology, Mineralogy, and Hydrology of U.S. Playas, AFCRL Rept. 65-266, p. 73-104.

Neal, J. T., and Motts, W. S. (1967) Recent geomorphic changes in playas of western United States, J. Geol. 75(No. 5):511-525.

Appendix A

Figures A1 to A12 show well logs, soil moisture contents, and ground water information from test holes drilled in 1966.

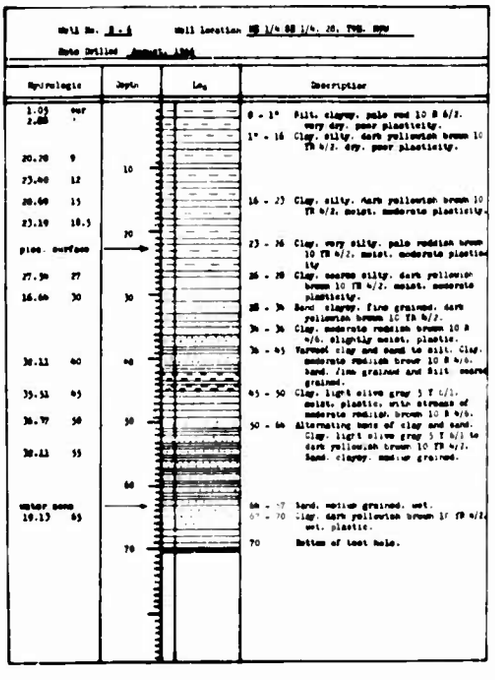

Figure A1. Log 1, Rogers Playa, Test Hole 6

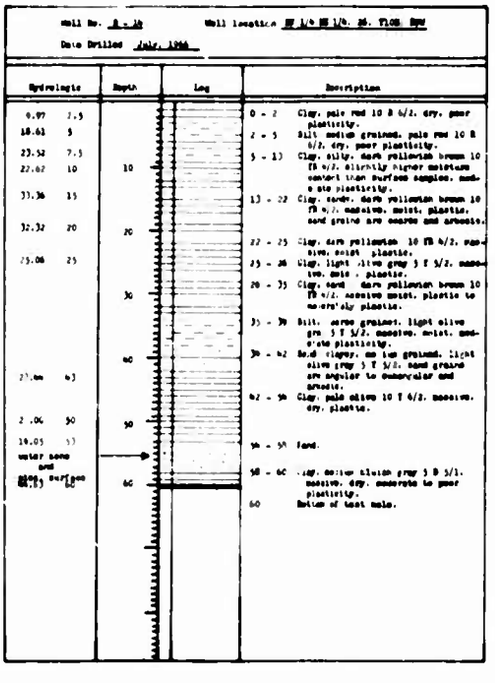

Figure A2. Log 2, Rogers Playa, Test Hole 14

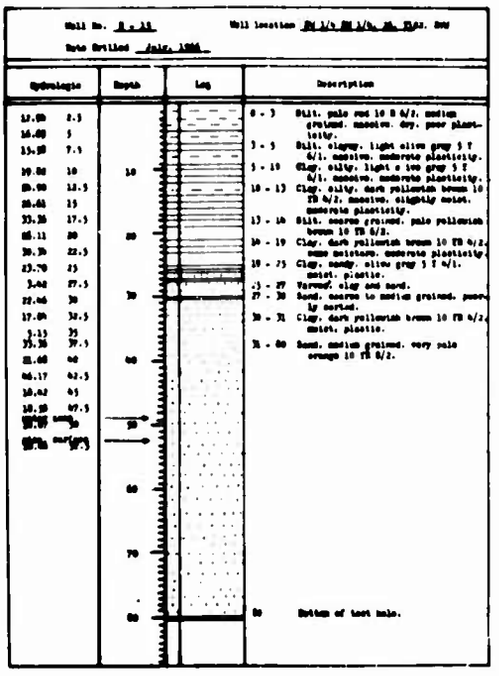

Figure A3. Log 3, Rogers Playa, Test Hole 15

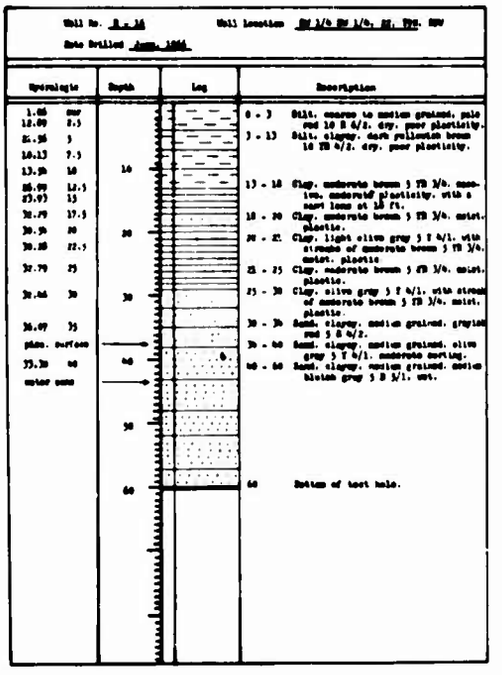

Figure A4. Log 4, Rogers Playa, Test Hole 16

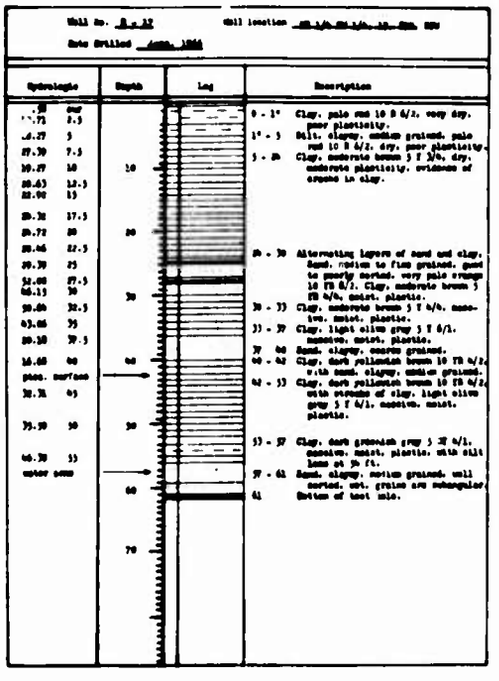

Figure A5. Log 5, Rogers Playa, Test Hole 17

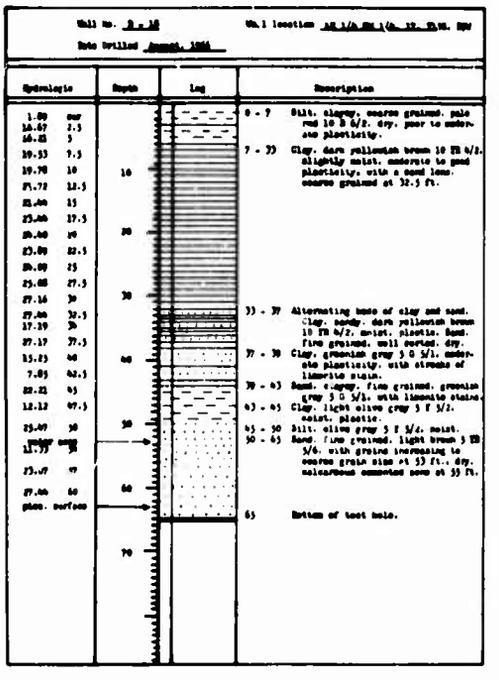

Figure A6. Log 6, Rogers Playa, Test Hole 18

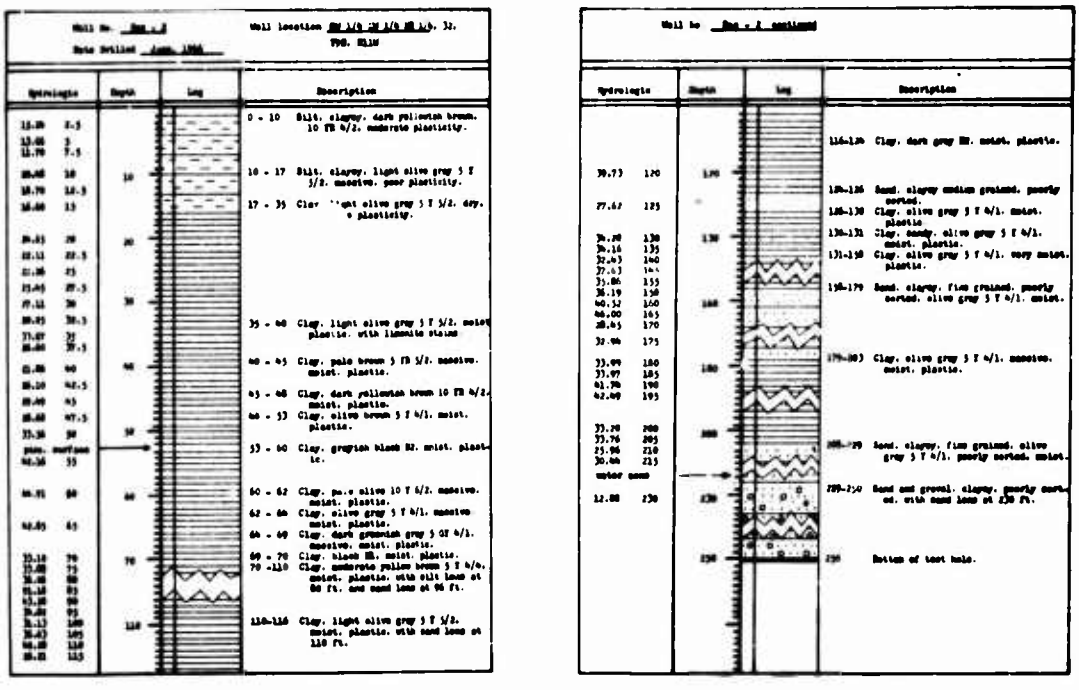

Figure A7. Log 7, Rosamond Playa, Test Hole 2

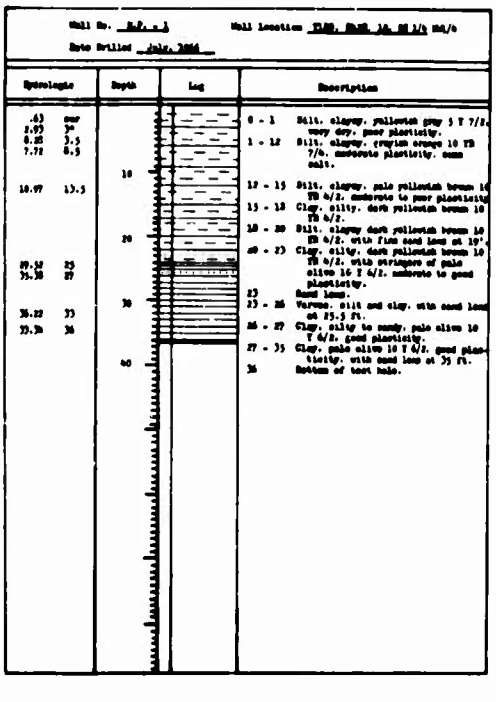

Figure A8. Log 8, North Panamint Playa, Test Hole 1

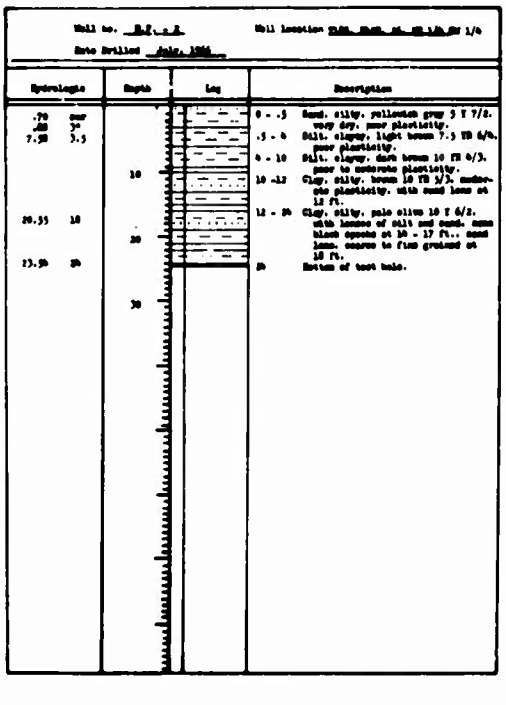

Figure A9. Log 9, North Panamint Playa, Test Hole 2

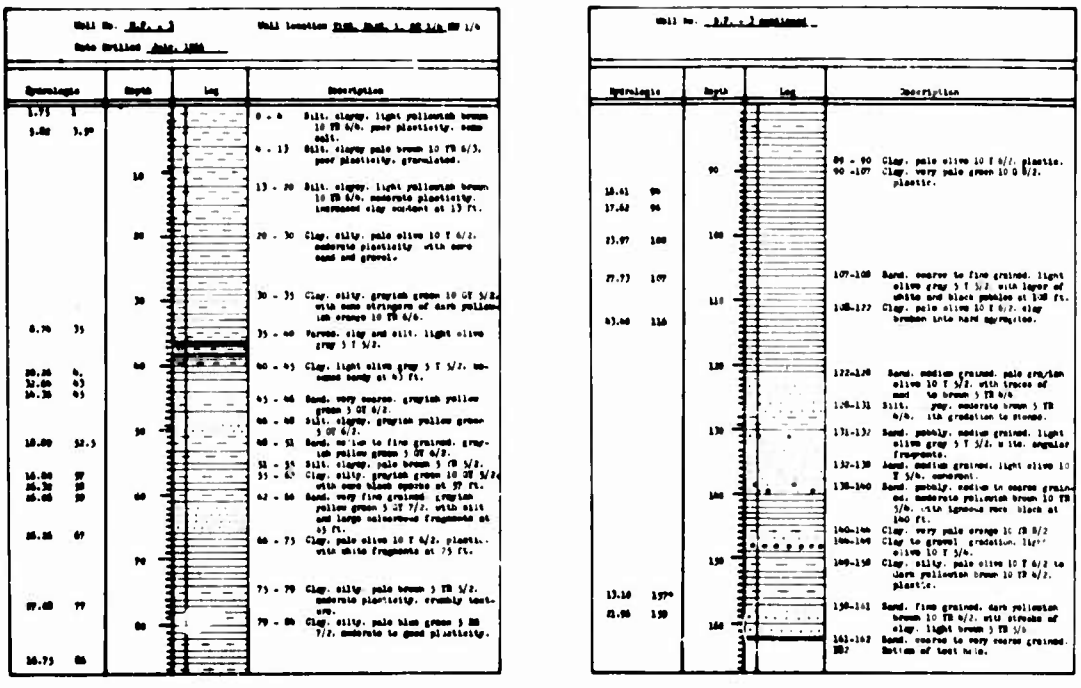

Figure A10. Log 10, North Panamint Playa, Test Hole 3

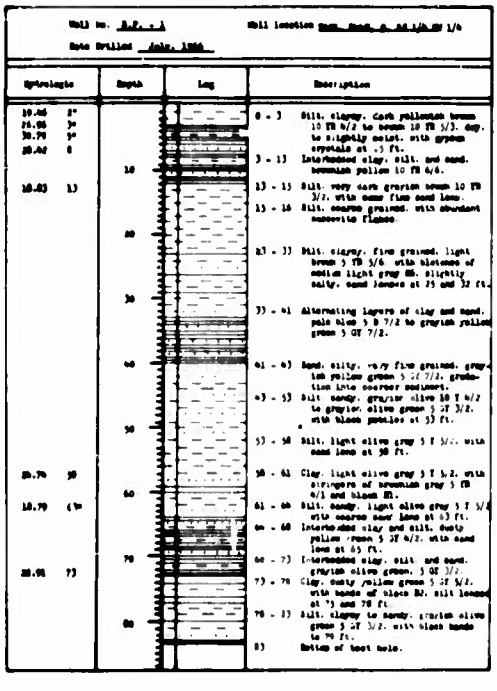

Figure A11. Log 11, South Panamint Playa, Test Hole 1

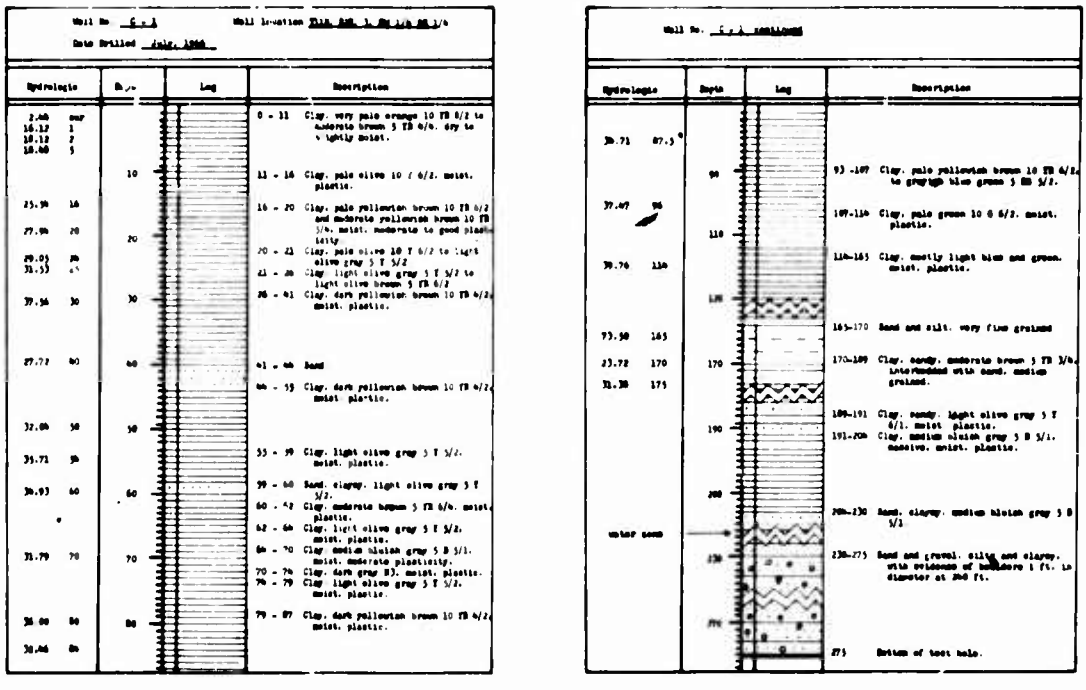

Figure A12. Log 12, Coyote Playa, Test Hole 1

Appendix B

Figures B1 to B7 are graphs showing change of soil moisture contents with depth for test holes drilled in 1965 and 1966.

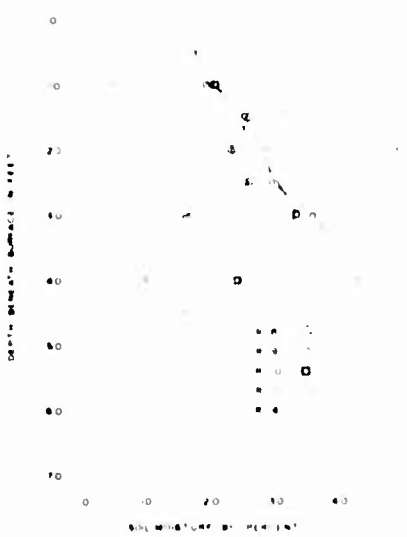

Figure B1. Graph 1, Soil Moisture Content for Test Holes 4, 8, 9, 10, 11, Rogers Playa

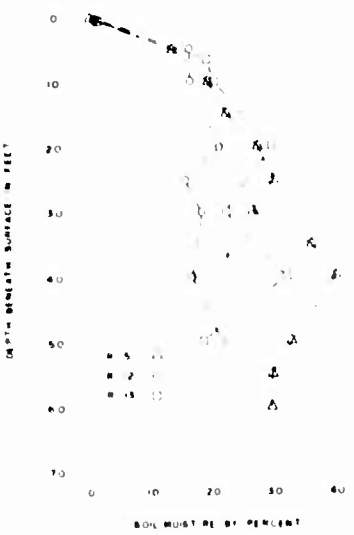

Figure B2. Graph 2, Soil Moisture Content for Test Holes 5, 12, 13, Rogers Playa

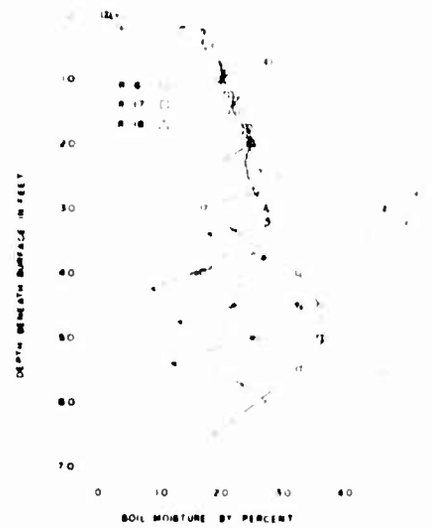

Figure B3. Graph 3, Soil Moisture Content for Test Holes 6, 17, 18, Rogers Playa

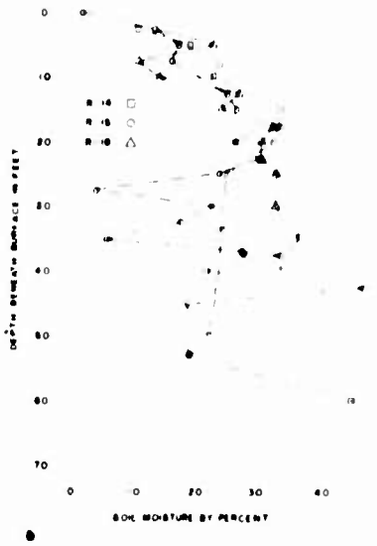

Figure B4. Graph 4, Soil Moisture Content for Test Holes 14, 15, 16, Rogers Playa

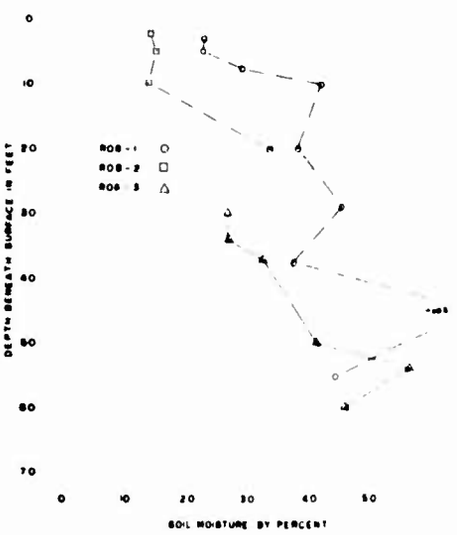

Figure B5. Graph 5, Soil Moisture Content for Test Holes 1, 2, 3, Rosamond Playa

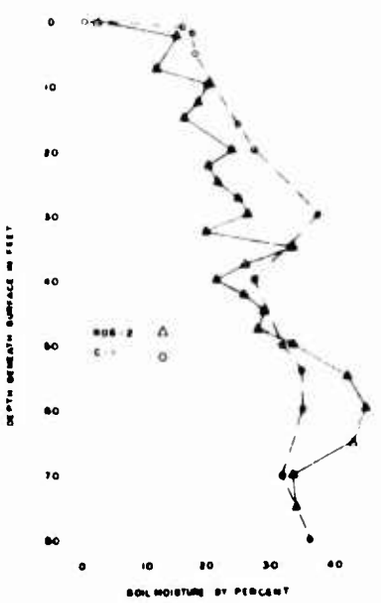

Figure B6. Graph 6, Soil Moisture Content for Test Hole 2, Rosamond Playa, and Test Hole 1, Coyote Playa

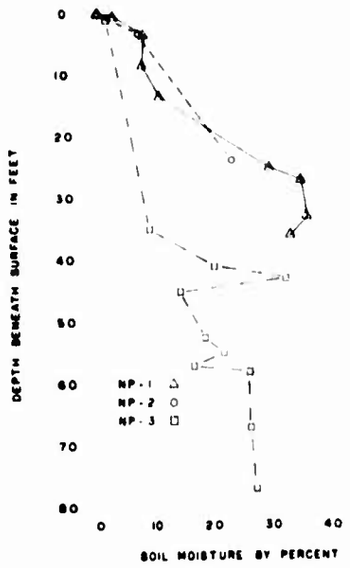

Figure B7. Graph 7, Soil Moisture Content for Test Holes 1, 2, 3, North Panamint Playa

Contents

IV. Geologic Characteristics of Seven Australian Playas

D. B. Kinsley, C. C. Woo, and G. E. Stoertz
Military Geology Branch
United States Geological Survey
Washington, D.C.

Abstract

Field evidence and laboratory analyses of playa sediments from Western and South Australia suggest that the Tertiary laterite which had been uniformly developed areally and vertically was subjected to erosion in the east due to the Kosciusko Uplift of late Tertiary time. In the west, laterization continued until the climate became arid just after the Kosciusko Uplift. The post-Tertiary arid conditions are reflected in the unweathered detrital feldspars (> 200 mesh fractions). This suggests that the clays rich in kaolinite are inherited products of laterization during the earlier tropical climate. Diagenesis is proposed as an explanation for the direct correlation between the soluble salt and kaolinite content of the clays, while both are inversely proportional to the montmorillinite and chlorite, and have no correlation with illite content.

The margins of extensive dune fields, which are now covered by recent sediments at Lake Frome, South Australia, are part of the dune system of interior Australia. This system is buried at its marine margins by tidal muds. These relationships support the thesis that interior Australia was dry and windy during the Pleistocene when sea level was lower. The recent sedimentary cover represents higher sea level and a somewhat moister climate.

Prepared under PRO-CP-67-820 with partial funding from Air Force Weapons Laboratory, Kirtland AFB, N.M.

1. INTRODUCTION

1.1 Definition

Playa, the Spanish word for beach, shore, or strand, has lost this meaning in the United States and has come to mean the flat, central portion of a closed desert basin. Playas are found throughout the desert areas of the world. In South America, they are termed salinas; in North Africa, sebkhas or shotts; and in Australia, they are usually referred to as lakes, although playa is used in the geologic literature.

Playas are the flattest of all landforms, commonly having a gradient of less than 20 cm per km (Neal, 1965, p. vii). They are composed of generally fine materials with some coarser fractions. Their peripheral areas often adjoin wet zones at the foot of alluvial plains.

There are three types of playas, based on the nature of their sediment. Playas that were previously occupied by lakes are generally underlain by a thick sequence of lacustrine sediments. Other playas, formed as the result of the deposition of medium to fine sediments beyond the peripheral alluvial fans and periodically occupied by shallow ephemeral lakes, are underlain by a sequence of interbedded lacustrine and alluvial sediments. Playas which may be inundated only infrequently and grade into pans are thinly veneered surfaces that reflect but little deposition over long periods of time. Such playas, where extensive, have poorly delineated boundaries.

Subtle environmental changes in precipitation, evaporation, wind, and temperature may cause playa surfaces to alternate between dry and hard, and wet and soft. Water-table fluctuations may produce micro-relief features such as contraction fissures or salt expansion ridges.

The lakes that previously occupied many playas formed during cooler wetter periods of the Pleistocene epoch. These periods have been termed "pluvials." The synchroneity of glacial with pluvial stages has been demonstrated in the United States by Russell (1889) at Mono Lake, by Gilbert (1890) for ancient Lake Bonneville, and by Antevs (1954) for New Mexico. Recently, Morrison and Frye (1965) have presented a comprehensive study which firmly establishes the synchroneity of the eastern part of the midwest United States glacial section with the C-14 dated sections from Lakes Bonneville and Lahontan. The concept of glacial-pluvial synchroneity is generally accepted, but it is periodically challenged by those who argue that precipitation was reduced in desert areas during periods of glacial advance. Flint (1947, p. 469) has pointed out that this argument assumes a closed atmospheric system and ignores the fact that Pleistocene glacial climates were characterized by intensified wind activity over the then still extensive ocean surfaces.

Pluvial lakes occupied many closed depressions within several of the present desert areas of the earth. These lakes reflected climatic change characterized by a higher precipitation/evaporation ratio. Ahnert (1960, p. 140) has pointed out that these lakes did not indicate the nature of the pluvial regimen, that is, the type and distribution of the Pleistocene pluvial rainfall. This information must be obtained from indirect evidence such as alluvial fills or buried vegetation which might suggest the seasonality of the pluvial rainfall.

There was a worldwide change in climate, with the consequent recession of the ice sheets and glaciers approximately 12,000 years before present (B.P.). The temperate zones became warmer and many of the desert areas became warmer and drier as a result of less precipitation and/or higher evaporation. The previously extensive pluvial lakes had marked their boundaries on the landscape by carving wave-cut cliffs, or depositing well-sorted beach gravel. These diagnostic features, when found today, merely establish that the "lacustrine playa" was occupied by a lake more extensive than the present boundaries of that playa. The absence of wave-cut cliffs and peripheral beaches may be the result of erosion or deposition, or a Pleistocene history of little or no pluvial lake expansion beyond the present playa boundary. In these latter cases, the stratigraphy of the playa deposits may provide the information required for genetic interpretation.

1.2 Purpose

The purpose of this study is to examine briefly Australian playas in order to compare them with similar features in the western United States and with playas in desert areas throughout the world. Because of their responsiveness to environmental changes, playas are significant indicators of climatic change and have been used for this purpose by Leopold (1951), Broecker and Orr (1958), and Reeves (1966).

1.3 Scope

The field work in Australia was conducted from 1 June to 14 July 1967, and consisted of ground investigations at seven playas. In Western Australia observations and sample collections were made at Lakes Austin, Carey, and Raeside; in South Australia similar studies were made at Lakes Gairdner, Harris, Torrens, and Frome. See Figure 1. An aerial reconnaissance was made of Lakes Frome, Eyre, and Torrens; and Lake George in New South Wales, an actual lake that is periodically desiccated, was visited.

Representative samples have been subjected to X-ray diffraction analysis of their clay minerals and light-mineral constituents. Both light and heavy minerals have been analysed qualitatively and quantitatively by optical methods. All samples have been described as to their relative particle size and salt constituents, and fossil identification has been made in several samples.

1.4 Previous Knowledge

Lake Eyre, one of the largest salt playas in the world, was investigated by Johns and Ludbrook (1963) in connection with a study of evaporites and brines. They concluded that the salts derived from "oceanic sources transported to the present situation through the agency of wind and an internal drainage system." The historical development of the lake is summarized as follows:

1) Lacustrine sedimentation in Lake Dieri (ancestral Lake Eyre) was more or less continuous from Cretaceous to early Tertiary.

2) Duricrust formation was followed by folding in the basin sediments, with rupture along well defined lineaments in the marginal areas.

3) Humid conditions prevailed in late Tertiary.

4) During the Pleistocene, the onset of aridity and the cutting off of outlets to the ocean resulted in reduction of the lakes in this region to playas, and the large lake to tributaries to intermittent creeks. The giant marsupials, such as diprotodon, became extinct.

5) Shallow brackish water sedimentation terminated approximately 40,000 years ago at the site of Lake Eyre.

6) Desiccation and the development of an extensive sand dune desert was accompanied by deflation. The floor of present Lake Eyre, 60 ft (18 m) below sea level, dates back some 20,000 years.

7) Modern lake sediments, 10 to 15 ft (3 to 4.5 m) thick over the surfaces of the large southern bays of Lake Eyre (North), generally consist of gypsiferous silt with a salt crust.

From a study of Lake Torrens, Johns (1964) drew the following conclusions:

The depositional basin originated in early Tertiary and there have been no subsequent marine incursions. The basin has gradually subsided accumulating almost 1,000 ft (300 m) of fresh-water lacustrine sediments. Evaporite sequences suggest a closed lake during arid intervals.

Lake Gairdner was studied by Johns (1966), who reached the following conclusions:

1) The lake extended gradually westward during the Quaternary and accumulated an alternating sequence of salt and windblown sands.

2) The upper sediments contain up to 80 percent gypsum, and are underlain by sands. Halite, common throughout the sequence, forms a crust over most of the lake surface. Detrital quartz is a major component of the lake sediments, and calcite, kaolinite, pyrite, and limonite are constant minor constituents throughout.

3) Composition of the lake brines reflects origins from sea water, but the potash content of the brines is lower than that of sea water. Available potassium contents show a range from 0.28 percent to 0.74 percent as compared with 1.1 percent for sea water.

2. DISTRIBUTION AND ENVIRONMENT OF AUSTRALIAN PLAYAS

2.1 Clay- and Silt-Floored Playas

Silt- or clay-floored playas are widely distributed, being most common in the southern part of Western Australia and in South Australia. These surfaces occupy approximately 20,000 square miles. Virtually all of the areas are in part silt or clay floored. On maps, the larger playas are generally identified as lakes, dry lakes, or salt lakes, and the smaller ones as claypans. Frequently these different terms are used arbitrarily in identifying playas that are identical in practically all respects. Similarly, the symbols by which playas are shown on maps include solid blue water tints, swamp and marsh symbols, cross-hatched symbols representing intermittent lakes, brown dots representing sand, and open areas without a symbol. Gregory (1914, p. 657-658) points out that the lakes of Western Australia are not lakes, but a series of salt claypans, and although their usually waterless condition is well understood, their title of lakes is too firmly established to be displaced. According to David (1950, p. 40-41) the name salt lake is also really a misnomer, since they are normally dry and they never contain any but very thin deposits of salt.

David reported (1950, p. 40-41) that there are almost 200 known salt lakes, which range in area from a few acres to 1,200 sq. miles, and which he describes as follows: "The floor of a lake may be of solid rock, extraordinarily smooth and level; sometimes this is covered with a thin layer of sand and silt, and exceptionally the detritus extends down to very considerable depths, as in Lakes Cowan and Dudas. In the former a bore passed through 277 feet of silt."

Waite (1917, p. 418) has stated that "claypans, . . . though extremely boggy in wet weather, dry with such a hard surface that foot of man or hoof of horse leave little or no impression." Madigan (1945, p. 133) describes the small claypans east of Lake Eyre as being "of all sizes and shapes from round ones a mile across to narrow ones 20 miles long, occur[ring] sporadically in this

undulating sea of sand . . . The floors are absolutely flat sand-free clay surfaces, of a buff colour. They were at times rather boggy, but during droughts, when the surface is crusty and gypseous, they can be crossed by motor vehicles. It appears that the eddies caused by the depression, together with the smoothness of the floor, keep the floors swept clean of sand."

2.2 Salt-Encrusted Playas

Salt crust, characteristic of some playas and formed by the evaporation of flood water or of ground water, may range in thickness from a fraction of an inch to at least 18 inches. The salt crust is commonly thickest in the lowest part of the playa, but a patchy appearance is common over the entire surface. The playa surfaces are so nearly flat and so large that a particular flood will not necessarily cover the entire lake floor. The distribution of salt may then depend on where the wind happened to blow the last remaining sheet of salt water before it evaporated (Madigan, 1944, p. 155).

In many places, such as on Lake Dora, the salt crusts are a smooth safe surface for a vehicle. Bonython (1956, p. 69) said that a jeep, having reached the thick salt crust of Lake Eyre (North), by running over planks laid on the soft lakebed where the gap between the land and the salt was narrowest (near Prescott Point), was able to travel at 40 mph on a smooth surface, most of which was as firm as concrete.

The water table is generally very close to the surface and beneath the salt there is commonly a thick layer of soft clay containing gypsum crystals and saturated with brine. This would afford little support to the salt crust which would probably act somewhat like a layer of ice floating on water. A few lakes, for example, Lake Macdonnell, as measured in 1921, are known to have had salt crusts up to 17 in. thick. There is no definite information about lakes having thicker crusts.

2.3 Rock-Floored Playas

The area in which rock is actually exposed at the surface probably constitutes at most a small percentage of the surface of the rock-floored playas, and is most commonly along their western margins. Commonly there are extensive areas of rock floor covered by a thin layer of silt or clay, the thickness of the surficial cover increasing toward the east. The water table generally lies at shallow depths beneath the surface so that the unconsolidated cover is commonly moist. The distribution of rock floors on Lake Goongarrie has been mapped in considerable detail by J. T. Jutson. A description of Lake Goongarrie playa follows and may exemplify the conditions that exist on parts of other playas.

Lake Goongarrie, in Western Australia, is located at lat 30°02'S., long 121°13'E. The playa, which is 11 miles long and covers an area of about 50 sq miles, is situated about 1 mile east of the railway between the towns of Comet Vale and Goongarrie, in the North Coolgardie Goldfield.

The rock floors of the playa occupy a considerable area of its western part, and can be traced for a mile from west to east. They are either devoid of detritus, possess a mere film, or are covered by 2 or 3 in. of fine silt. Jutson (1918, p. 120-123) has described the microrelief in this way: "In places [the rock floors] are slightly furrowed, along the strike of the rocks, but this does not destroy the 'billiard table' character of the floors. The actual plane of the surface may be slightly inclined or undulating, but precise levelling is needed to determine the directions of slope. So horizontal, however, are some of the rock surfaces that when rain falls (unless it be long continued) it simply rests on such surfaces without flow. . . . the occurrence of the bare rock floors [is] most striking, . . . possessing the appearance of having been recently swept by a gigantic broom."

The playas specifically studied in this paper are shown in Figure 1.

2.4 Climatology

2.4.1 WEATHER CYCLE

Temperate Australia is characterized by a steady succession of anticyclones belonging to the great subtropical belt. Traveling from west to east they move at an average rate of 500 miles a day. Wedges of lower pressure between these anticyclonic cells are extensions from the equatorial belt in the north and the temperate low-pressure belt in the south.

The northerlies which blow ahead of the low-pressure troughs during the warmer months in southern Australia, carry intensely hot and dry air from the desert interior. The southerlies or southwesterlies which displace them originate over a cool ocean and are consequently cool and moist. Their influence can be felt 150 to 200 miles inland (Australia, CSIRO, 1960, p. 22), and they are often associated with rain during the winter. The spring months may include a few very hot days.

2.4.2 TEMPERATURE

The summer is warm to hot and maximum temperatures above 100°F are common in inland Australia. The winter is warm in the north but the temperature falls at higher latitudes.

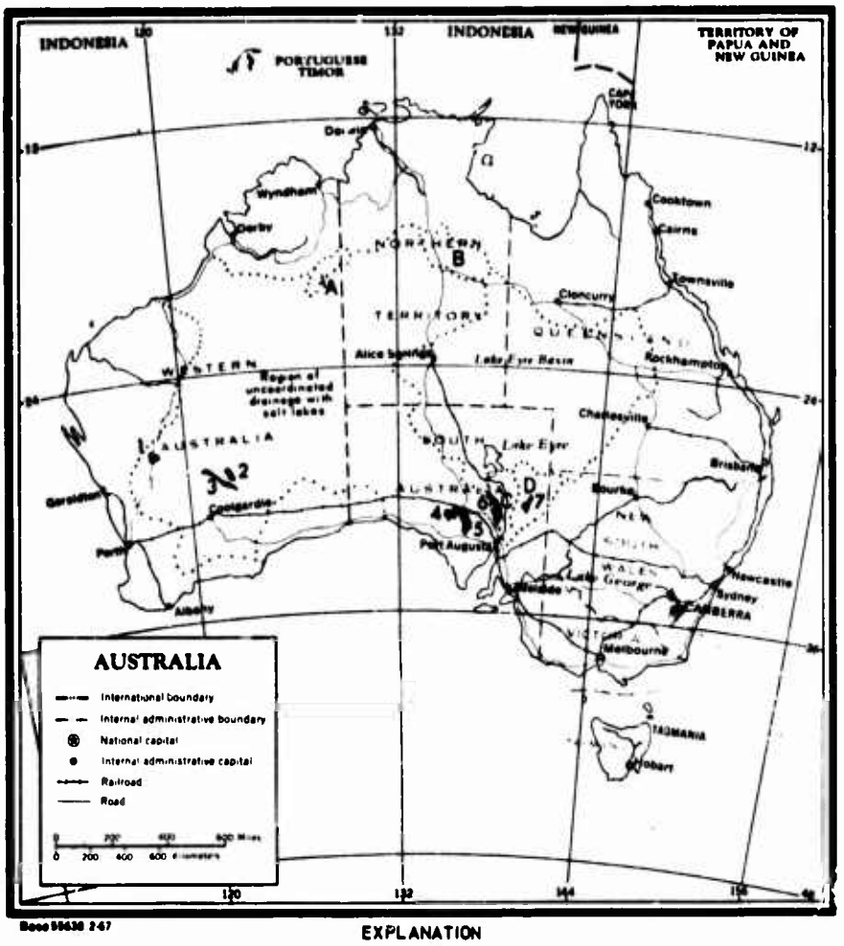

Figure 1. Location of Playas and Drainage Basins

2.4.3 PRECIPITATION

Figure 2 indicates that the wetter areas are confined to the coastal strips and to the mountains of the southeast and east. During the summer (Figure 3), a monsoonal low-pressure area forms over the intensely heated northern part of Australia and the associated rain reaches close to the Tropic of Capricorn, diminishing in amount from north to south. South of the tropic it is dry. During the winter (Figure 4), the high-pressure belt dominates the tropic and the north is dry, while the south receives regular rain associated with the temperature

low-pressure belt. The amount of this rain gradually diminishes inland. In South Australia, the north-south ranges cause relatively heavy rain on the western slopes and rain shadows to the east. The desert zone lies too far away from the tracks of the rain-bearing storms to benefit regularly either in summer or in winter. Erratic rainfall and drought are recurring events over much of Australia. The map of variability (Figure 5) is plotted as the mean deviation percent of the average rainfall. Variability increases inland and northward. Figure 6 shows the departure of Australian annual mean rainfall variability from world mean variability.

3. GEOLOGIC CHARACTERISTICS OF SEVEN PLAYAS

3.1 General Geology

The southwestern part of Western Australia which includes Lakes Austin, Carey, and Raeside (Figures 7 and 8) is underlain by granite and gneiss, part of the Archean basement of the continent. The granite and gneiss form plains traversed by folded belts of metamorphosed sedimentary rocks in hills up to 150 m high, and of greenstone in lower, more rounded hills (Mabbutt, 1961, p. 101). Alluvium covers 40 percent of the area. The erosional land surface consists of an upper surface with a fossil laterite, termed the Old Plateau (Jutson, 1934, p. 96-96), and a lower surface, generally eroded between 25 and 75 ft below, termed the New Plateau. The laterite is generally interpreted as having formed under a humid climate on a broadly undulating plain which was uplifted in the late Tertiary to form the interior plateau of Australia (Woolnough, 1927, p. 25-26). The laterite is considered to be of early to middle Tertiary age. The New Plateau erosion cycle was initiated by the uplift, but was subsequently affected by the change to a drier climate. Widespread local alluviation occurred during the early stage of desiccation. Increasing aridity later resulted in eolian reworking of the sandy lateritic solls of the Old Plateau to form sand plains (Mabbutt, 1961, p. 102).

Lakes Torrens and Frome (Figure 9) occupy part of a geosynclinal belt which extends 800 km from the Lake Eyre depression to the Southern Ocean. Sediments which were deposited in the geosyncline during the Precambrian and Cambrian were metamorphosed, in part to massive beds of quartzite. These resistant beds dominate the landscape as hills up to 300 m above the adjacent plains and valleys (Twidale, 1967, p. 95). The faulted and slightly compressed strata have been subjected to several subsequent cycles of erosion during which structures in the resistant strata have been etched out. An undulating erosional

Figure 2. Annual Mean Rainfall (In.)

Figure 3. January Mean Rainfall (In.)

Figure 4. July Mean Rainfall (In.)

Figure 5. Percentage Mean Variability from Annual Mean Rainfall

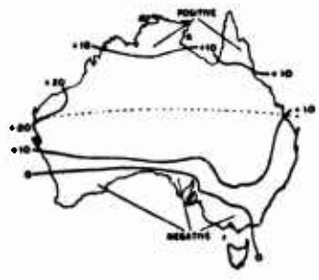

Figure 6. Departure of Australian Annu Mean Rainfall Variability from World Mean Variability

(From Commonwealth Scientific and Industrial Research Organization of Australia

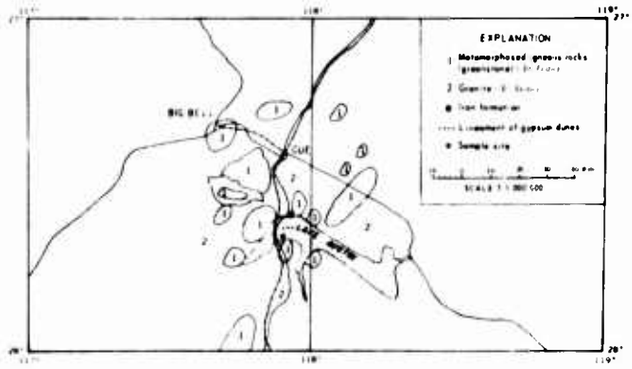

Figure 7. Geologic Map of Lake Austin

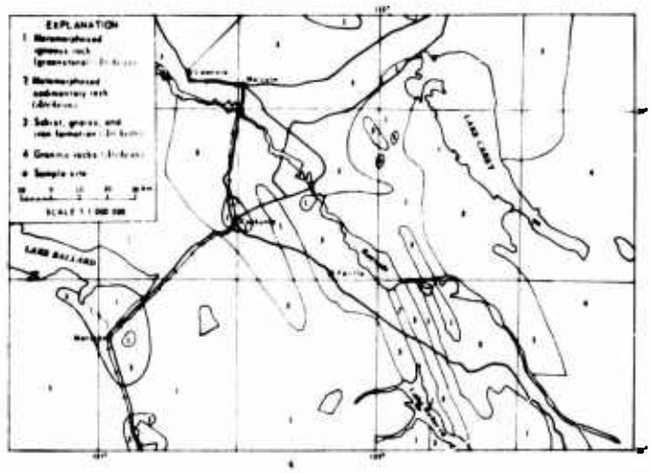

Figure 8. Geologic Map of Lakes Raeside and Carey

surface truncates the bedrock structure and cuts across lacustrine sediments of Triassic age. Below this high surface are remnants of a system of old valley floors and piedmont plains eroded across the less resistant argillaceous sediments between the quartzites. These ancient valley floors, which are younger than the high level surface and probably of mid-Tertiary age, have been dissected and in many districts all but removed. New plains of erosion have developed in many valleys and basins. There are thus three erosional surfaces represented in the area dominated by the Flinders Ranges.

Lakes Harris and Gairdner are partly surrounded and underlain by rhyolite, and quartz-feldspar prophyries (Figure 10). Because of the numerous rock-cored

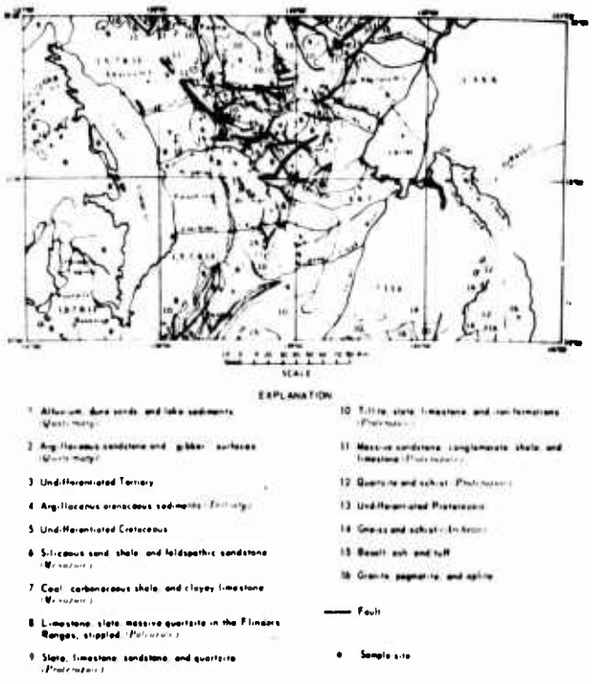

Figure 9. Geologic Map of Lakes Torrens and Frome

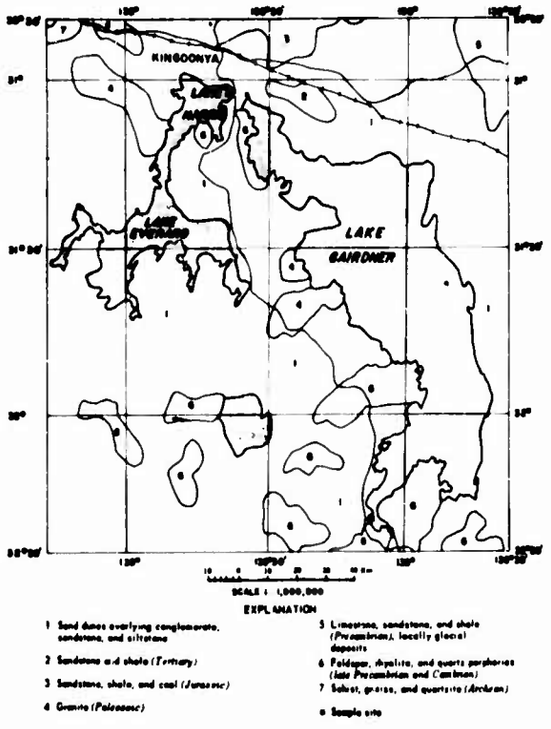

Figure 10. Geologic Map of Lakes Harris and Gairdner

islands, it is reasonable to assume that the lake deposits are relatively shallow (Johns, 1966, p. 7). The porphyry has a strong rectilinear joint pattern northeast-southwest and northwest-southeast. Erosional widening along major joints has resulted in broad, flat-bottomed, alluvium-filled valleys. Red loam flats and sand plains extend from the shores to low rounded hills around the lakes. Stony tableland remnants to the north of Lakes Harris and Gairdner are the approximate boundary of the shallow marine transgression of the Mesozoic. The tableland is formed of siltstones, boulder beds, and gravels with a duricrust surface.

3.2 Surface Hydrology

Lakes Austin, Carey, Raeside, Harris, and Gairdner belong to the "region of uncoordinated drainage with salt lakes." See Figure 1. There are no permanent streams and the intermittent streams flow only after a heavy rain, their waters being quickly dissipated in the plains. Jutson (1934, p. 98) describing the salt lakes in "Salinaland," a subdivision of the region of uncoordinated drainage, has stated, "They are usually found along and in fact constitute the main drainage lines of the division; and they may be a few hundred yards or several kilometers wide (using this term where the length is much greater than the width) or in diameter (if the lake is more or less circular). The lakes may be isolated, but in some places they are strung loosely together, with divisions of varying width. They are usually dry, but after a heavy rain, a thin sheet of water may spread over their surfaces. Unless, however, the rain be continued, the water evaporates with extraordinary rapidity, leaving a deposit of salt and usually of gypsum on the floors of the lakes."

Lakes Torrens and Frome (Figure 1) are centers of independent basins of interior drainage. The environment is similar to those of the lakes within the region of uncoordinated drainage, but their evolution has been different.

3.3 Stratigraphy and Mineralogy

Playa sediments were collected at six playas from dug pits and/or auger holes up to 1.9 m deep, 100 m from the shore (Table 1). The samples were processed to determine moisture content and percentage by weight of soluble salt. Eleven of the clay samples, representative of each playa, were examined by X-ray diffraction before moisture determination to insure that no endellite was present, All of the clay samples were then analysed by X-ray diffraction. The heavy minerals were separated from the > 200-mesh fraction with bromoform, and the mineralogy was determined.

Table 1. Data from Playa Samples

Sample	Location	Moisture content %	Soluble-salt % by weight	Total sample <200-mesh fraction	Total sample >200-mesh fraction	Detrital material (gypsum & salt removed) <200-mesh fraction	Detrital material (gypsum & salt removed) >200-mesh fraction
1	Austin	25.00		54.0[2]	46.0	100.0	
2	Austin	18.7[1]	11.6	27.1	61.3[3]	100.0	
3	Austin	14.0[1]	9.7	59.0	31.4	83.7	16.3
4	Carey	15.8	8.7	62.1	29.0	68.3	31.7
5	Carey	16.2	11.4	71.7	17.0	80.8	19.2
6	Carey	16.7	7.8	79.4	12.8	86.1	13.9
7	Carey	22.5	6.6	77.6	15.8	83.0	17.0
8	Gairdner	18.3	10.8	23.8	65.4	34.4	65.6
9	Gairdner	22.2	9.8	39.2	51.0	43.4	56.6
10	Gairdner	16.7	7.8	37.4	54.9	40.5	59.5
11	Harris	26.8	9.4	67.1	23.6	76.4	23.6
12	Harris	30.6	13.5	74.8	11.7	86.5	13.5
13	Harris	17.1	6.1	26.5	67.4	28.2	71.8
14	Harris	19.8	5.4	27.9	66.8	29.5	70.5
15	Torrens	23.5	5.0	39.7	55.4	61.6	38.4
16	Torrens	29.8		63.0[2]	37.0[3]	99.4	0.6
17	Torrens	26.3	4.7	52.0	43.2	54.8	45.4
18	Torrens	22.6	4.9	38.8	56.3	40.8	59.2
19	Frome	2.0	2.4	trace	97.6	trace	100.0
20	Frome	24.1	5.2	78.4	16.4	82.7	17.3
21	Frome	16.9	6.0	24.4	69.6	26.0	74.0
22	Frome	15.1	5.2	12.4	82.0	13.2	86.8
23	Frome	17.5	5.6	19.6	74.6	20.9	79.1

1 Leakage of the container - the moisture contents here are the partial moisture contents, not true moisture contents - probably close to No. 1.

2 Soluble salts included.

3 Almost all gypsum crystals.

Estimates of the clay minerals were made on X-ray diffractograms, by comparing relative intensity as reflected in the area under the peak. Optical point-counting was used for the mineral constituents of the > 200-mesh fractions. Only 100 to 500 points were counted for each sample, and so the percentage figures are only indicative of the true composition. The Wentworth scale (Krumbein and Pettijohn, 1938, p. 80) is used in this study.

Because considerable rain fell 2 to 3 weeks before sample collection on the playas, the sediments were sticky and wet. In spite of disparate geographic locations, these wet conditions were comparable at all sites.

The percentage of moisture, the percentage of soluble salts, total > 200-mesh fraction and < 200-mesh fraction, and > 200-mesh fraction and < 200-mesh fraction with gypsum and salts removed are listed in Table 1. The descriptions of the several playas are treated separately. Samples from Lake Raeside were not processed because of unavoidable mixing during collection. They were from the same geologic province as the samples from Lake Carey and had similar topographic relationships.

3.3.1 LAKE AUSTIN

Lake Austin is close to the divide between the interior basins of uncoordinated drainage and the Indian Ocean drainage.

The lake is elongated east-west (Figures 7 and 11). There is a low ridge about 10 m high of bare rock composed of folded, lean iron formation at the middle part of the north bank, and a low, elongated gypsum dune on the south bank. A section of the dune is cut by the highway from Magnet to Cue (Figures 12, 13, and 14). A very low gypsum dune 3 to 7 m high with an east-west trend forms an island in the middle of the playa.

Descriptions and analyses of the Lake Austin samples are given in Table 2. The three samples show that the lake sediments above the water table are composed principally of chemical precipitates and a very minor amount of fine red clay (Figure 15). The > 200-mesh fraction of Samples 1 and 2 is almost entirely gypsum of sand size. The gypsum grains become finer upward from the coarse scaly gypsum crystal layer. Only the > 200-mesh fraction of Sample 3 was examined with the microscope. See Table 2. The quartz grains are rather angular with rich inclusions, commonly wavy extinction, and some well-developed platy structure, indicating that they are probably principally derived from metamorphic rocks. Some of the grains which were coated with needles of gypsum may have been counted as gypsum.

3.3.2 LAKE CAREY

Lake Carey is bounded at its north shore by cliffed knobs (Figures 8 and 16) composed of iron formation and rising 50 to 75 m above the playa surface. The playa sediments are rather thin, overlying gravel below the cliffs or resting directly on bedrock farther from the shore (Figure 17). Description and analyses of Lake Carey samples are listed in Table 3. Sample 7, the bottom sample at the site, is actually a yellowish-white siltstone 46 cm below the surface of the playa. Some dunes are still active along part of the shore (Figure 18) or on the playa. They are composed of quartz sands.

Figure 11. Flooded Lake Austin Crossed by a Causeway. View north-northwest, 21 May 1967.

Figure 12. Road Cut through a Dune of Gypsum Sand. Beds dip south; dune trends east-west. View west, 21 May 1967.

Figure 13. Case Hardened Surface of Gypsum Dune with Polygonal Patches. Cracks between polygons are filled with later efflorescent gypsum crystals derived from capillary movement of solutions along cracks, 21 May 1967.

Figure 14. Flooded Lake Austin. View northwest from gypsum dune south of the lake, 21 May 1967.

Figure 15. Small Domes and Buckles in the Gypsum-Salt Crust Caused by Crystallization Expansion during Evaporation of Saline Solutions along Polygonal Cracks below the Crust, 21 May 1967.

Table 2. Description and Analyses of Lake Austin Samples

Pit section east of highway

Sample	Depth (cm)	Description
	0 - 0.5	White salt crust (5 YR 8/1) slightly effervescent with dilute HCl
1	0.5 - 7.6	Red gypsum crystals (2.5 YR 4/6), sand size
	7.6 - 22.9	Reddish-brown silty clay
2	22.9 - 35.6	Reddish-brown moist silty clay with medium-grain gypsum crystals
	38.1 - 40.6	A layer of crowded gypsum crystals in black mud of uniform 3 mm size having a bi-convex tabulated crystal habit; they are translucent white very similar to fish scales; not effervescent with HCl
	45.7	Water table
3	50.8 - 63.5	Wet, reddish-brown clay

Estimated Clay Mineral %

	Sample 1	Sample 2	Sample 3
Kaolinite	100.0%	47.4%	43.9%
Montmorillonite	0.0	28.3	0.0
Illite	0.0	24.4	40.9
Chlorite	0.0	0.0	15.2
	100.0	100.1	100.0

Sample 3: > 200 mesh fraction

Sp. gr. < 2.8 (light minerals)	
Gypsum	63.7%
Quartz	30.9
Manganese or manganese stained spheroids	1.6
Plagioclase	1.4
Potash feldspar	2.4
	100.0

Sp. gr. > 2.8 (heavy minerals)	
Opaques (magnetite)	48.9%
Hematitic and mostly limonitic opaques	35.1 (reddish felted granules)
Green amphibole	9.7
Biotite	1.4
Celestite	5.0
	100.1

Figure 16. Lake Carey from a Knob Containing Iron Formations Approximately 50 Meters above the Playa Surface. View south, 22 June 1967.

Figure 17. Polygonal Cracks in Soft Clayey Silt near the Lake Carey Sample Site (Samples 4, 5, 6, and 7), 100 Meters South of the North Shore, 22 June 1967.

Figure 18. Vegetation Partly Buried by Active Sand Dunes along the North Shore of Lake Carey. View south, 22 June 1967.

Table 3. Description and Analyses of Lake Carey Samples

Pit Section

Sample	Depth (cm)	Description
	0 - 1	Pinkish-white 5 YR 8/2 salt crust
4	5 - 6	Dark reddish-brown silty clay (2.5 YR 3/4)
5	10 - 11	
	20 - 21	Dark reddish-brown clay with manganese mottled stain structure. Manganese stains increase downward.
6	30 - 31	
	31 - 33	Light yellowish-brown silty clay (2.5 Y 6/4)
	45.7	Water table
7	46	Yellowish-white siltstone

Estimated Clay Mineral Percentages

	Sample 4	5	6	7
Kaolinite	62.2%	41.0%	38.1%	29.1%
Illite	16.2	20.8	23.0	0.0
Chlorite	21.6	38.2	38.8	0.0
Montmorillonite	0.0	0.0	0.0	70.9
	100.0	100.0	99.9	100.0

Light-mineral (Sp. gr. < 2.8) Composition of > 200 mesh fraction

	Sample 4	5	6	7
Quartz	82.0%	85.8%	91.0%	7.9%
Clay-coated fragments and rocks	12.0	5.2	2.1	0.0
Manganese grains and spheroids	3.0	1.8	3.7	0.0
Plagioclase	1.5	2.2	1.1	1.8
Potash-feldspar	1.5	4.9	1.6	1.2
Claystone rock fragments	0.0	0.0	0.0	75.6
Siltstone rock fragments (up to 20 mm in diameter)	0.0	0.0	0.0	13.4
	100.0	99.9	99.5	99.9

The quartz grains derived from metamorphic rocks show wavy extinction and platy structure; those in Sample 4 are smaller in average grain size (silt-very fine sand) and are heavily coated with clayey materials. Samples 5 and 6 are cleaner, well sorted, rounded, and coarser (fine sand). Some quartz grains contain numerous inclusions and some contain none, but those not strained are probably hydrothermal in origin. Sample 7 is actually partly weathered bedrock. The heavy minerals of the four samples are almost all composed of magnetic iron-ore fragments probably derived from the nearby iron formation. There is only a very small trace of well-rounded zircon. A needle-shaped, colorless, well-preserved prism of celestite is the only heavy mineral found in Sample 6.

3.3.3 LAKE RAESIDE

Samples from Lake Raeside (Figures 8 and 19) were significantly mixed during collection by auger, because they were wet and sticky. For this reason and because of similarities in the geology and topography of Lakes Raeside and Carey, samples from Lake Raeside were not processed.

3.3.4 LAKE GAIRDNER

Lake Gairdner lies in an elongated northwest-southeast depression which is separated from Lake Torrens by the Andamooka Range and Arcoona Plateau (Figure 10). The playa is underlain by rocks of the Archean basement, similar to those of Western Australia. There is higher local relief adjacent to gibber plains (stony deserts) and an extensive rhyolite formation along the south and southwestern shores. Iron formations and rhyolite were gently folded, forming ridges and knobs which stand above the less resistant schist and gneisses of the crystalline basement rocks.

The samples (Table 4) were taken 0.8 mile west-northwest of the southern tip of the lake (Figure 20). The surface was covered with a thin white crystalline gypsum-salt crust (Figures 21 and 22). Recent water marks near the shore were composed of two parallel lines of scum formed by dead insects.

The quartz grains of the three samples are mostly well rounded, but some are poorly rounded. The angularity of the rhyolite grains and the large quantities of large-grain opaque particles occurring in the heavy-mineral fractions indicate that these are locally derived. The well-rounded quartz grains, zircon, and rutile must have been of multicycled origin.

The > 200-mesh fractions are very fine sand. The clay fractions of the samples are very poor in clay minerals; only a very insignificant peak of the (001) of kaolinite indicates the presence of this mineral in all three samples. Under the petrographic microscope, the samples show numerous line and quartz particles and the kaolinite present is probably in the > 10 percent range. The

Figure 19. Partly Vegetated, Wet, Clayey-Silt Sediments at Lake Raeside. View southeast, 23 June 1967.

Table 4. Description and Analyses of Lake Gairdner Samples

Pit Section

Sample	Depth (cm)	Description
	0 - 0.5	White crystalline gypsum-salt crust
8	0.5 - 1.5	Partly manganese-stained red silty sand with salt
9	1.5	
	9 - 11	Red silty sand
	16 - 18	
	18	Water table
10	18 - 21	Compact or semi-indurated red silty sands

Sample 8: Mineral Composition of > 200 mesh fractions (Sample 9 & 10 Similar)

Light minerals (Sp. gr. < 2.8)		Heavy minerals (Sp. gr. > 2.8)	
Rhyolitic rock fragments*	55.3%	Opaques	93.8%
Quartz	38.1	Leucoxene and earthy nonoxides grains	10.4
Carbonate (calcite or dolomite?)	2.4	Zircon	2.9
Plagioclase	1.4	Rutile	0.4
Potash-feldspar	0.6	Others	2.5
Other rock fragments: slate or claystone	1.1		
	98.9		100.0

*Some fragments made up of feldspar or largely of feldspar were counted as rhyolitic rock fragments.

Figure 20. Southwest Embayment of Lake Gairdner from 3-Meter-High Hill along Southwest Shore. View east, 30 June 1967.

Figure 21. Salt Crust 0.5 Centimeter Thick with Weakly Developed Polygonal Pattern Overlying Soft, Moist, Red Silt in Southwest Embayment of Lake Gairdner. View southeast, 30 June 1967.

Figure 22. Sample Site (Samples 8, 9, and 10) in Southwest Embayment of Lake Gairdner. Salt crust 0.5 centimeter thick overlying soft, moist, red silt, 30 June 1967.

rich lime in the fine-clay fraction was probably redeposited from the white chalky bottom of small playas developed between the sand dunes in the surrounding area. These between-dune playas are generally small. The flat limy bottom is hard and generally devoid of any vegetation except some of the salt-resistant pig grasses.

3.3.5 LAKE HARRIS

Lake Harris is the northern part of an irregularly shaped playa whose southern extension is called Lake Everard. Lake Harris is almost in the same trend and can be regarded as the northwest extension of Lake Gairdner, but the two are separated by a low land bridge with occasional low isolated hills interspersed with gibber plains and sand flats.

Unlike the southern end of Lake Gairdner where the area surrounding the lake is composed of gibbers (pebbles) and solid bedrock, the shore area of Lake Harris is entirely dunes, mostly covered by vegetation (Figures 10 and 23). The section of the sample pit (Table 5, Figure 24) is as follows: The sediments of the top half-meter are sandy silt which contains a very small percentage of gypsum crystals about 1 mm to as large as 3 mm in diameter, having a bi-convex, flat disc-form crystal habit. The sands are generally subrounded but range from very angular to very well rounded indicating both fluviatile and eolian origins. Samples

Figure 23. Low, Active Sand Dunes along Northeast Shore of Lake Harris. View west, 1 July 1967.

Figure 24. Wet, Red Clayey-Silt Sediments at Sample Site (Samples 11, 12, 13 and 14) 50 Meters from Northeast Shore of Lake Harris. View west, 1 July 1967.

Table 5. Description and Analyses of Lake Harris Samples

Pit Section

Sample	Depth (cm)	Description
11	0 - 5	Reddish-brown sandy silt, gypsiferous, to depth of 45 cm
12	30 - 35	
	46	Water table
13	121.9 - 137.2	Brownish-red coarse sediments, from 46-198 cm depth
14	182.9 - 198.1	

Size Analysis

Sample	Depth (cm)	% of Total Sample Passing > 20 Mesh
11	0 - 5	trace
12	30 - 35	6.5
13	121.9 - 137.2	18.6
14	182.9 - 198.1	34.8

Estimated Clay Mineral %

	Sample			
	11	12	13	14
Kaolinite	28.8%	45.2%	27.7%	27.8%
Illite	26.9	42.9	72.3	72.2
Montmorillonite	44.2	11.9	0.0	0.0
	99.9	100.0	100.0	100.0

> 200 Mesh Fractions

Light Minerals (sp. gr. < 2.8)

	Sample		
	11	12	13 & 14
Quartz	68.2%	86.0%	85 - 90%
Gypsum	18.3	0.2	est. 1
Rhyolitic rock fragments	13.5	12.3	10 - 15
Plagioclase	0.0	0.4	1 - 3
Potash-feldspar	0.0	0.4	1 - 3
	100.0	99.3	

Heavy Minerals (sp. gr. > 2.8)

	Sample	
	11	13
Opaques	21.1%	60.2%
Iron cutan	10.0	13.4
Yellowish needles in felted speroids (probably some sulfate)	15.9	0.0
Amphibole	3.1	0.0
Biotite	trace	0.0
Tourmaline	0.6	0.0
Zircon	trace	15.6
Rutile	2.3	8.6
Monazite	0.0	0.5
Kyanite	0.0	0.5
Celestite	47.0	0.0
	100.0	98.8

13 and 14 are considerably coarser with grains up to 5 mm in diameter or granules and are probably derived from coarse granitic rocks. On the whole, the sediments become coarser with depth, and also with the increase of percentage by weight in the > 200-mesh fractions. See Table 1. The heavy minerals of Samples 12 and 14 are very similar to those of Sample 13. There are also similarities between the heavy minerals of Lake Harris and those of Lake Gairdner.

Four types of origin are proposed for these heavy minerals:

1) Some are authigenic. The celestite and surrounding sediments are particularly rich in gypsum. They contain long needle-shaped, perfect crystal prisms terminated with a dome, which are too delicate to have been transported with the sediments.

Those transported with the sediments came from three sources:

2) Heavy minerals derived from redeposited broken iron or manganese films, called cutans (Brewer, 1960), formed under arid conditions, were precipitated from iron, manganese, or alumina-bearing pore solutions along exposed surfaces, such as cracks or vugs, in unconsolidated or semiconsolidated sediments. They are probably similar in composition and origin to the desert varnish on the gibbers.

Cutans occur in all the heavy-mineral fractions of the Lake Harris sediments. They are peculiarly magnetic; very thin films exhibit delicate laminations in red, dark brown, or even black. The sooty black cutans are rich in manganese. They are too delicate to have been transported very far. In Sample 13, some cutans exhibit peculiar forms similar to microscopic australite in that highly polished glossy disc-shaped granules have concentric rings.

These peculiar forms may be explained as follows. The cutan begins as a soft plastic film with high water content. The highly glossy upper surface is impermeable and airtight. When it is baked by the sun, bubbles of steam are formed. Repeated cooling and heating of the surface creates a wrinkle in the cutan bubble, which eventually cracks, allowing the steam to escape. Alternatively, vugs that were first created by steam bubbles which escaped in the process of drying, may then be coated by cutan assuming the same shape as the bubble. The cutan was deposited from the pore solution in the mud surrounding the evaporation vug or pipe.

Since only the highly glazed cutan has these peculiar forms, the cutans may have formed in a very shallow depression where the water contained colloidal particles of iron or manganese oxides in colloidal clay. The clay was precipitated last to create the impermeable film. This would not explain how the elongated gas escape pipes were formed. But the theory is attractive because iron formation fragments without iron cutan constitute a very large part of the opaques of Lake Gairdner, which is relatively close to iron formation outcrops. Lake Harris is farther away from the iron formation outcrops and therefore the iron fragments, when introduced into this distant area, are colloidal in form. It is not known why the cutans are highly magnetic.

3) Heavy minerals derived from relatively younger formations are the green amphibole and biotite. They are not resistant to intense weathering or to attrition during transport, and they are probably of first cycle sedimentation origin.

4) Heavy minerals with a high order of persistence (Krumbein and Pettijohn, 1938, p. 516) derived from ancient rocks are the zircon, rutile, tourmaline, kyanite, and monazite. The mineral grains are very small, almost silt size, and extremely well rounded, some with highly polished surfaces. They are minerals of the Archean crystalline basement rocks and have experienced a multicycle sedimentation history.

3.3.6 LAKE TORRENS

Lake Torrens (Figures 9 and 25) occupies an Eocene sedimentary basin, the middle segment of the St. Vincent Gulf sunkland. The basin is formed by a broad downwarp of the upper Proterozoic clastics which include minor dolomite beds of

Figure 25. North End of Andamooka Island, West Side of Lake Torrens. Water-stained zone from recent inundation in foreground. View southwest from 700-meter altitude above playa, 15 June 1967.

Cambrian age. Since the Eocene, 300 m of lake sediments have been deposited (Table 6). The basement rocks of the basin are mostly gently dipping to flat lying. The upper Proterozoic rocks which crop out at its east margin form a range with 2,000-m relief. The steep bank of the west shore is composed of flat-lying bedrock believed to be the upthrown block of a fault or a series of step faults, as revealed by geophysical prospecting and drilling (Johns, 1964). The fault extends southward to Port Augusta and northward to the north end of the lake. The only surface evidence of the faults are the roughly aligned springs at the surface of the lake. The eastern convex shoreline is separated from the unfaulted Flinders Ranges horst by a vast, very gently sloping plain composed of alluvial fans and extensive gibber flats. A sloping sand plain of nearly east-west trend, containing old and active younger dunes, extends beyond the southern tip of the lake into Spencer Gulf, as the Port Augusta corridor. The basin is abutted on the north by terrain of high relief and an east-west ridge of Tertiary and Cretaceous sediments separates the lake drainage from that of Lake Eyre to the north.

The sediments collected from Lake Torrens are all fine silty sands with various amounts of gypsum crystals (Figure 26). The gypsum forms a hard solid crystal layer 7 cm thick having a 3-cm white layer of sand grains on top and a 4-cm layer of coarse crystals at the bottom. The sample descriptions and analyses are listed in Table 7.

Figure 26. Patchy Salt Crust Overlying Wet Clayey Silt at Sample Site (Samples 15, 16, 17, and 18) 30 Meters West of East Shore of Lake Torrens. Sand dunes along shore in background. View east, 2 July 1967.

Table 6. Lake Torrens Sediments (Johns, 1964)

Age	Thickness	Description
Quaternary*	54 ft	Brown, partly blue clays with sporadic gypsum crystals and thin beds of silt and sand
	43 ft	Gypsum sands with impure quartz grains
	137 ft	Brown silty clay, partly sandy
	27 ft	Red brown clayey sand with laminated silts
Tertiary		
Miocene	232 ft	Dolomitic sequence: pale gray-green to white mudstone with silty mudstone and breccia dolomites. The chief impurities are clays of halloysite and palygorskite. This sequence may be correlated with the 150-ft thick Miocene Stadunna Dolomite measured in a drilled section of Lake Eyre sediments.
Miocene	105 ft	Mudstone-siltstone sequence: upper 78 ft gray mudstone with lignitic fragments, occasionally dolomitic, mineralogically cherty fine-grained quartz and montmorillonite; top 13 ft also pyritic, dominantly of quartz with kaolinite and subordinate illite clays; lower 37 ft finely laminated lignitic silt-stone gradational at top from the above mudstone.
Lower or Middle Eocene	279 ft	Sand sequence: carbonaceous, gray-brown, fine- to coarse-grained quartz sands with mudstone beds. The well-preserved pollen indicates that lack of pollen above this horizon is due to shallow water and more oxidized conditions.

* In the upper part of the Quaternary section, the clay minerals are composed of kaolinite and illite with minor calcite. The lower part of the section contains kaolinite and dehydrated halloysite.

Table 7. Description and Analyses of Lake Torrens Samples

Pit Section

Sample	Depth (cm)	Description
	0 - 0.5	Gypsum surface crust
15	0.5 - 14	Light-brown gypsiferous sandy silt
	19 - 21	Hard, white compact gypsum sand
16	21 - 28	Dark-brown coarse gypsum crystal
	47	Water table
17	52 - 77	Reddish-brown silty sand from depth of 47-125 cm
18	113 - 125	

Light Minerals (sp. gr. <2.8), >200 mesh fraction

	Sample 15	16	17	18
Gypsum	58.0%	90.0%	trace	0.0%
Quartz	40.0	7.0	83.0%	84.0
Plagioclase	1.0	0.0	1.0	1.0
Potash feldspar	1.0	0.0	1.0	1.0
Siltstone or chert	2.0	0.0	5.0	10.0
Limestone or dolomite	0.0	0.0	10.0	4.0
Clay	0.0	3.0	0.0	0.0
	100.0	100.0	100.0	100.0

Estimated Clay Mineral %

	Sample 15	16	17	18
Kaolinite	22.0%	29.0%	20.3%	15.0%
Illite	18.1	54.8	25.4	25.0
Montmorillonite	59.9	16.1	54.2	60.0
	100.0	99.9	99.9	100.0

Heavy Minerals (>2.8 sp. gr.), >200 mesh fraction

	Sample 15	17
Opaques	20.1%	76.4%
Siderite	3.0	0.0
Epidote	2.0	3.4
Actinolite	trace	1.1
Muscovite	2.3	0.0
Biotite	0.8	0.0
Tourmaline	0.0	3.4
Zircon	1.4	trace
Rutile	0.2	trace
Barite and celestite	41.2	0.0
Celestite	0.0	15.7
Felted yellowish-red needle crystal aggregates	28.0	0.0
	99.0	100.0

3.3.7 LAKE FROME

Lake Frome occupies the southern end of a depression at the east side of the Flinders Ranges horst (Figures 9, 27, and 28).

Figure 27. West Shore of Lake Frome with Offshore Bars and Spits in Right Foreground. View southwest from 700-meter altitude above playa, 14 June 1967.

Like Lake Torrens, Lake Frome is separated from the Flinders Ranges by a wide strip of land composed of a piedmont talus-cone belt, an alluvial and gibber plain, and a wide belt of sand-dune-covered gibber plains (Figure 29). Similar plains stretch from the lakeshore eastward and southward. Northward Lake Frome merges with the Great Artesian Basin.

Descriptions and analyses of the Lake Frome samples are listed in Table 8. The > 200-mesh fraction of Sample 19 is fine-sand, two-thirds of which contains well rounded grains of eolian origin. The rest of Sample 19 is subrounded and subangular like the major part of the grains of Sample 20, which is of fluviatile origin, of smaller grain size, and rich in micas and fibrous vegetable matter. Sample 21, also similar to Sample 19, is a mixture containing a higher percentage of eolian sands. Samples 22 and 23 are almost entirely well-rounded eolian sands and therefore are probably old sand dune materials (Figure 30). The sands are clean and light-buff colored as compared with the brown to reddish-brown sands of Samples 21, 20, and 19, which are partly coated with iron oxides.

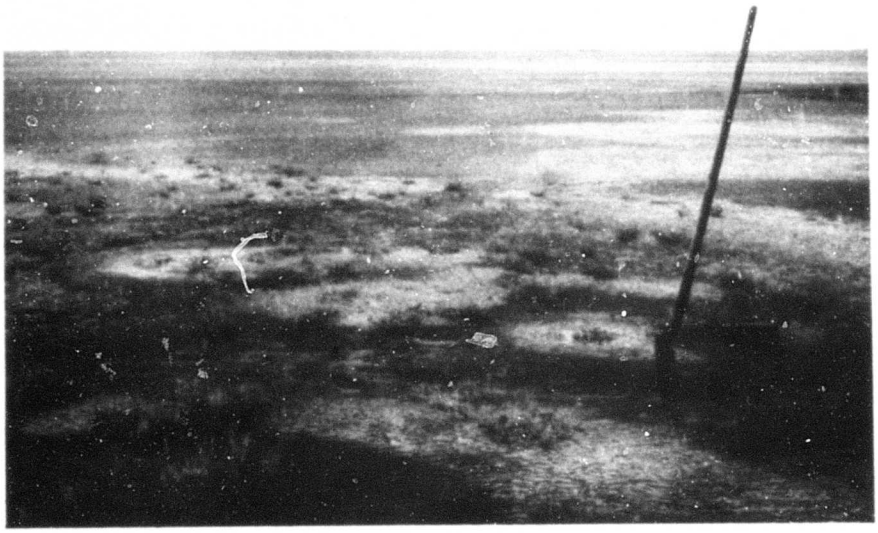

Figure 28. Ripple Marks in Silty Surface Sediments of Lake Frome at Site of Samples 19, 20, 21, 22, and 23. Lighter areas are slightly raised and drier, and thus are subjected to more eolian erosion. View southeast, 4 July 1967.

Figure 29. Active Sand Dunes along West Shore of Lake Frome, East of Balcanoona. View southeast, 4 July 1967.

Table 8. Description and Analyses of Lake Frome Samples

Pit Section

Sample	Depth (cm)	Description
19	0 - 7	Sand
20	7 - 34 29 - 34	Brown silty clay
	46	Water table
	46 - 51	Pebble-size gravel
21	66 - 76	Brown silty sand
22	100 - 112	Brownish-gray sand
23	149 - 159	Gravel

Estimated Clay Mineral %

	Sample 19	20	21	22	23
Kaolinite	14.9%	22.4%	24.5%	12.3%	10.0%
Illite	35.1	32.7	35.1	32.4	32.0
Montmorillonite	50.0	44.9	40.4	55.3	0.0
Chlorite	0.0	0.0	0.0	0.0	58.0
	100.0	100.0	100.0	100.0	100.0

Sample 19: >200-mesh fractions

Light Minerals (sp. gr. <2.8)		Heavy Minerals (sp. gr. >2.8)	
Quartz	87.3%	Opaques	70.9%
Siltstone fragments	11.1	Magnetite (octahedious)	8.4
Grayish greenstone, trace of reddish limestone or dolomite	0.9	Actinolite	0.4
		Tremolite	6.3
		Siderite	8.4
Plagioclase	0.3	Apatite	2.1
Potash-feldspar	0.3	Zircon	0.4
		Rutile	0.8
		Tourmaline	1.3
		Chlorite	0.6
		Biotite	trace
		Muscovite	trace
		Epidote	trace
	99.9		99.6

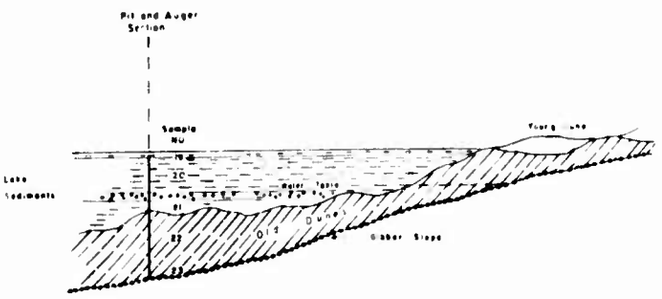

Figure 30. Sketch of the Possible Stratigraphic Relationships of Old Dunes and Playa Sediments at Lake Frome

The light and heavy minerals of the > 200-mesh fraction of Samples 20, 21, 22, and 23 are similar to those of Sample 19. The quartz grains all have wavy extinction, indicating metamorphic origin. Some grains show platy structure and others have strained platy structure forming the core of the grain. Unstrained quartz is overgrown outside the grain. Traces of gypsum sand present in Samples 19 and 23 are rounded grains of probable eolian origin.

The most interesting feature of the sediments is the presence of shell fragments in all the samples examined. All the samples contain ostracods; a microscopic size helix snail was found in Sample 19; and five well preserved Gyrogonites of the Charophyta were found, one in Sample 21 and four in Sample 22. Chara is a fresh-water algae which may also live in brackish water. It is

not likely that the finding of Chara Gyrogonites would mean a fresh-water environment for the lake sediments. It is more likely that these Gyrogonites were brought into the lake with the sediments by floods and their original fresh-water habitats were billabongs (ponds) along intermittent watercourses. The Chara is still one of the important aquatic plants of present day billabongs within the drainage basin of Lake Frome.

Except for minor variations mostly in the relative proportions of the heavy minerals, the samples, except Sample 19, are similar. The heavy minerals can be divided into two groups; the zircon-rutile-tourmaline group, and the actinolite-tremolite group. The former is very fine-grained, well-rounded, and has a high order of persistence. Most of the grains have been derived from old crystalline basement rocks and probably experienced a multicycled sedimentary history. The second group is subangular to angular, having well-preserved crystal faces and large grain size. It is composed of minerals of low order of persistence and was subjected to less abrasion. It may represent at most a second cycle of sedimentation. Siderite, apatite, muscovite, biotite, and the opaques (probably hematite, limonite, and leucoxene) also belong to this group.

3.4 Classification of Playas Studied

Relationships among the data listed in Table 1 were tested. No direct correlation was found either between moisture content and soluble salts, or between grain size and soluble salts. However, there is a positive correlation between moisture content and the <200-mesh sized material. A plot of soluble salts against <200-mesh fraction with gypsum and soluble salts removed (Figure 31) clearly indicates the relationships of the sediments of the different lakes studied. Three groups are recognized:

A. Lake Austin and Lake Carey group; Precambrian shield depression of Western Australia

B. Lake Torrens and Lake Frome group; Flinders Ranges marginal depressions

C. Lake Gairdner and Lake Harris group; Gawler Range depressions

Group A is characterized by a high percentage of both soluble salts and fine-grained sediments. The fineness of the playa sediments along with the large amount of salts and gypsum both as playa sediments and as dunes suggests that they are derived from either an older interior basin or were formed under extremely arid climatic conditions on a tectonically stable terrain.

Group B is characterized by low content of soluble salts and by varied but coarser-grained sediments in a tectonically active area. Drill records of Lake Torrens indicate a well-drained sedimentary basin of Tertiary age. The Tertiary

Figure 31. Relationship of Soluble Salts and Coarse Fractions with Gypsum and Salts Removed

sediments became progressively finer until the deposition of Miocene dolomite, which suggests that the catchment basin attained very low relief. At that time intense chemical weathering predominated. The eventual isolation of the basins, probably during the Pliocene Kosciusko Uplift, and a change from humid to arid climate resulted in the deposition of the upper 260 ft of Quaternary red and brown clastics that includes a 43-ft-thick bed of gypsum. In view of the steep western bank and the high Flinders Ranges not more than 20 miles away, the rather fine grained upper sediments are probably an expression of the continued aridity of the area.

Group C is intermediate, being similar to A in its rather high soluble salts content and to B in the generally coarse grain of its sediments.

3.5 Clay-Mineralogy of the Playa Sediments

Clays, as the final product of weathering, are subjected to late diagenetic alterations which reflect climatic and hydrologic conditions. When the climate is dry, the weathering of the parent rocks is retarded and produces very minor amounts of clay minerals. The soil is therefore rich in fragments of unaltered parent rocks and inherited clay minerals. The kinds of clay minerals present are largely a function of leaching of the alkalis or other cations of varied solubility from the system. This is largely determined by the duration of leaching and the pH values of the leaching solutions, which in turn are determined by climate and relief. Kaolinite or kaolinitic minerals are the predominant clay mineral or minerals produced in granitic, well-drained terrain. This terrain is the product of a wet climate with soil rich in humic or mineral acid, and steep slopes. In the terrain within the zone of uncoordinated drainage, the ground water is rich in alkalis or other cations, and the formation of illite is favored in the presence of K^{+} and montmorillonite or chlorite in the presence of Mg^{++}, Fe^{++}, and Al^{++}.

Investigations reported by Grim (1953, p. 341, 354) and Kerr and Langer (1965, p. 60-69) indicate that montmorillonite and illite are the dominant clay minerals in arid interior basins. As further reported by Grim (1953), Knox's studies of solonetz (saline or alkali) soils showed no kaolinite.

In contrast, kaolinite is omnipresent in the Australian playa sediments and this must be regarded as one of their outstanding characteristics. The kaolinite ranges from 10 to 100 percent of all the clays (Figure 32).

Plots were made of soluble-salt content against the different clay minerals present (Figures 32, 33, and 34). With increase in kaolinite content, there is an increased salt content. Conversely, montmorillonite and chlorite content increases with decreasing salt. There is no apparent correlation with salt and illite content. The correlation is accentuated by combining the content of montmorillonite, chlorite, and illite (Figure 35).

The abnormally high content of kaolinite in Australian playa sediments is primarily inherited from kaolinite-rich laterite, the product of intense lateriza-tion throughout the Australian continent during early to mid-Tertiary time. The hot humid climate in which the laterite was formed was also responsible for the formation of the duricrust, an extremely thick silica-rich horizon beneath the laterite. A considerable amount of alkali and other soluble cations must have been removed from the continent to the sea. The lack of these salts and an arid climate permitted the kaolinite to enter the playas without severe alteration until the salinity of the playas increased. The subsequent formation of clays other than kaolinite (montmorillonite or chlorite and illite) is due to the diagenesis of the kaolinite in the presence of K^+, Mg^+, and other cations in the soluble salts. Thus, low kaolinite should be associated with low soluble salts and with high montmoril-lonite or chlorite and illite, or vice versa (Figures 32 and 35).

The kaolinite content is plotted against depth in Figure 36. The variation curves of kaolinite from playas in Groups B and C are strikingly similar to, but distinguishable from the curves from playas in Group A. With the exception of the uppermost samples from the playas, the kaolinite content generally decreases with depth. It is possible that this is the result of progressive diagenetic alteration of kaolinite into montmorillonite or chlorite, and illite.

The effect of time can also be detected by the relationships between mont-morillonite and chlorite in the samples. The occurrence of montmorillonite is incompatible with that of chlorite (Figure 33). In a marine environment mont-morillonite may be altered into illite and the chloritic materials (Grim, 1953, p. 352). It is known to be unstable and is generally not found in sediments older than Mesozoic, with the exception of a few bentonite beds. Sample 7 is an altered bedrock of Precambrian bentonite clay probably of volcanic origin containing two-thirds montmorillonite and one-third kaolinite. The kaolinite is probably the

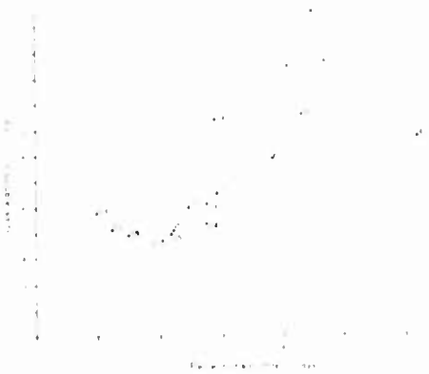

Figure 32. Relationship of Soluble Salts and Kaolinite Content

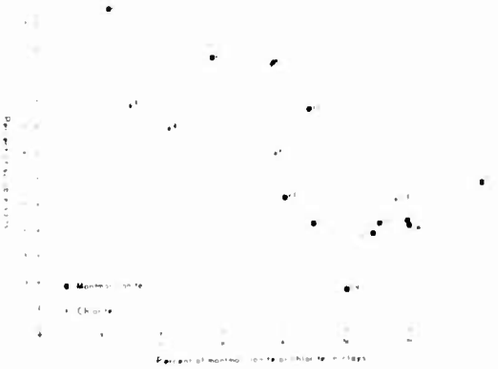

Figure 33. Relationship of Soluble Salts and Montmorillonite or Chlorite Content

Figure 34. Relationship of Soluble Salts and Illite Content

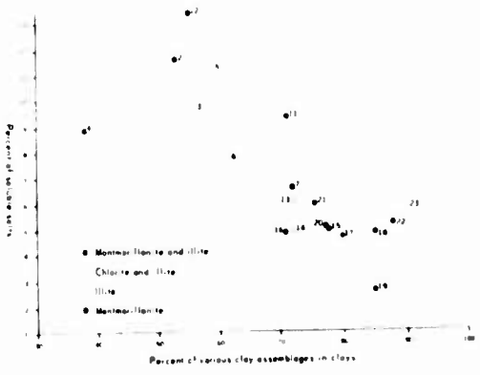

Figure 35. Relationship of Soluble Salts and Clay Assemblages

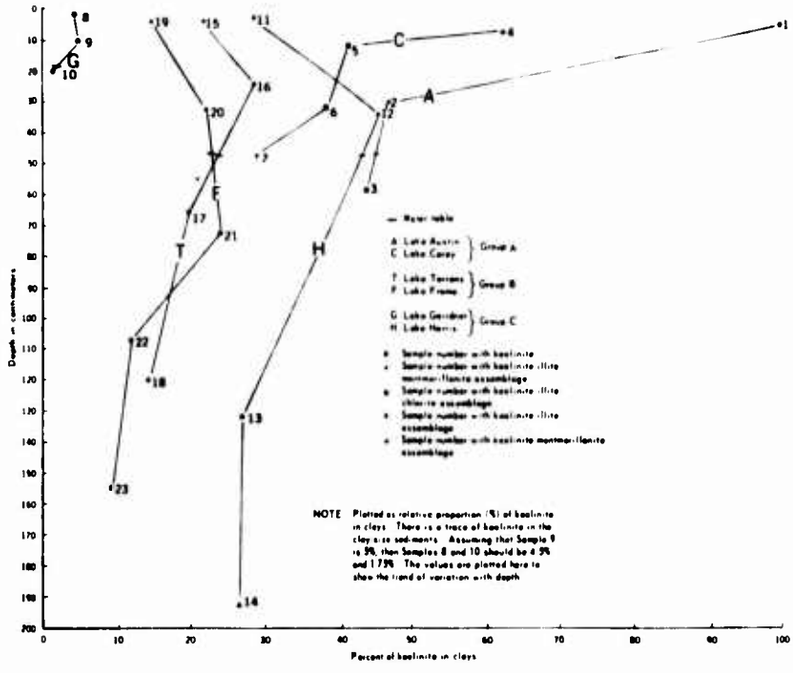

Figure 36. Relationship of Kaolinite Content and Depth

alteration product of the early Tertiary laterization from montmorillonite, and is similar to the example described by Altschuler and others (1963). In the playa sediments, occurrences of kaolinite-illite-chlorite assemblages are subordinate to those of kaolinite-illite-montmorillonite and in two cases occur only in the lowermost samples collected, indicating a preference for sediments of older age. Four out of five chlorite assemblages occur in samples from Western Australia playas (Figure 36) which suggests that the playas of Group A are older than those of Groups B and C.

The highest kaolinite content in the sediments of each playa is found about 10 to 20 cm above the water table, which is also about the level of accumulations of authigenic gypsum crystals. A layer of solid gypsum may be present. The interstitial spaces of the gypsum-crystal layer are usually filled with bluish-black mud. This mud and the brine at the ground-water level generally have a slightly putrid odor that indicates hydrogen sulfide. Therefore, the color of the mud is probably due to fine-grain pyrite crystals. With the hydrogen sulfide and pyrite in the oxidizing environment above the water table, sulfur-oxidizing bacteria should be active, producing sulfuric acid. An acidic condition retards the conversion of kaolinite into montmorillonite or illite so that the kaolinite content in these samples is high. This also probably accounts for the unusually high

kaolinite content of Sample 21. Immediately on top of the bed of Sample 21 is a pebbly gravel aquifer 10 cm thick. The moving ground water must have contained more oxygen, facilitating the activity of sulfur-oxidizing bacteria. The downward leaching of organic remains of these bacteria probably furnished the organic nutrient for the sulfur-reducing bacteria in the anaerobic conditions below the water table. Since the bluish-black mud occurs near the surface under the salt crust of Lake Austin, the same mechanism can also explain the high kaolinite content of Sample 1.

Clays absorb K^+; this is known as K- fixation in diagenesis (Keller, 1964). For instance, illite can be formed even with the addition of potash fertilizer to soils (Grim, 1953, p. 343-344). This explains why, even with a high potash-bearing prophyry country rock (K_2O=5.12-5.7 percent) surrounding Lake Gairdner, the brine of the lake yielded no higher potassium than the brines of the other interior basins of South Australia. Potassium at Lake Gairdner ranged from 0.28 to 0.74 percent, which is lower than the percent for sea water (1.1 percent) (Johns, 1966, p. 10). Due to arid conditions, potassium was not released into solution and the detrital prophyry entered the lake as fresh rock sand. Figure 45 shows that the range of illite in the lake sediment is between 20 and 40 percent regardless of the content of soluble salts. This suggests that potassium salts were partially removed during the period of laterization. The more than 70 percent illite in Samples 13 and 14 (Figure 34) (the lowermost samples collected at Lake Harris) could have been a glauconitic illite where Ca^+ and Na^+ could also have entered into the mineral composition. The conditions that favor formation of glauconitic illite rather than chlorite are not known. It might be that illite formed in the presence of local sources of K^+ from a buried evaporite.

The uppermost playa samples (Figure 36) exhibit sharp deflection in kaolinite content, either increasing (Western Australia playas) or decreasing (South Australia playas). The relationships are not well understood except for Sample 1. The Old Plateau of Western Australia was not dissected after its uplift, which left the laterite soil cover widely distributed, while over South Australia the laterite surface was dissected and the remnants are patchy; in places the duricrust once buried beneath the laterite is now exposed and forms the resistant cap rock of mesas. Therefore, the smaller kaolinite content in the uppermost sample of the playas in South Australia could be due to diminishing kaolinite supplies. The small content of kaolinite in the clay sediments of all the Lake Gairdner samples strongly suggests that the catchment area of the lake was stripped of the weathering product or soils at the tin e of the deposition of the sediments. The area is now covered with bare rock and gibbers.

Figures 37 and 38 show the soluble salts and grain-size variation with depth. Figures 36 and 38 show that kaolinite tends to be associated with finer grain size. This relationship does not conform to that of clay minerals formed under marine conditions, where kaolinite tends to be coarser grained and occurs in near-shore sediments and both montmorillonite and illite are finer grained and occur in deep-water sediments.

3.6 Detrital Material of the Playa Sediments

The > 200-mesh fractions of the playa sediments all show the presence of fresh feldspar. This feldspar and the sands, predominantly of eolian origin, reflect the arid conditions under which the sediments were deposited and strongly suggest that the clays in the playa sediments are not derived from the weathering of the country rocks which supplied the detrital material. Both the light- and heavy-mineral fractions indicate that the sediments are from a local source. For instance, in the Lake Gairdner samples, porphyritic rhyolite and iron-ore fragments are important in both the light- and heavy-mineral fractions, but in the Lake Harris samples such materials are subordinate. This can be explained by the greater distance from the outcrops of these rocks to the sites of deposition.

Figure 38 shows that detrital grain size generally becomes coarser with depth except in the uppermost samples, which could mean a repetition of the coarser grained sediments, and the initiation of a new erosional cycle or eolian activity.

The heavy minerals yield celestite of authigenic origin, closely associated with gypsum. In one sample from Lake Torrens, barite was found. The gypsum crystals from this lake are in short prisms instead of showing bi-convex tabular habit. Whether the crystal habits of gypsum were related to impurity of the other alkaline earths that were present is yet to be answered.

4. CONCLUSIONS

This investigation of Australian playas was a brief reconnaissance that did not permit drilling or other examination of the subsurface deeper than 2 meters. The field data represent the most recent geologic time although some of the material seen in the western samples may be as old as late Tertiary.

The Tertiary climate of interior Australia was characterised by humid tropical conditions that prevailed over all the playas studied in this report, just as the present arid climate prevails over all these playa areas. There is no evidence that in the period between the Tertiary and the present, individual

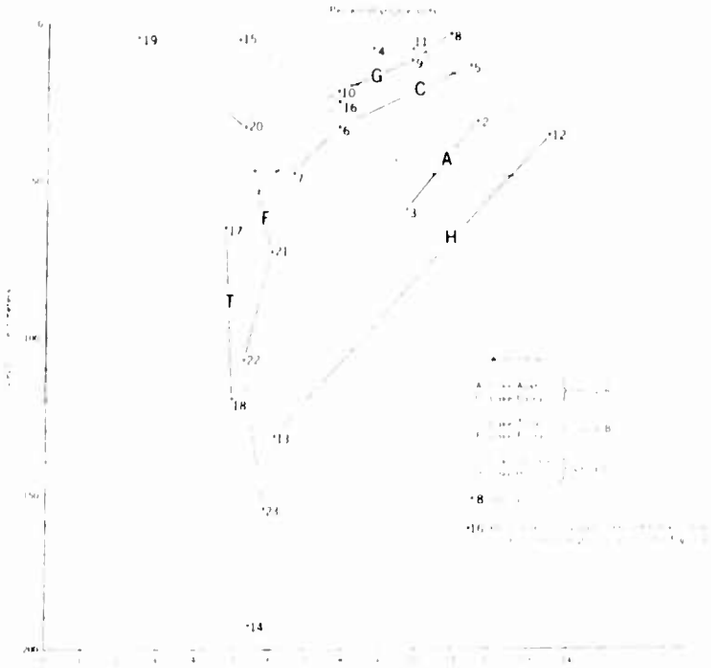

Figure 37. Relationship of Soluble Salts and Depth

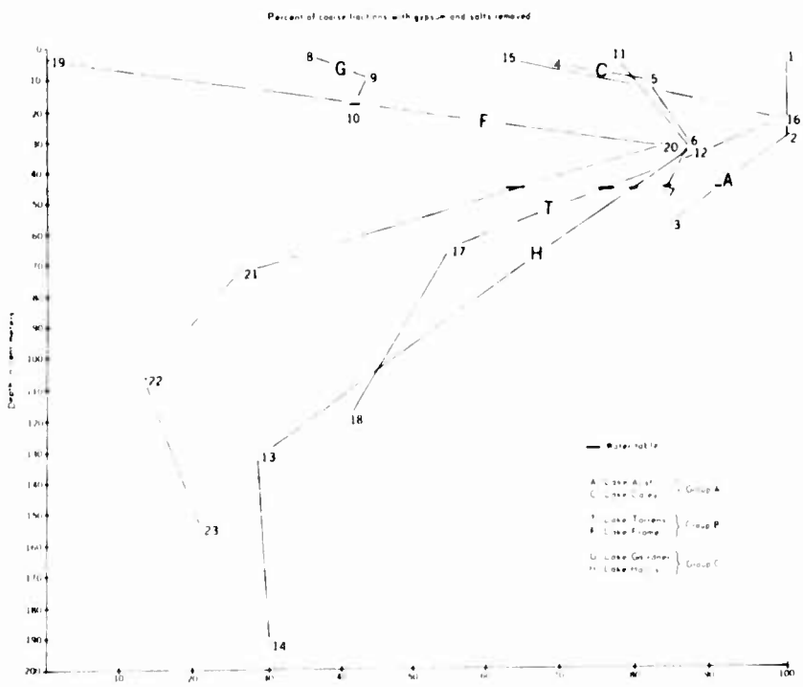

Figure 38. Relationship of Coarse Fractions with Gypsum and Salts Removed, and Depth

playas experienced different climate conditions nor is there any evidence to suggest that the onset of aridity in late Tertiary time occurred sequentially rather than uniformly over all the playas.

Areal differences in the composition of the several playas can not therefore be explained by differential weathering due to areal climatic variations.

There is an extensive laterite cover in Western Australia which diminishes eastward until only patches of dissected laterite remain in South Australia. This distribution is reflected in the kaolinite and soluble salt content derived from the laterite, which is higher in western playas and lower in the eastern playas. Laterization is a tropical weathering process which depends on a warm moist climate. But its progress downward and its ultimate thickness depend on a stable surface not subjected to accelerated erosion. The Kosciusko Uplift of late Tertiary time began just before the change from a humid tropical to an arid climate. In the east there was significant crustal deformation, but in the west there was merely epeirogenic uplift. The laterization which had been uniformly developed areally and vertically was now subjected to erosion in the east. In the west the laterization continued until the climate became arid. The fact that detrital grain size is coarsest in the easternmost playas, intermediate at Lakes Harris and Gairdner, and finest in the western playas is evidence of this distribution of tectonism.

The post-Tertiary arid conditions are reflected in the unweathered detrital feldspars (> 200-mesh fractions). This suggests that the clays rich in kaolinite are inherited produtts of laterization during the earlier humid tropical climate. Diagenesis is proposed as an explanation for the correlation between the scluble salt and kaolinite contents of the clays, while both exhibit an inverse correlation with montmorillinite and chlorite, and no correlation with illite content.

Recent strandlines immediately peripheral to the present shoreline of Lake Eyre are related to historical flooding. Otherwise, there is no evidence, in Western or South Australia of beaches or of wave-cut features which might indicate that the playas visited had previously been occupied by more extensive lakes. This suggests that Pleistocene periods of glacial advance, which are represented by pluvial lakes in the United States and elsewhere, were not times of significantly increased precipitation in the interior of Australia. The stratigraphy at Lake Frome suggests that old dunes are buried beneath the most recent playa sediments. Galloway (1965, p. 615), discussing Australia, points out that the "immense, homogenous system of longitudinal dunes, now stabilized, extends across the heart of the continent through more than twenty degrees of latitude." See Figure 39. Therefore, he argues, "There is good reason to postulate a considerable degree of climatic uniformity at times during the Pleistocene."

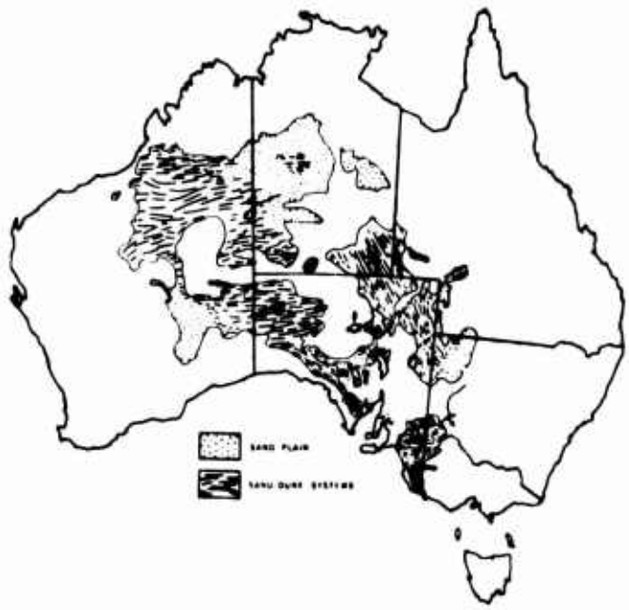

Figure 39. Recorded Distribution of Sand-Dune Systems and Sand Plains

Quoting Wright (1962) and Thom (1961), Galloway cites evidence for linear inland dunes passing below present tidal flats or sea level. Johns and Ludbrook (1963, p. 34) have pointed out that extensive deflation occurred in central Australia during the period 40,000 to 20,000 years B.P. Therefore, sea level was lower during the Pleistocene periods of glacial advance which also coincided with a period of intense eolian activity in Australia. Since the water table is the ultimate base for eolian activity, the Lake Frome section suggests a lower water table during a period of previous eolian activity. If the older dunes are in fact Pleistocene dunes, they were formed during a period which was windier, colder, but drier. The dunes were subsequently covered by playa sediments during a period characterized by a higher water table. Thus, Australia may have experienced no true pluvial period comparable to that which has been well documented in the United States. The post glacial (?) climate as inferred from the Lake Frome section has been more moist than the period during which the dunes were formed (presumably a late glacial period). These relationships are in agreement with the ideas expressed by Galloway.

Refererences

Ahnert, F. (1960) The influence of Pleistocene climates upon the morphology of cuesta scarps on the Colorado Plateau, Assoc. Am. Geographers Annals 50(No. 2):139-156.

Altschuler, Z. S., Dwornik, E. J., and Kramer, H. (1963) Transformation of montmorillonite to kaolinite during weathering, Science 141(No. 3578):148-152.

Antevs, E. (1954) Climate of New Mexico during the last glacio-pluvial, Jour. Geology 62:182-191.

Australia, Commonwealth Scientific and Industrial Research Organization (1960) The Australian Environment, C.S.I.R.O. and Melbourne University Press, p. 151.

Bonython, C. W. (1956) The salt of Lake Eyre - its occurrence in Madigan Gulf and its possible origin, Royal Soc. of South Australia Trans. 79:66-92.

Brewer, R. (1960) Cutans: their definition, recognition and classification, Jour. Soil Sci. 11:280-292.

Broecker, W. S., and Orr, P. C. (1958) Radiocarbon chronology of Lake Lahontan and Lake Bonneville, Geol. Soc. Americ Bull. 69:1009-1032.

David, T. W. E. (1950) The Geology of the Commonwealth of Australia, 3 Vol., Edward Arnold, London.

Flint, R. F. (1947) Glacial geology and the Pleistocene Epoch, John Wiley & Sons, 589 p.

Galloway, R. W. (1965) Late Quaternary climates in Australia: Jour. Geology 73(No. 4):603-618.

Gilbert, G. K. (1890) Lake Bonneville: U. S. Geol. Survey Mon. 1, 438 p.

Gregory, J. W. (1914) The lake system of Westralia, Geog. Jour., 43:656-664.

Grim, R. E. (1953) Clay Mineralogy, McGraw-Hill Book Co., Inc., 384 p.

Johns, R. K. (1964) Investigation of Lake Torrens, South Australia Dept. of Mines, 29 p.

Johns, R. K. (1966) Investigation of Lake Gairdner Grids G6 and H6, South Austral Dept. of Mines, Rept. Bk. No. 62/103, G. S. No. 3448, D. M. 1348/60, 13 p.

Johns, R. K., and Ludbrook, N. H., 1963, Investigation of Lake Eyre, South Australia Dept. of Mines, Rept. of Inv. No. 24, 104 p.

Jutson, J. T. (1917) Erosion and the resulting landforms in sub-arid Western Australia, including the origin and growth of the dry lakes, Geog. Jour. 50:418-437.

Jutson, J. T. (1918) The sand ridges, rock floors, and other associated features at Goongarrie in sub-arid Western Australia; and their relation to the growth of Lake Goongarrie, a "dry" lake or playa: Royal Soc. of Victoria Proc., 31(n.s.):113-128.

Jutson, J. T. (1934) The physiography (geomorphology) of Western Australia, Western Australia Geol. Survey Bull. No. 95, 366 p.

Keller, W. D. (1964) Processes of origin and alteration of clay minerals, in Soil Clay Mineralogy, Rich, C. I., and Kunze, G. W., Eds., A symposium, Chapel Hill, N. C., U. of N. C. Press, pp. 3-77.

Kerr, P. F., and Langer, A. M. (1965) Mineralogical features of Mojave Desert playa crusts, in Neal, J. T., Ed., Geology, Mineralogy, and Hydrology of U. S. Playas, AFCRL Environmental Research Paper No. 96, pp. 31-72.

Krumbein, W. C., and Pettijohn, F. J. (1938) Manual of Sedimentary Petrography, D. Appleton-Century Co., 549 p.

Leopold, L. B. (1951) Pleistocene climate in New Mexico: Am. Jour. Sci. 249:152-168.

Mabbutt, J. A. (1961) A Stripped Land Surface in Western Australia, Inst. British Geographers, Trans. and Papers, No. 29, p. 101-114.

Madigan, C. T. (1930) Lake Eyre, South Australia, Geog. Jour. 76:215-240.

Madigan, C. T. (1944) Central Australia, Oxford Univ. Press, 316 p.

Madigan, C. T. (1945) The Simpson Desert Expedition, 1939, Royal Soc. of South Australia Trans., Pt. I, Vol. 69, p. 118-139.

Morrison, R. B., and Frye, J. C. (1965) Correlation of the Middle and Late Quaternary Successions of the Lake Lahontan, Lake Bonneville, Rocky Mountain (Wasatch Range), Southern Great Plains, and Eastern Midwest Areas, Nevada Bur. of Mines, Rept. 9, pp. 1-45.

Neal, J. T. (1965) Geology, Mineralogy, and Hydrology of U. S. Playas, AFCRL Environmental Research Paper No. 96, 176 p.

Reeves, C. C., Jr. (1966) Pluvial lake basins of west Texas, Jour. Geology, 74:269-291.

Russell, I. C. (1889) Quaternary History of Mono Valley, California, U. S. Geol. Survey, 8th Ann. Rept., Pt. I, pp. 261-394.

Stoertz, G. E. and Hasser, E. G. (1961) Areas Including Sites Suitable for Expedient Airstrips in Australian Deserts and Semideserts, U. S. Air Force Geophysics Research Directorate, AFCRL Air Research and Development Command, 96 p.

Twidale, C. R. (1967) Hillslopes and pediments in the Flinders Ranges, South Australia, in Landform studies from Australia and New Guinea, Jennings, J. N., and Mabbutt, J. A., Eds., Natl. Univ. Press, Canberra, Australia, pp. 95-117.

Waite, E. R. (1917) Results of the South Australian Museum Expedition to Strzlecke and Cooper Creeks, Royal Soc. of South Australia Trans. and Proc., Vol. 41, pp. 405-658.

Woolnough, W. G. (1927) The Duricrust of Australia, Royal Soc. of New South Wales Jour. and Proc., Vol. 61, pp. 24-53.

BLANK PAGE

Contents

V. Geomorphology of Three Kavirs in Northern Iran

Daniel B. Krinsley
Military Geology Branch
United States Geological Survey
Washington, D.C.

Abstract

The distribution of three kavirs in northern Iran as well as the presence or absence of peripheral lacustrine deposits suggest that the Pleistocene climate of northern Iran was similar to the present climate, except that the precipitation/evaporation ratio was higher due to decreased summer temperature.

This Pleistocene climatic regime resulted in extensive lacustrine expansion at Daryacheh Rezaiyeh (Lake Urmia), and probable expansion at Sabzevar Kavir. At the Great Kavir, where it was cooler and windier but not wetter than at present, there is no evidence that a lake ever existed.

1. INTRODUCTION

This report describes geologic observations made on selected kavirs (playas) in northern Iran during eight weeks of field study in 1965 and 1966. Previous information on these kavirs is sparse and little known in the United States.

The history of the kavirs of Iran is of considerable interest to students of Pleistocene geology as there has been speculation that the kavirs may have

Prepared under PRO-CP-67-820 with partial funding from Air Force Weapons Laboratory, Kirtland AFB, N.M.

contained semipermanent lakes concurrently with Pleistocene glaciation. This condition has been demonstrated in the United States, North Africa, and Australia. The present study is directed primarily toward this aspect of the recent geological history, but also includes related geologic observations. Studies elsewhere have shown that playas are dynamic landforms; that is, they continually undergo change with time, and in response to environmental variation.

2. SABZEVAR KAVIR

2.1 Geography and Climate

Sabzevar Kavir is a clay playa of the ground-water discharging type, which is centered at 36°10'N.; 56°40'E. (Figure 1). Approximately 85 percent of the kavir occupies the western part of its basin and a narrow extension borders the eastern tributary stream. The kavir is 122 km in longest dimension (east-west) and 8 to 30 km in width (north-south) with a total area of 2,025 sq km. The drainage basin occupied by the kavir is 408 km long (east-west) and 240 km wide (north-south) with a total area of 56,527 sq km. The basin to playa ratio is 28:1.

The kavir lies southeast of the Elburz Mountains in a region which receives from 10 to 20 cm of precipitation per year. The rainy period starts in November and continues through spring with as much as 8 cm of precipitation during the period March through April. Only a trace of rain is recorded in June. The period July through October is extremely dry, although there may be an occasional cloudburst. The location of a large dune field along the southern and eastern margins of the kavir is evidence that the prevailing winds are from the north and west. The winds are frequently strong as indicated by sharply etched ventifacts. During the night of August 27, 1966, strong winds threatened to carry away a large field tent which had to be restaked to avoid destruction. Wind gusts were estimated to be about 100 km per hr.

2.2 Regional Geology and Topography

Sabzevar Kavir is at an altitude of approximately 800 m. It is dominated to the north by a generally northwest-trending ridge that reaches altitudes of 2,000 to 2,900 m. The ridge is composed of ultrabasic intrusive rock which contains several magmatic segregations of chromite. The ultrabasic rock is flanked by volcanic rock of Eocene age along its northern side and by conglomerates of Miocene-Pliocene age along its southern side. Along the eastern margin of the kavir, there are dissected mountains which range in altitude from 1,200 to 1,500 m. These are composed of volcanic rock of Eocene age; evaporites, shale, and mudstone of

Figure 1. Location Map

Miocene age; and rhyolitic lavas of Paleozoic age. Copper ore in the form of chalcocite, cuprite, malachite, and chrysocolla occurs in mineralized zones along the walls of Eocene formations, filling fissures and impregnating eruptive rocks.

The mountains south of Sabzevar Kavir form a breeched amphitheatre opening to the kavir. The ridge line ranges in altitude from 1,200 to 1,800 m and is composed of Eocene volcanic rocks, Upper Cretaceous basic igneous and sedimentary rocks with siliceous shale and limestone, and Miocene red sandstone, sandy shale, siltstone, local pebble horizons, and massive evaporites at the base. All of these rocks to the south are faulted.

2.3 Hydrography

Sabzevar Kavir receives the runoff of numerous peripheral streams and the seasonal waters of two master streams, the Rud-e-Qal'eh-ye-Mureh and the Rud-e-Kal-Shur (Figure 2).

The Mureh heads in the Elburz Mountains and drains the basin surrounding Jajarm before flowing south to Sabzevar Kavir. After receiving the Shur as a major tributary in the form of several distributaries, the Mureh drains the southwest part

of the kavir and then flows south to the Dasht-E-Kavir. From its headwaters to the Dasht-E-Kavir, the Mureh is 320 km long. The Shur flows west from the mountains above Nishabur for 240 km to its junction with the Mureh in Sabzevar Kavir.

The Mureh enters the kavir from the north, 12.8 km east of Abbasabad. The single channel subdivides into numerous distributaries which fan out over an area of approximately 440 sq km (Figure 2) before rejoining a main channel in the southwest part of the kavir. The Shur enters the kavir from the east and maintains its identity for 19.2 km in the principal part of the kavir before it subdivides into many distributaries. These distributaries are less well defined than are those of the Mureh, and disappear into the kavir for short distances before reappearing to join into tributaries which eventually enter the Mureh.

A large alluvial fan encroaching upon the kavir from the north margin, east of the Mureh, has imposed a third drainage system on the northeast surface of the kavir. Some of its channels enter the Mureh system but most of them maintain a separate identity along the northeast part of the kavir.

An incised channel, segments of which are covered with salt, lies 3 m below the surface of the kavir, in the central area (Figure 2). This channel receives distributaries from the Mureh and Shur Rivers at almost right angles, which suggests that it is cutting headward due to a reduced base level (uplift or lowered water table) and has captured the distributaries.

2.4 Surface Conditions

Sabzevar Kavir is bordered by alluvial fans with margins that are rather sharply delineated (Figure 3). At present, the alluvial fans are encroaching upon the kavir, as is clearly shown at the toe of the large fan immediately east of the Mureh. Old maps of the area do not show the present extent of this large fan. The alluvial fans have slopes of 15° to 20° along the north and west margins of the kavir, and slopes of 5° to 10° along the south margin.

North of the kavir, and resting on the alluvial fans are a series of fine sandy silt with clay deposits which form terraces at altitudes of 892, 879, and 874 m (Figure 2). On the basis of their morphology and composition, the terraces are considered to be beaches which were emplaced at the margin of a lake which once covered the present area of Sabzevar Kavir.

Within the margins of the kavir, seven types of surface units have been delineated (Figure 3). Several units are composites and many boundaries are transitional. Figure 3 was prepared from aerial photos taken during the latter half of June 1955 with the result that surface conditions shown are those of the relatively dry period (Figure 4). However, the surface of the kavir is one of ground-water discharge throughout and ground water is believed to lie everywhere within about 3 m of the surface. It is not clear whether ground water flows out of the southern

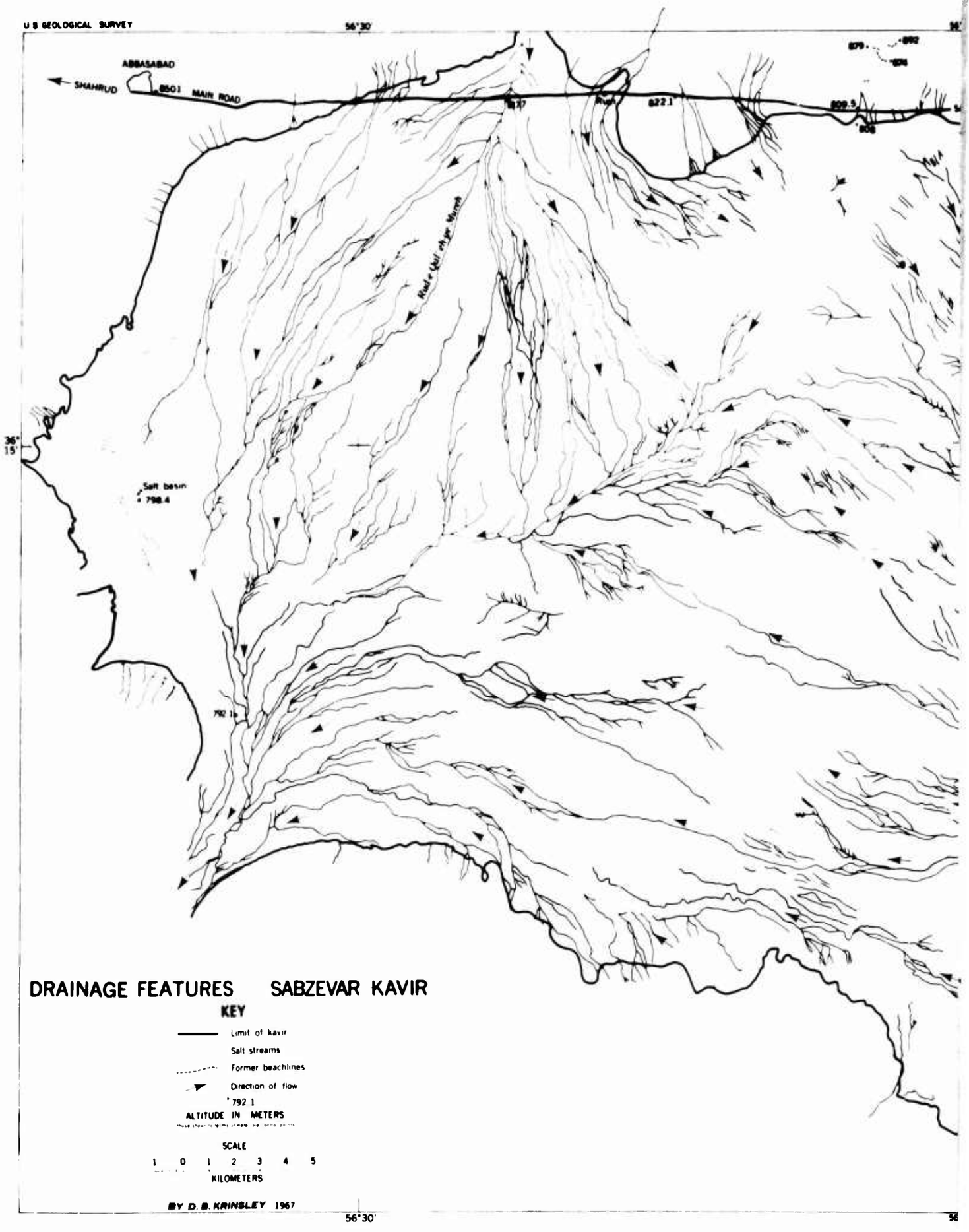

Figure 2. Map of Drainage Features, Sabze

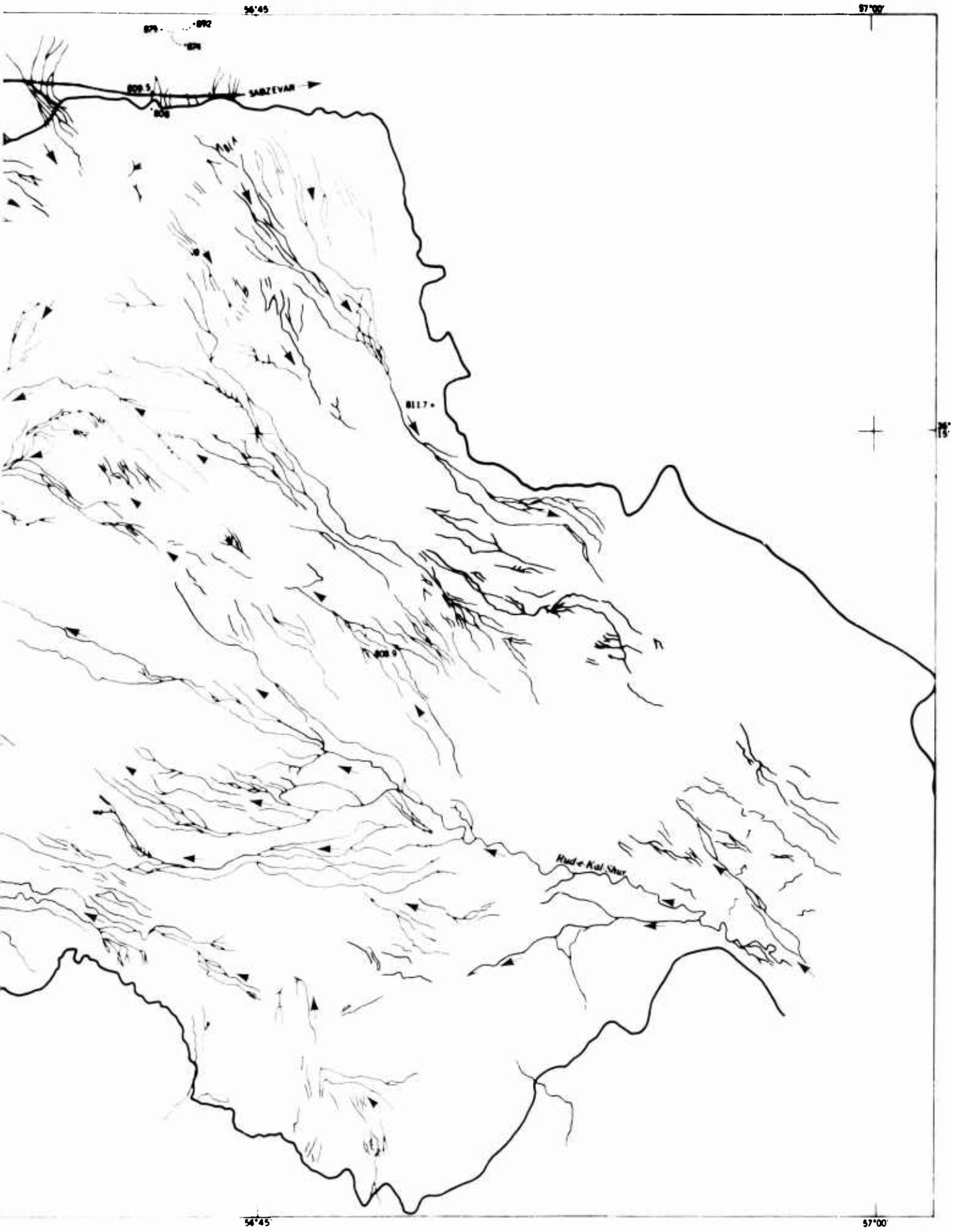

ap of Drainage Features, Sabzevar Kavir

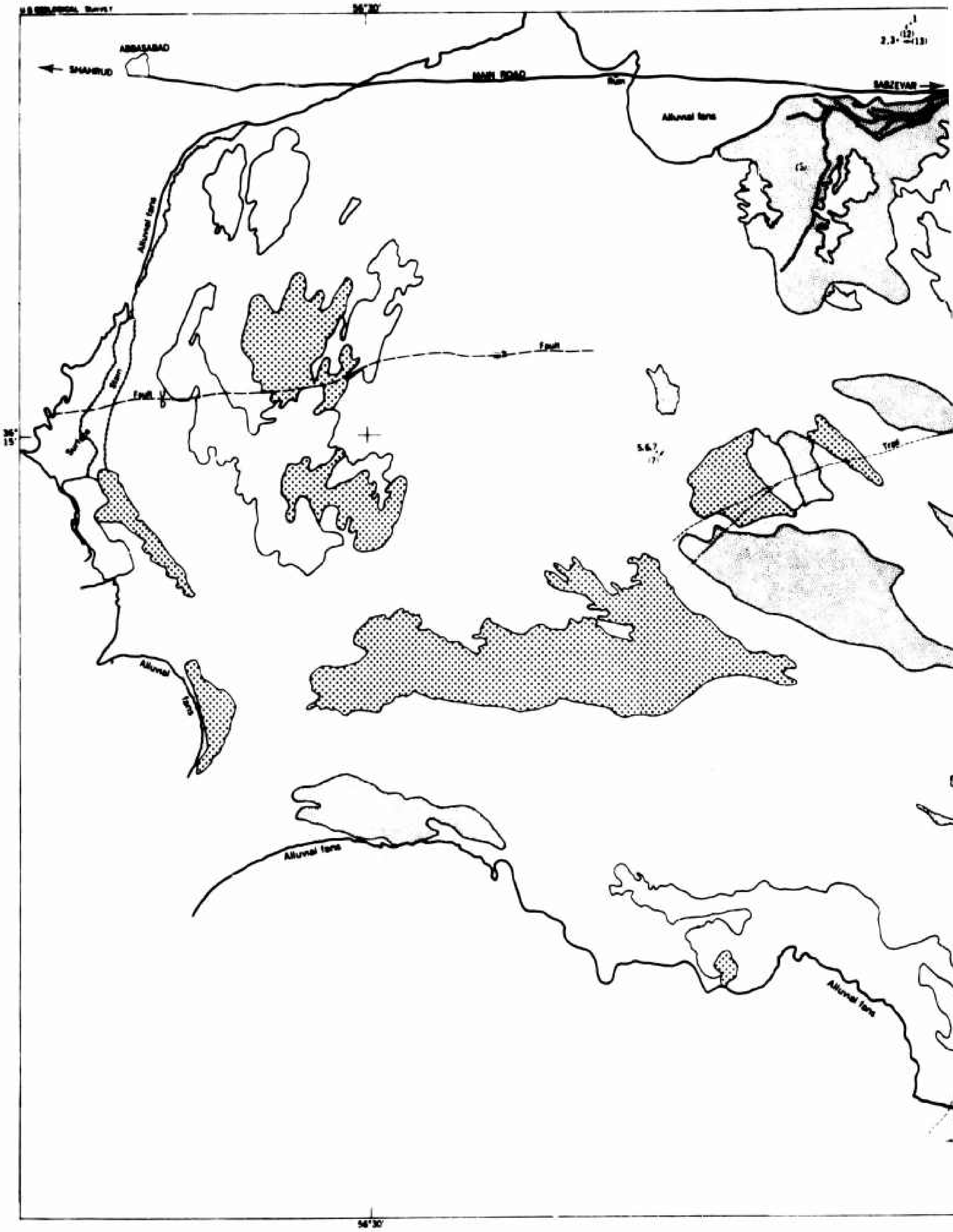

A

Figure 3. Map of Surface Features, Sabz

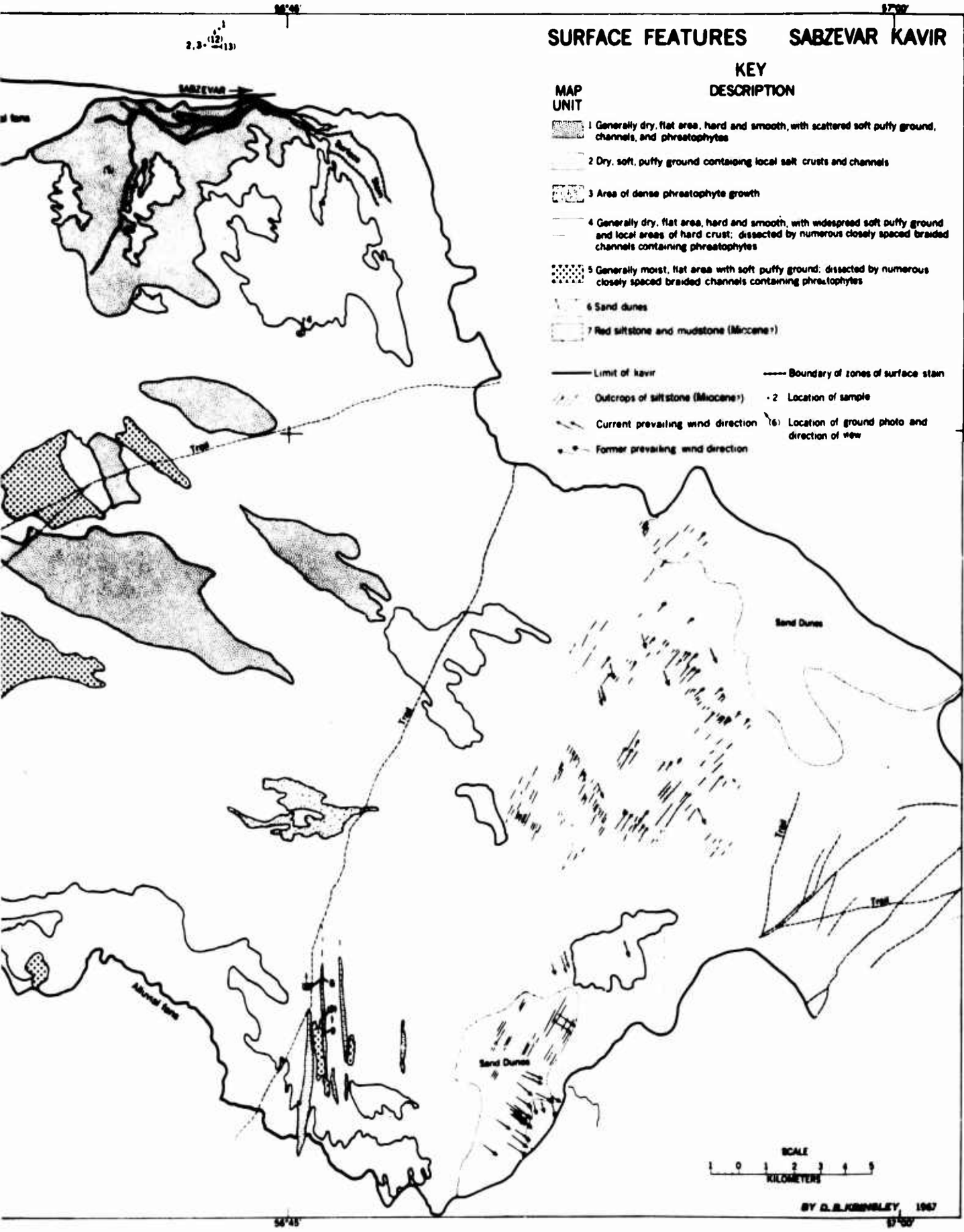

. Map of Surface Features, Sabzevar Kavir

end of the basin, but this is possible as the general state of the surface is not one of heavy salt accumulation. Eight photos (Figures 4 to 9, 12, and 13) illustrate some details of the surface conditions within the kavir.

Map Unit 1 (Figure 3) is generally dry and flat, consisting mainly of hard, smooth areas but with scattered puffy ground, channels, and preatophytes. The microrelief of the hard areas is generally less than 3 cm but is as much as 5 cm locally. Puffy ground is found in patches, and along dry channels. The channels associated with the hard areas are generally less than 25 cm deep and 3 m wide although the sides are often sharply eroded vertical cuts. These channels are abrupt discontinuous features, which are part of the distributary system. Phreatophytes occur singly or in small groups, frequently adjacent to patches of puffy ground or along channels. Hard, dry compact surfaces (Figure 5) are normally associated with a deeper ground-water level than that occurring at Sabzevar. The existence of this type of crust within a ground-water discharging kavir can be explained by frequent surface flooding. These surfaces contain standing water during the rainy season, as has been observed on numerous playas in the western United States. At Sabzevar, the hard surface was observed to have greater areal extent in August 1966 than in September 1965, presumably because of flooding during the rainy winter of 1965-1966. Map Unit 1 occurs in the northeast, central, and southwest parts of the kavir. It occupies a total of 91 sq km or 5 percent of the mapped area.

Map Unit 2 contains dry, soft, puffy ground and locally includes salt crusts and channels. The microrelief of the puffy ground ranges from 5 to 15 cm. Many variations of this type of surface exist, but it is generally capable of supporting normal vehicular traffic, with minor rutting. Moist plastic sediment is generally encountered at shallow depths. The local salt crusts are generally 5 mm thick and may be either flat and smooth or warped in tentlike forms associated with puffy ground (Figure 6). Channels are generally less than 25 cm deep and 3 m wide with sides that are generally modified into rounded shoulders. Map Unit 2 is rather widely distributed, and occupies a total of 161 sq km or 9 percent of the mapped area.

Map Unit 3 includes two small areas of dense phreatophyte vegetation near the central part of the kavir. The phreatophytes, apparently a variety of pickleweed approximately 1 m high, are concentrated along channels about 2 m below the general surface of the kavir. Map Unit 3 occupies a total of 8 sq km or 0.4 percent of the mapped area.

Map Unit 4 is generally dry and flat consisting of hard smooth areas with widespread soft puffy ground and local areas of hard crust. This terrain is dissected by numerous closely spaced braided channels containing phreatophytes. Map Unit 4 is very widely distributed and occupies a total of 1,380 sq km or 75 percent of the mapped area. The deepest channels observed within Map Unit 4 were in

Figure 4. Vertical Aerial Photo of Central Part of Sabzevar Kavir, Scale 1:60,000, 19 June 1955

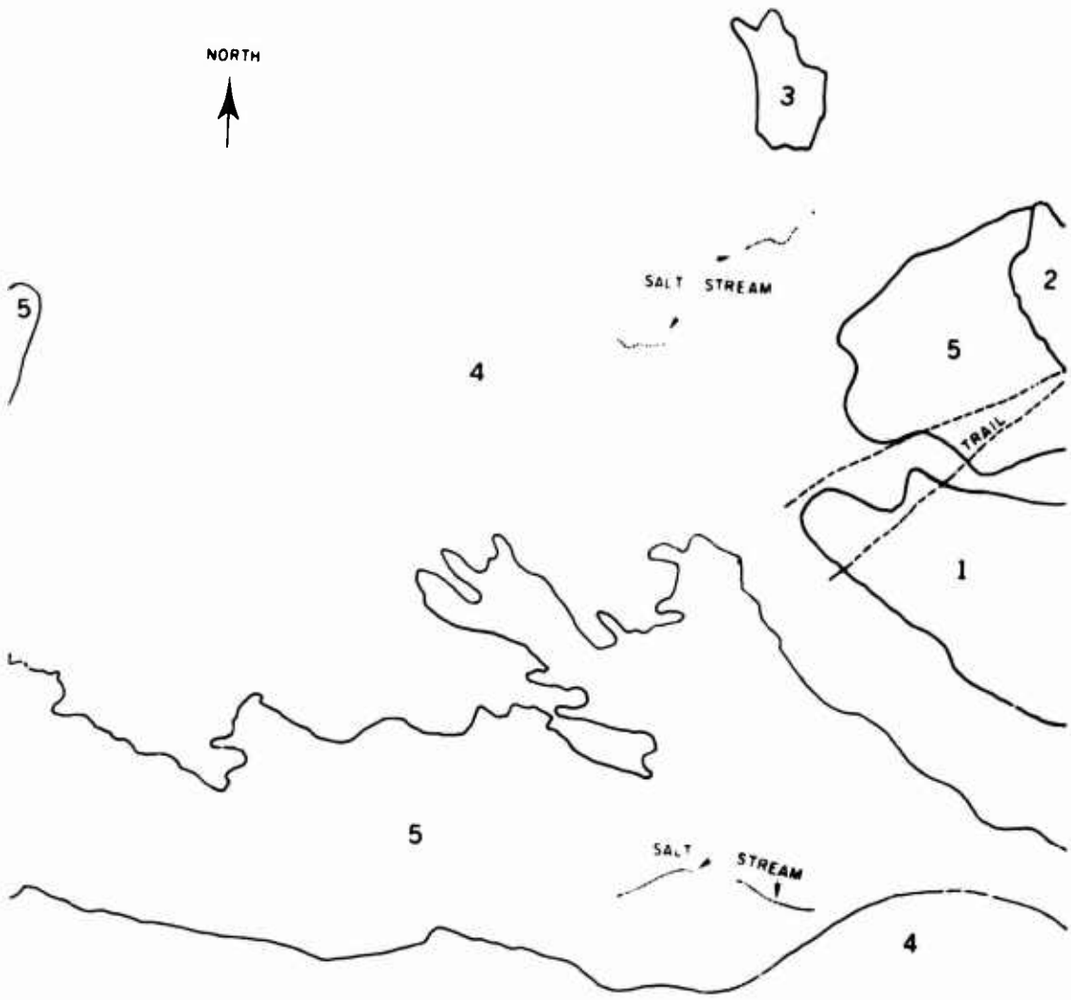

Figure 4a. Overlay for Figure 4. Numbers refer to map units shown in Figure 3.

the central part of the kavir where they are 3 m deep and 10 m wide at the deepest part but widen to 30 m within 1 m of the kavir surface. One channel was filled with wet salt 15 cm thick resting on a layer of wet black clay approximately 20 cm thick. The wet salt occurred in a segment of the channel and its initial and terminal boundaries were sharp (Figure 7).

Map Unit 5 contains generally moist, flat areas with soft puffy ground and is dissected by numerous closely spaced braided channels containing phreatophytes. These moist areas lie mainly on the periphery of the fan of the Mureh in the west-central part of the kavir. The map unit occupies a total of 104 sq km or 6 percent of the mapped area.

Map Unit 6 contains extensive dune fields which are distributed in two areas in the eastern part of the mapped area. It is estimated that the relief ranges from 3 to 6 m with most dunes less than 4 m high. Sand dunes in the southern area are vegetated and apparently stabilized. Their orientation suggests that they formed when the prevailing wind was from 304° to 308° true north. Current blowouts and dunes at the noses of Miocene outcrops suggest that the present prevailing wind is from 340° to 343° true north. Map Unit 6 occupies a total of 73 sq km or 4 percent of the mapped area.

Bedrock of presumed Miocene age is exposed in the southeastern part of the kavir in narrow zones trending north-south (Map Unit 7, Figures 8 and 9). The rock consists of siltstone and mudstone with salts generally in the form of halite

Figure 5. Hard, Dry Crust with Small Desiccation Polygons

Figure 6. Salt Crust (0.5 mm thick) Overlying Dark Reddish-Brown (5YR3/3) Fine Sand and Silty Clay (Sample 4) Within an Area of Dry, Soft, Puffy Ground (Map Unit 2), 28 August 1966

Figure 7. Salt Stream (Namak Safid) in Central Part of Kavir. Area is generally dry and flat with widespread soft puffy ground (Map Unit 4). View northeast, 26 August 1966, location of samples 5, 6, and 7.

Figure 8. Transverse Section Through a Ridge of Miocene(?) Bedrock. Bluff is 5 m high. View north, 28 August 1966, location of sample 8 (from base of bluff).

Figure 9. Ridge of Miocene(?) Bedrock, 10 m High Above Kavir. View south, 28 August 1966, location of sample 9 (from surface crust).

or gypsum. To the east and northeast there are numerous small outcrops of similar rock in which the bedding trends are northeast rather than north, suggesting a fault between the two areas. Map Unit 7 occupies 3 sq km or less than 1 percent of the mapped area.

A recent fault scarp can be seen in the northwest part of the kavir. Along its western extent the north side appears to be a few meters higher than the south side. The north side has moved to the east relative to the south side as indicated by the offsets of streams normal to the fault.

Peripheral areas of the kavir are subject to periodic inundation which is indicated by concentric zones of surface stain, noticeable in the west and northeast (Figure 3).

2.5 Sedimentary Analyses

Nine samples of surficial material were collected for sedimentary analysis (Figures 3 and 10). Particle size distribution was determined by the hydrometer method, and particles were inspected for roundness. All samples were examined for pH content and conductivity and inspected for possible fossil content.

Because most of the samples are of very fine texture, only the particles smaller than 0.1 mm were measured. The generally high salt content caused flocculation in all cases, but within different time intervals. Repeated flocculation required that several samples be washed and centrifuged six times. Three of the beach and kavir samples are well graded (1, 5, 7, Figure 11) and three are poorly graded, considering the narrow range of particle size (2, 3, 4, Figure 11). There is no apparent correlation between the geographic or vertical position of the samples and their curves. Because of the repeated washings of the samples, a small weight of soluble material was lost. This has the effect of lowering the percent weight values but not changing the relative positions of the curves.

The pH values of the sample solutions were measured before and after flocculation (Table 1). The same unit concentration of each sample was prepared in distilled water and mixed with a sonic horn. Readings of pH were taken immediately and again more than 24 hours later, following flocculation. There is no apparent correlation between the pH values of the samples and their geographic or vertical position within the section. The highest pH, sample 6 (8.15), and the lowest, sample 7 (7.20), occur in the same section (Figure 10).

The conductivity of each sample with the same unit concentration was also measured in a solution of distilled water that had been mixed with a sonic horn (Table 1). As can be seen by examining Table 1 in conjunction with Figure 10 the data indicate that conductivity is related to both geographic location and vertical position within a section. At any one locality, conductivity is considerably greater at or near the surface than at depth. For example, the value for sample 2 is about

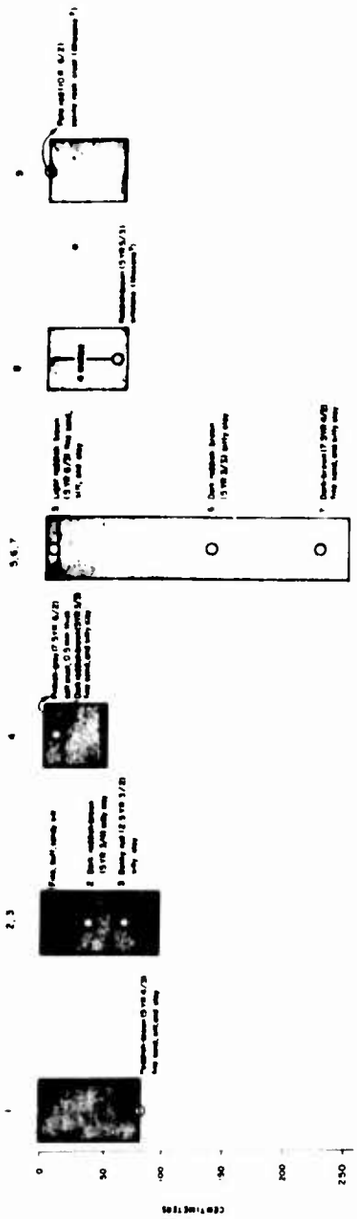

Figure 10. Sections at Sample Locations, Sabzevar Kavir. Sample locations shown on Figure 3.

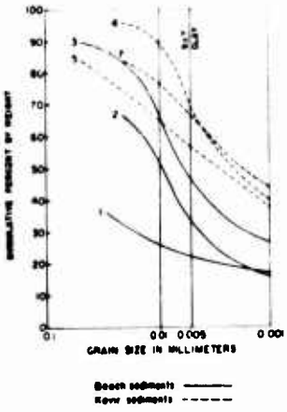

Figure 11. Mechanical Analyses of Fine Fraction of Beach and Kavir Sediments at Sabzevar Kavir

Table 1. pH and Conductivity. Bracket indicates same or related section.

Kavir	Sample	A pH of Solution	B pH of Flocculant*	B less A	Conductivity in micro mho units	Approximate increase in conductivity due to concentration through capillarity
Sabzevar Kavir	1	7.50	8.30	+0.80	400	
	2	7.35	7.85	+0.50	1,100	2x
	3	7.55	8.10	+0.55	600	
	4	7.65	8.45	+0.80	6,000	
	5	7.70	8.40	+0.70	10,250	
	6	8.15	8.75	+0.60	2,800	5x
	7	7.20	8.50	+1.30	2,200	
	8	7.50	8.35	+0.85	4,250	7x
	9	7.50	8.10	+0.60	30,000	
Dasht-E-Kavir	1	7.25	7.90	+0.65	>40,000	

*Flocculant formed more than 24 hours after the solution had been mixed and measured by hydrometer.

twice that for sample 3, sample 5 is about five times sample 7, and sample 8 (near sample 9 although not in the same section) is about seven times sample 9. This relationship is ascribed to a concentration of salts by capillary movement of ground water toward the surface. This process has been most effective near the center of the kavir, as seen in the increasing conductivities from sample 1 on the perimeter through samples 2 and 4 to sample 5 at the center. This relationship seems clear despite the slight differences in depth among these samples. The high values for samples 8 and 9, near the edge of the kavir, probably result from the longer time the process has been at work in the Miocene bedrock.

The samples were microscopically examined and no fossils were observed. All particles are generally extremely angular with only a low percentage showing roundness.

2.6 Subsurface Conditions

The water table ranges from 2 to 3 m in depth within a zone 4.5 km wide along the north margin of the kavir. The incised channel approximately 3 m below the general surface in the center of the kavir is covered with wet salt. These data together with the widespread occurrence of puffy ground indicate that the water table is at shallow depth, probably not exceeding 3 m throughout most of the kavir.

The presence of deeper channels, 6 to 10 m deep, in the southwest part of the kavir suggests that in this area the base level is lower and that the general level of the adjacent water table has also been lowered.

The subsurface bedrock profile is unknown. Outcrops are numerous in the southeast part of the kavir, but bedrock is not exposed elsewhere, even in the deepest channels. Borings did not exceed 3 m because of caving below the water table, but no bedrock was encountered.

2.7 Beaches

There are three distinct levels at altitudes of 892, 879, and 874 m in an area 2 to 3 km northeast of Sabzevar Kavir (Figures 2, 12, 13, and 14). The highest level is 8 m wide with a slope of 7°. It abuts a steeper bedrock slope (14°) and falls off downslope with a gradient of 20°. Levels 2 and 3 are wider but less well developed and slope down into the alluvial fan at low angles.

The levels are composed of fine sandy silt with clay (Figures 10 and 11). Considering the narrow range of grain sizes, samples 2 and 3 are generally poorly graded and their curves resemble the curves of beach sands. Sample 1 is better graded though coarser. Conductivity measurements indicate a concentration upward through capillarity but values are considerably lower than those of the kavir samples (Table 1).

On the basis of their morphology and sedimentary analyses, the levels may be beach deposits which were emplaced at the margin of a lake. Although not visited on the ground, several other levels were mapped by means of aerial photos and their locations are shown in Figure 2. The configuration and freshness of the levels in the western part of the kavir suggest recent occupancy by a body of water; this area is also the lowest part of the kavir.

Although adequate topographic data are lacking, the present lower course of the Mureh, between Sabzevar Kavir and the Dasht-E-Kavir (Figure 1) may have been impounded. The present altitude of the Mureh channel between the kavirs is

Figure 12. Sabzevar Kavir. High beach (892 m) in middleground is partly covered by grass. Note structure is steeply dipping to left. View north, 27 August 1966, location of sample 1.

Figure 13. Sabzevar Kavir. Low beach (874 m) limit against steep rock face with thin talus veneer. View west, 27 August 1966, location of samples 2 and 3.

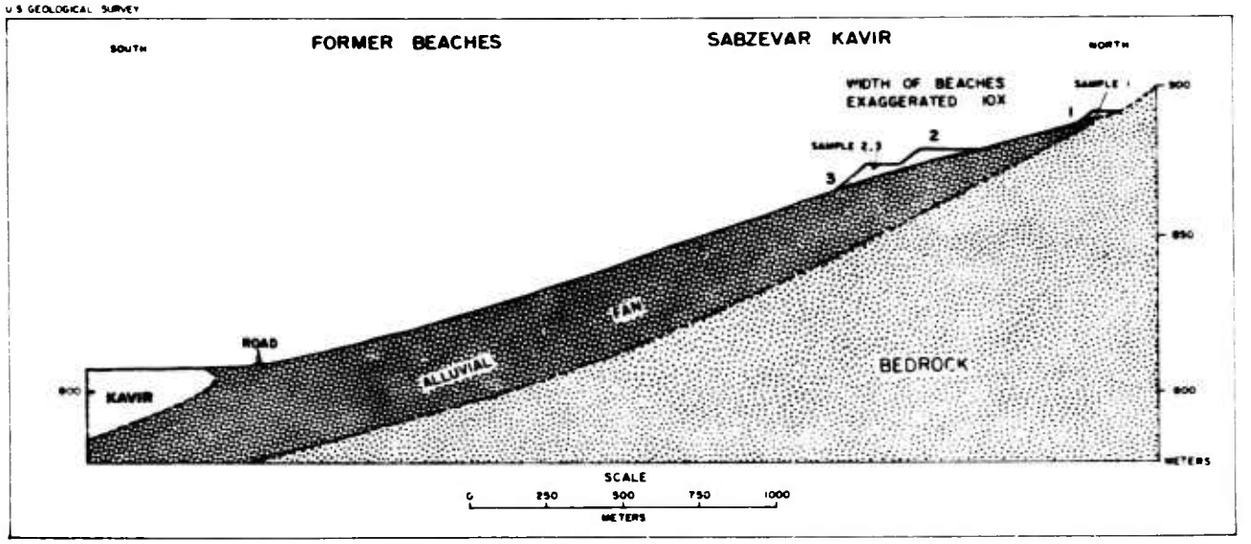

Figure 14. Sabzevar Kavir, Former Beaches

609 m. The mechanics of creating a dam 283 m high are formidable in view of the present absence of sufficiently high terrain adjacent to the channel.

The area of and adjacent to Sabzevar Kavir is unstable (note the recent fault across Sabzevar Kavir) and recent crustal movements are indicated at Damghan Kavir. It is possible that the Dasht-E-Kavir represents a recent tectonic basin (late Pleistocene) and Sabzevar Kavir may have been uplifted during this same period. In the absence of more topographic evidence, additional mechanisms for impoundment would be purely speculative.

The levels peripheral to the kavir are of the same general age on the basis of their proximal positions, morphology, and profile development (conductivity). They appear to be fresh and consequently young. In the absence of specific chronologic data, the author suggests that they may represent the deposits of a lake that reached its maximum extent during the Würm glacial period. The levels in the western depression within Sabzevar Kavir may represent occupancy within the last 100 years during a period of heavy winter precipitation. They may also represent the area occupied by a small lake during the "little ice age," from 3000 to 1850 years before the present.

2.8 Conclusions

Sabzevar Kavir may be the bed of a Pleistocene (Würm) lake which existed during a period when temperatures were 4°C lower than at present (Bobek, 1937, p. 153). The present drainage of Sabzevar Kavir empties into the Dasht-E-Kavir which lies at an altitude of less than 609m, 283 m below the level of the late Pleistocene lake. In the absence of present topographic evidence for the site of the lake impoundment, it is hypothesized that tectonic activity might have provided the required mechanism by tilting the basin to the south, toward the Dasht-E-Kavir during the late Pleistocene.

After the lake was drained, the dry lake sediments were then subjected to wind erosion and dunes were formed in the southeast part of the kavir. The prevailing wind was therefore from the northwest. Photographic evidence suggests that some of the dark-toned dunes (vegetated and stabilized) were formed by prevailing winds which blew from 304° to 308° true north. The current blowouts and dunes indicate that the present prevailing wind is from 340° to 343° true north. The author can only speculate that the former wind direction represents a modification of the prevailing wind due to climate changes during the "little ice age."

The present kavir is undergoing erosion by the Mureh drainage system, as indicated by the incision of the stream system into the kavir deposits.

3. DASHT-E-KAVIR

3.1 Description

The Dasht-E-Kavir is the largest interior desert area in Iran and occupies an irregular depression in the surface of the Iranian Plateau between the northern Elburz Mountains and the Central Ranges (Figure 1). It extends 370 km from west to east and ranges in width from 64 km to 240 km north-south, the average being 160 km. The lowest point is 700.0 m in the eastern basin and the highest is 1,170.0 m in the central basin.

The Dasht-E-Kavir contains several types of surfaces (Figures 15 to 19). Most of the area, perhaps as much as 60 percent, consists of folded Miocene and older rocks which have been eroded to low rolling plains. The Miocene rock, which consists in large part of evaporites, has weathered to such an extent that the original bedding planes are masked in depressions, but are still visible on domes or anticlinal structures (Figure 19). The eroded structures are covered at the margins of the kavir by alluvial fans (dasht) and merge within the kavir with closed depressions to form thick salty silty-clay deposits which characterize true kavirs.

The true kavir basins occupy approximately 30 percent of the entire Dasht-E-Kavir. Within these basins, which have been filled by layers of salt and silty clay, additional salt may be deposited by capillary movement of brine upward to the kavir surface with the consequent evaporation at the surface. The salt precipitated at the surface expands during crystallization. Repeated cycles of salt crystallization together with thermal expansion of the salt due to solar heating alternately buckle and crack the salt surface. The compression ridges which arise by this process form polygonal patterns. Old compression ridges may be eroded by the wind into sharp pinnacles (Figure 18).

There is evidence that the kavir basin fill is transgressing both on the dasht as well as on the erosional surfaces of the Miocene (Bobek, 1963, p. 407). There is no evidence that these Miocene surfaces were ever covered by water or kavir sediments, and no beaches have been observed by either Bobek or this author.

A third surface consists of drained kavir areas adjacent to the dasht or eroded Miocene structures. These drier surfaces represent approximately 10 percent of the Dasht-E-Kavir and locally contain hard, flat, smooth areas (Figure 16).

3.2 Sedimentary Analysis

A single sample was obtained from a kavir basin and analysed in the laboratory. It consists of dark reddish-brown (2.5YR3/4) silty clay characterized by unusual deliquescence. It is thought to correspond to similar material described by Bobek (1959, p. 17) and referred to by the local name "charbeh." Because of its

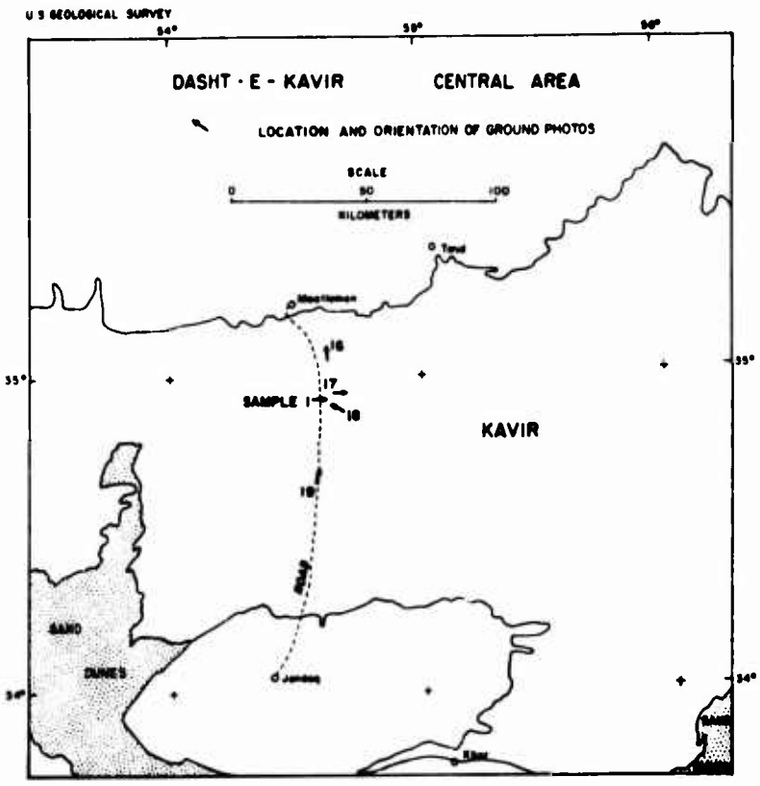

Figure 15. Dasht-E-Kavir, Central Area Location and Orientation of Ground Photos

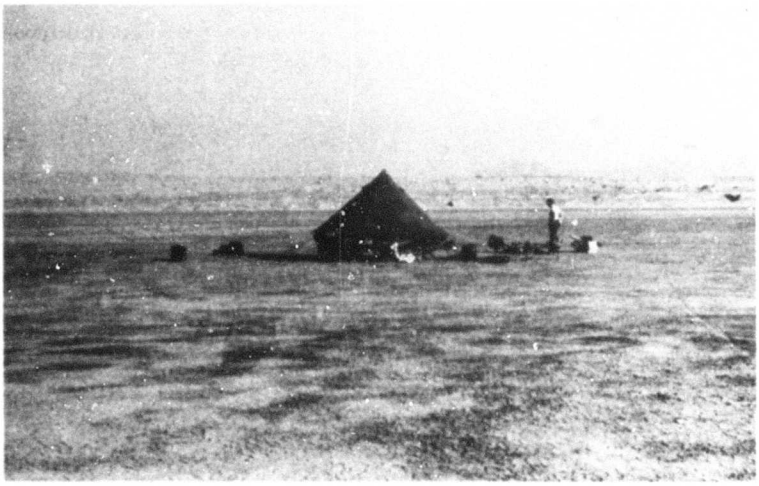

Figure 16. Campsite on the Dasht-E-Kavir, 19 km Southeast of Moalleman. Surface is hard, dry, smooth, and flat. View north toward folded Miocene sediments, 2 September 1966.

Figure 17. Surface of Soft Powdery Silt, 37 km Southeast of Moalleman. Rut is 7 cm deep. View east along anticlinal dome of Miocene, 2 September 1966.

Figure 18. Salt Ridges and Spires up to 53 cm High in a Depression 40 km Southeast of Moalleman. View northwest, 2 September 1966.

Figure 19. The Road Between Moalleman and Jandaq, 62 km Southeast of Moalleman. The rolling terrain has a rough hard surface with local relief up to 30 cm. The tonal differences between the darker middleground and the lighter foreground and background are due to moisture which reflects the salt (lithologic) differences of the shallow, underlying Miocene bedrock. View northeast, 2 September 1966.

extremely high salt content, no attempt was made to measure particle size distribution by hydrometer. The pH values (Table 1) correspond to those of other kavir sediments, but its conductivity exceeded the capacity of the measuring instrument. No fossils were observed under microscopic examination, and the grains were generally angular.

3.3 X-ray Analysis

An X-ray analysis resulted in the identification of halite, quartz, and calcite. Another significant constituent, unidentified by X-ray, is considered likely to be calcium chloride because of its deliquescence and conductivity.

3.4 Conclusions

The field evidence suggests that the vast Dasht-E-Kavir is a post-Miocene plain which has been subjected to uninterrupted arid erosional processes for a considerable length of time. There is no evidence to indicate that the kavir was inundated during the Pleistocene. On the contrary, the data on Sabzevar Kavir and Damghan Kavir support the thesis that during the Würm period when basins immediately adjacent to the Elburz Mountains were in fact areas containing lakes through increased runoff because of lower evaporation rates, these basins were actually cut off from the Dasht-E-Kavir.

If Lake Sabzevar at its maximum level of 892 m had actually been connected with the Dasht-E-Kavir, then the lake would have flooded not only the Dasht-E-Kavir but the Dasht-E-Lut as well. Evidence for such a body of water has not been found. In fact, such evidence is not likely to be found since the climatic requisites for such an extensive body of water are impossible within the physical framework of the existing climatic zones. The present precipitation is entirely inadequate to fill such a lake and there is no evidence that there was a dramatic shift in the precipitation belts of the area during the Pleistocene. Similar reasoning may be applies to the extremely high present evaporation rates.

4. DARYACHEH REZAIYEH

4.1 Description

Daryacheh Rezaiyeh (Lake Urmia) in northwest Iran (Figure 1) occupies an area of 4,000 sq km during the low water period in autumn and 6,000 sq km during the high water period of snow melt in spring. The mean depth of the lake is 5 m and its greatest depth probably does not exceed 15 m. The lake has no outlet and its salinity is 148,000 ppm (Langbein, 1961, p. 18), about three-fifths as saline as the Dead Sea and comparable to Great Salt Lake (138,000 ppm).

The mean altitude of the lake level is 1,274 m. The shoreline consists of a belt of salty mud of varying width, with some stretches of salt-encrusted rock along steeper headlands. Extensive flats of solonchak soils along the northeast and southeast margins of the lake lie 3 to 5 m above the lake and suggest very recent emergence. Coextensive with the solonchak flats but at slightly higher levels of 5 to 26 m above the lake, there are older, better drained and extensively cultivated plains. Above these levels are scattered remnants of older terraces which are related to the late Pleistocene Lake Rezaiyeh. Bobek (1937, p. 165-174) has calculated that the former lake existed under a hydrologic regimen characterized by lower evaporation (mean air temperature 5°C lower than present based on depression of the snowline in the Zagros Mountains), but a precipitation similar to that of the present.

The mean annual temperature for Rezaiyeh, along the west-central side of the lake, is 13.1°C with a maximum of 37.0°C. Total precipitation is 306.4 mm. These data correspond to a net evaporation of 960 mm from the lake surface, which is approximately 85 percent of the evaporation from a fresh water body of similar extent.

A large percentage of the precipitation that falls at Rezaiyeh is lost through evapotranspiration. The evidence that the margins of the lake have recently emerged indicates that the present evaporation rate at the lake surface exceeds runoff received plus ground-water recharge.

Similar observations have been made along the Caspian Sea where the lake level has fallen at the rate of 3 cm/yr during the last 30 years. The climate has become slightly more arid.

5. SUMMARY

Field observations made during the summer of 1966 and analyses of samples permit the following conclusions:

1. A lake existed at the present site of Sabzevar Kavir during a period of cooler climate probably corresponding to the latest Pleistocene period (Würm).

2. At their maximum extent, these lakes were not connected with the Dasht-E-Kavir.

3. The Dasht-E-Kavir was not inundated during the Pleistocene but remained essentially as it is today, a vast interior desert.

4. The late Pleistocene climate of Iran was more compartmented than that of other countries in similar latitudes. The mountains were glaciated, with a depression of the snowline of 800 m in the Elburz Mountains. The immediate southern flanks of these mountains experienced reduced evaporation rates sufficient to create

a surplus of water and lakes formed in depressions. However, the desert areas experienced no pluvial climate.

5. The evidence suggests that the climate is currently more arid than it has been in the recent past.

6. Detailed measurements of the conductivity of the source of sediments may permit estimates of the relative ages of unconsolidated deposits whose upper horizons are being enriched with salt transported upward through capillarity.

Acknowledgments

The author wishes to express his gratitude to Captain James T. Neal, USAF, of the Air Force Cambridge Research Laboratories, who actively contributed to this report by participating in the collection of the field data, and whose many suggestions have improved the general presentation of the results. Mr. A. Victor Rossi assisted with the field measurement program; Mr. Edward G. Hasser assisted in the laboratory and with the processing of the mechanical analyses; and Mr. Ching Chang Woo provided the mineralogic analysis of one of the samples.

References

Bobek, H. (1937) Die Rolle der Eiszeit in Nordwesteran, Zeit für Gletscherkunde, 25:130-183.

Bobek, H. (1959) Features and Formation of the Great Kavir and Masileh, Arid Zone Research Centre Pub. No. 2, 63 p.

Bobek, H. (1963) Nature and implications of Quaternary climatic changes in Iran, UNESCO, Symposium on Changes of Climate, Rome, October 1961, pp. 403-413.

Langbein, W. B. (1961) Salinity and Hydrology of Closed Lakes, U. S. Geol. Survey Prof. Paper 412, 20 p.

Wright, H. E. (1961) Pleistocene glaciation in Kurdistan, Eiszeitalter und Gegenwart, 12:131-164.

Contents

VI. Satellite Monitoring of Lakebed Surfaces

James T. Neal, Capt, USAF
Air Force Cambridge Research Laboratories
Bedford, Massachusetts

Abstract

Playas (dry lakebeds), situated in arid regions of the world, are useful as emergency aircraft landing sites and as indicators of the hydrologic environment. A factor that has limited their use is the inability to intermittently monitor surface changes that occur as a result of rain. A partial solution in monitoring them is through the use of satellite sensor data. Reflectance changes that indicate soil moisture or compositional variations (which in turn affect trafficability) have been observed on Gemini color photographs and Nimbus AVCS (Advanced Vidicon Camera System) imagery. The best data that is currently available is the Gemini color photography; several hundred playas have been photographed in North America, Africa and Asia. Existing television and infrared imaging systems are marginal for use in observing playas, but future systems with improved resolution that are now under development will provide additional useful data. The use of infrared and false-color films from orbital altitudes will provide advantages in discriminating moisture variations as well as improving low-visibility conditions.

1. INTRODUCTION

Playas (dry lakebeds) are landforms that have surfaces which change with time. This aspect of playa geology is covered in Chapter II of this report and

further discussed in the literature (Neal and Motts, 1967). An example of such change may be seen in short-term rainstorms which flood playa surfaces and rearrange the soils. See Chapter II. It is therefore of interest to explore the possibility of continuously monitoring playas from a remote sensor platform, which would essentially eliminate the need for repetitive field examination. Airphotos taken from conventional aircraft have proved especially useful (Neal, 1965). In spite of their established value, conventional photographs are expensive and difficult to obtain on a recurring basis.

A variety of earth-sensing satellites exist that were designed for other purposes but which appear to have some value in observing surface changes on playas. A satellite in polar orbit can examine every point on the earth periodically, and at intervals of as little as 12 hours. Already hundreds of space photographs and images of playas exist. Television and infrared images and color photographs taken from TIROS, Nimbus and Gemini satellites have been examined. The purpose of this paper is to evaluate these satellite sensor capabilities for observing playa surface changes, and thereby suggest which types of future systems will have value.

2. DISCRIMINATION OF PLAYA SURFACE FEATURES

The geologic surface features on playas that have been observed to change are relatively small in size (Table 1). In fact, most are difficult to see on 1/60,000 scale conventional aerial photographs. The principal exception lies in gross variations in moisture and composition which are visible even on extremely small scale photographs. This category of changes on playas is thus the only one that can be observed on satellite-derived images and photographs, because of the inherent small scale (1/100,000 and smaller). It is important to note that these moisture variations affect strength, saline concentration, and compaction. These properties are of utmost concern in trafficability considerations.

The basis for remote sensor discrimination of moisture or compositional variations on playas lies in the thermal and spectral reflectance properties of the various surfaces. For example, a hard, dry clay crust when moistened becomes dark, effecting an average reduction in reflectance of 30% in the visible spectrum. In addition, the increased moisture content alters the density and specific heat of the surface. The reflectance properties of other playa surface conditions vary in such a way that the surfaces may be qualitatively distinguished on conventional air photos as variations in gray tones (Neal, 1965). Frequently the reflectance differences are subtle, but on hard, dry crusts the moisture-induced reflectance changes are pronounced. Photographic examples of this darkening

may be seen in Chapter II of this report (Figure 1 and Figure 11). A large, regional darkening was observed by Lowman (1966c) on one of the GEMINI photographs that was taken over rain-soaked soil in west Texas.

Table 1. Photography of Surface Features on Lakebeds

Surface Feature	Dimensions (meters)	Optimum Scale
Salt ridges	1/3 - 1	1/20,000 and larger
Giant desiccation fissures	1/3 - 1	1/30,000 and larger
Windblown sand	1 - 2	1/30,000 and larger
Vegetation	1 - 5	1/40,000 and larger
Moisture and compositional variations (gross)	> 50	1/60,000 and smaller

One of the difficulties encountered in this study is that playas, being features of the desert, very rarely receive and retain moisture, and thus actual observations on moisture conditions are sparse. It is therefore necessary to determine what might be seen by observing natural objects having similar size, shape, contrast and visibility.

3. EXISTING SATELLITE SENSOR SYSTEMS

Four systems that have imaged the earth from orbiting satellites have been studied and are discussed in succeeding paragraphs. They are TIROS TV, Nimbus AVCS (TV), NIMBUS HRIR (infrared imagery) and Gemini color photography. Newer and more refined systems have been and are being developed for planetary studies, but none have yet been used for Earth orbital viewing.

3.1 TIROS TV

TIROS (Television and Infrared Observational Satellite), although designed primarily as a meteorological tool for observing clouds during the early 1960's, produced many good images over land. Playas were noted to be particularly visible on the television images, because their albedo is similar to that of clouds, and because of the contrast with the adjacent, less reflective desert alluvium.

TIROS had ground resolution no better than about 5 km, consequently only the largest of playas were discernible, and then only as light patches. Nonetheless, reflectance changes might be detected on the larger playa surfaces using such systems. Cronin (1963), in a study of several thousand frames from TIROS, noticed that the Black Rock Desert in northwestern Nevada was not always visible on different passes. This might have been the result of a rain, which could have effectively lowered contrast and visibility of the playa to the point of nondiscrimination.

3.2 Nimbus I AVCS (Advanced Vidicon Camera System)

The AVCS aboard the Nimbus I meteorological satellite produced about 27,000 high quality TV images over a period of 27 days in August and September, 1964. The satellite's elliptical polar orbit permitted near complete coverage of the globe and enabled the AVCS to resolve 1/2 km at perigee (423 km). This resulted in substantial improvement over TIROS and provided useful terrain data for the earth scientist, whereas in TIROS the data was marginal at best. The AVCS took triplets (a vertical and two oblique views) along the orbital path and thus obtained essentially contiguous coverage. System characteristics are described more completely by Nordberg (1965) and in the International Geophysics Bulletin (1965).

A brightness scale is included along the edge of each AVCS image. A constant intensity flash lamp illuminated a "gray-wedge" while each exposure was being made. This provides a brightness comparison on the picture that ranges from very dark to very bright, usually in about 8 levels of gray. This brightness scale can be used in playa studies in a semi-quantitative way, where the relative brightness of moist and dry surfaces can be compared and related to reflectance values.

Three examples of Nimbus I AVCS imagery that contain playas are shown here. They demonstrate optimum capabilities of the system at the altitudes of measurement. These examples represent a variety of playa surface conditions and environmental occurrence.

Figure 1, taken over northwestern Nevada, shows a variety of playa surface conditions ranging from hard, dry crusts (locations 2, 3, 6, 7, 16 to 19) to soft, dry, friable surfaces (locations 5, 8, 10, 14, 15). The latter frequently contain moist surfaces with accumulations of salt (see for example the central portion of the Humboldt Salt Marsh (15). Without prior knowledge of surface conditions, it would be difficult to identify the type of surface that exists on these playa. For example the gray-level of the hard, dry clay crust at Smith Creek Valley (19) is the same as the central salt core of the Humboldt Salt Marsh (15). However, it is known that these two playas change little from year to year, so that any pronounced change in the reflectance level of these surfaces would probably indicate a change in moisture, or surface flooding.

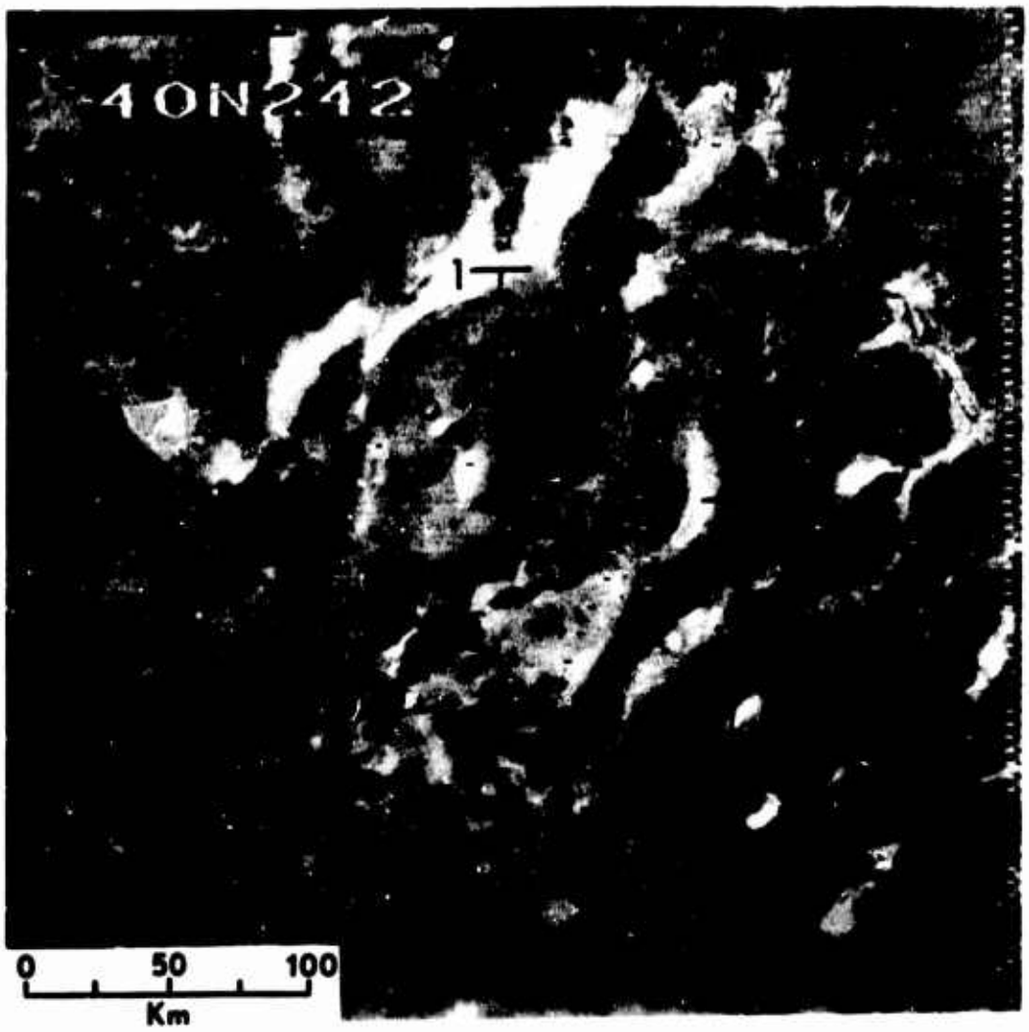

1 - Black Rock Desert (playa)
2 - Jungo Flats (playa)
3 - Pit-Taylor Reservoir (playa)
4 - Smoke Creek Desert (playa)
5 - Honey Lake Valley (2 playas)
6 - Bluewing Playa
7 - Adobe Flat (playa)
8 - Winnemucca Lake (playa)
9 - Pyramid Lake
10 - Buena Vista Playa
11 - Buffalo Playa
12 - Farmlands in lacustrine sediments
13 - Brady Playa
14 - Carson Sink (playa)
15 - Humboldt Salt Marsh (playa)
16 - Edwards Creek Playa
17 - Grass Playa
18 - Labou Flat (playa)
19 - Smith Creek Playa
20 - Big Smoky Playa
21 - Gabbs Playa
22 - Walker Lake
23 - Lake Tahoe
24 - Marshland (dark gray area)

Figure 1. NIMBUS AVCS Image, Northwestern Nevada, 17 September 1964, Orbit 285, Time 19-04-43. Good contrast separation between lakebeds (white and light gray), alluvium (intermediate gray), forested mountains (dark gray), and lakes (black) is apparent. Principal playas and lakes are listed above and keyed to numbers on the photo.

Black Rock (1) and Smoke Creek (4) Deserts on Figure 1 exhibit an essentially equal gray-level tone throughout, even though a variety of crustal types exist. This points out a limitation in the spectral discrimination capability of the system. The average reflectance values of these surfaces do not vary more than about 10 percent. Wet marshlands (24) show up lighter than the permanent lakes in the region (9, 22, 23). The darker forested mountains which separate the valleys that contain the playas are readily distinguished from the alluvial slopes immediately adjacent to the playas.

Figure 2, a Nimbus AVCS image taken over the Mojave Desert of southern California, shows good contrast separation between water, mountains, and alluviated valleys, but not all of the playas are visible. This is partly because of the small scale of the image. As in Figure 1, salt and dry clay surfaces have the highest reflectance values. The highly reflective salt core of Searles Lake (1) is particularly prominent.

The importance of contrast on low resolution images between lakebeds and surrounding terrain is especially significant, and can be observed by comparing Figures 1 and 2. In Figure 1 taken over northwestern Nevada, the light-colored lakebeds stand out prominently against darker alluvial slopes and heavily forested mountains. The Mojave Desert, on the other hand, is much higher in average regional albedo because the mountains are lower in elevation and have much less forest cover. The Mojave Desert as a whole is also considerably more sandy than the Nevada area shown in Figure 1, so that the lower contrast between lakebeds and surrounding terrain in the Mojave makes the lakebeds difficult to see.

Figure 3 taken over southern Iran again shows the playas as the brightest terrain features. The highly reflective white zones are salt on the surface. Lavar Maidan (1) and Sirjan Kavir (playa) (7) contain mixed surfaces; the brightest zones are salt and the adjacent lighter gray zones are clayey silts with lesser amounts of salt. Maidan-I-Gil (6) is a predominantly soft, dry friable-surfaced playa and is considerably less reflective than the salt surfaces. Lavar Maidan Daryacheh-I-Tasht, and Daryacheh-I-Bakhtigan were photographed one year later on the Gemini V mission and are shown for comparison (Figures 7 and 8). Comparison of reflectance levels of playa and adjacent terrain on the Gemini photos and the AVCS image reveals that the Daracheh-I-Bakhtigan and Daracheh-I-Tasht were largely free of water in 1964 during the Nimbus I mission, whereas during the Gemini V mission they were largely flooded. The value of using the two contrasting types of data is apparent.

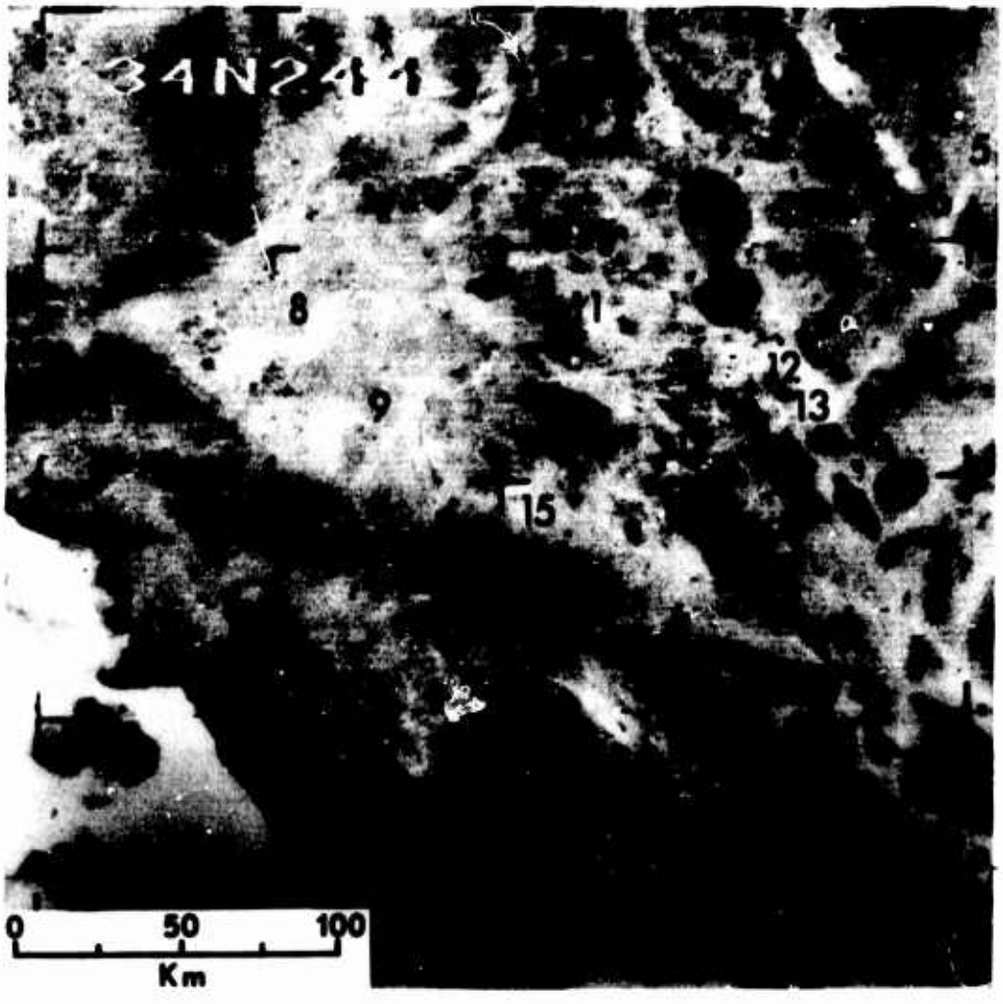

1 - Searles Lake (playa)
2 - Southern Death Valley
3 - Pahrump Valley
4 - Mesquite Playa
5 - Jean Playa
6 - Roach Playa
7 - Ivanpah Playa
8 - Rogers Playa
9 - El Mirage Playa
10 - Superior Valley Playas (3)
11 - Coyote Playa
12 - Soda Playa
13 - Devil's Playground (sand dunes)
14 - Lavic Playa (light) and Mt. Pisgah (dark)
15 - Lucerne Playa
16 - Los Angeles
17 - San Gabriel Mountains
18 - San Bernardino Mountains
19 - San Jacinto Mountains
20 - Salton Sea
21 - Tehachapi Mountains
22 - Clouds over Pacific Ocean
23 - Open water, Pacific Ocean

Figure 2. NIMBUS I AVCS Image, Mojave Desert, California, 17 September 1964, Orbit 285, Time 19-03-12. Contrast separation between lakebeds and surrounding terrain is much poorer than that shown in Figure 1. V-shaped pattern at left center of image outlines the Garlock and San Andreas Faults.

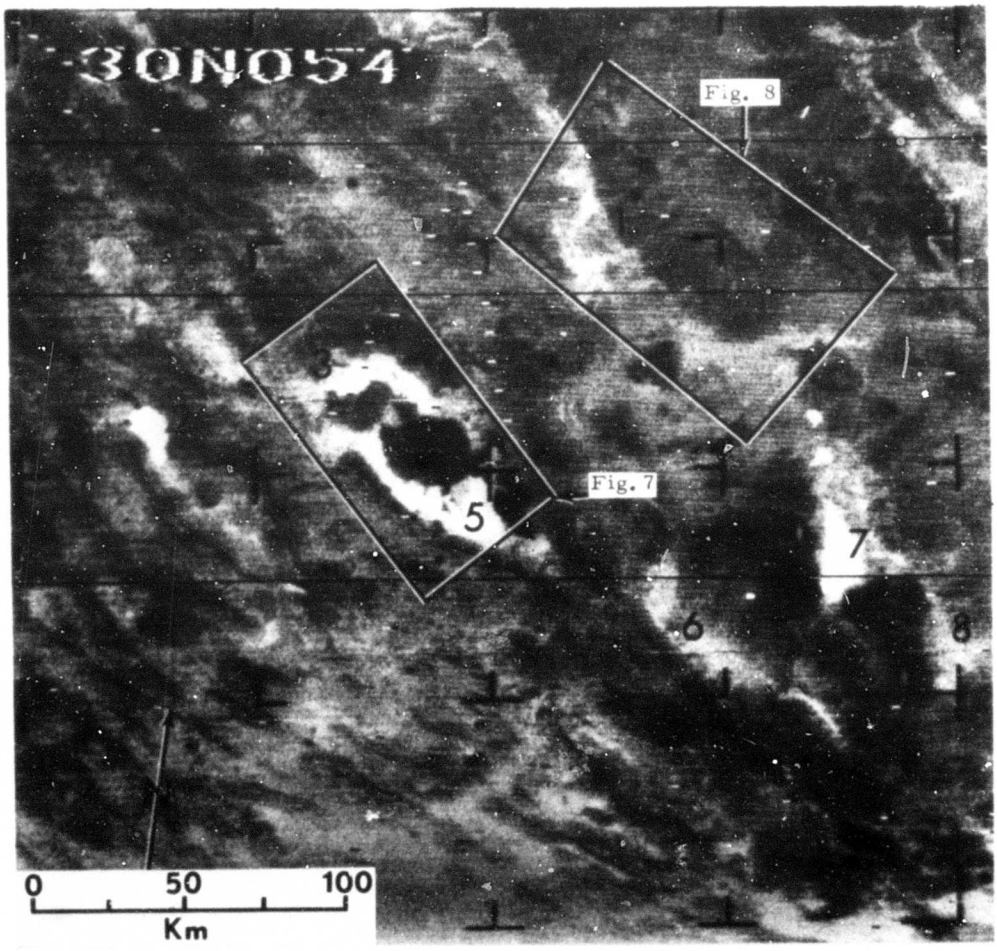

1 - Lavar Maidan (playa)
2 - Daryacheh-I-Maharly (playa)
3 - Daryacheh-I-Tasht (playa)
4 - Volcanic mountains
5 - Daryacheh-I-Bakhtigan (playa)
6 - Maidan-I-Gil (playa)
7 - Sirjan Kavir (playa)
8 - Ibrahimabad Kavir (playa)

Figure 3. NIMBUS I AVCS Image, Southern Iran, 20 September 1964, Orbit 323, Time 07-43-42.

Examination of the AVCS images shows that their utility in playa studies is limited, but that they do have considerable information content, especially when dealing with known conditions, and when used in conjunction with higher resolution photography such as from the Gemini missions. If the same AVCS were used from an altitude of 200 km (Nimbus I perigee was 423 km) the resolution would be about 500 meters and much more could be seen. However, the number of frames would at least quadruple, and the original usefulness as a cloud viewing device would be reduced because of a large increase in the number of images to be examined.

3.3 Gemini Color Photography

Color photography taken from the Gemini series of manned orbiting satellites in 1965-66 has provided excellent coverage of the low latitude regions of earth, in which much of earth's desert regions lie. From a visibility standpoint, deserts have probably been the best photographic subject, having generally less cloud cover than other regions. Also they are not covered by vegetation to the extent that other regions are. Playas usually have high albedo values, and high contrast separation between adjacent terrain units. Thus playas show up extremely well on the Gemini photography and more than one hundred have been viewed. The majority of exposures have been made with a hand-held 70 mm Hasselblad camera using conventional color emulsions.

The advantages of color in photographing terrestrial features from space have become significant. This is particularly true in the study of playas where variations in surface characteristics often show as subtle color differences between light gray and brown, but still have high overall albedo values. On black and white photos these subtle variations are often indistinguishable. Photography of terrain features from space is superior on color emulsions because approximately 20,000 separable colors, shades, and hues may be distinguished, whereas panchromatic emulsions record only about 200 shades of gray (Swanson, 1962). Above the atmosphere even fewer shades are visible. Subtle variations in water depth, soil moisture, and compositional variations are known to be more easily discerned with color film. Further, the better resolution of panchromatic film appears to be less significant when compared with color discrimination properties.

Numerous applications of the Gemini terrain photography have been made by earth scientists. Lowman's reviews (Lowman, 1966a, b, c; Lowman, McDivitt and White, 1966) of the various missions have provided an excellent overall insight into potential uses by geologists. U.S. Geological Survey scientists have examined numerous frames in detail (Tabor, 1966; Wolfe, 1966). Through the use of these high-quality, small-scale photographs, structural features in Egypt have been

mapped out (Abdel-Gawad, 1967) and several oil companies have filled in gaps in their existing regional geologic maps. Gettys (1965) has shown that bottom contours can be estimated in shallow off-shore locations. All of these studies have indicated that orbital photography has great scientific value and that small scale is no great hindrance, especially in areas of sparse knowledge. In many cases the small scale provides an overview hitherto impossible, by showing large regional relationships simultaneously on one picture.

Figures 4 and 5 are comparative photographs of Willcox Playa, Arizona, taken in June and August, 1965, during the Gemini IV and V missions. A wavy, dark zone (arrow) in the lower, central part of the playa, measuring 3 km long and 1/2 km wide, is visible on the June photo but not on the August exposure. The only known condition that can cause this darkening is an increase in soil moisture. Apparently the moisture had evaporated during the interval between the Gemini IV and V missions. Such an interpretation seems reasonable as the summer months are a period of intense evaporation.

Figure 6 is a conventional photomosaic made from photos taken from low-altitude aircraft reduced to the scale of Figures 4 and 5. Comparison of these three photographs shows graphically the quality of the small-scale photographs. The reduced low-altitude photo (Figure 6) is not significantly better than the Gemini photos.

Figure 7 shows two salt lakes in southern Iran that are partly covered with water. The original Gemini V color transparency shows clearly the color gradation from white to light blue to dark blue, and thus qualitatively indicates water depth. Studies of tonal variations in the water that show on one of the Gemini IV frames exposed over the head of the Gulf of California suggest that such color tones might be used to qualitatively estimate the depth of water (Gettys, 1965). Measurements of tonal values might be used to contour water depth. Figure 3, the Nimbus I AVCS image taken eleven months before Figure 7, revealed that the two lakes were nearly dry. Although the two types of image differ greatly in quality, it is apparent that they can be used together to provide useful data.

Figure 8, a Gemini V photo showing Lavar Maidan (a playa) in southern Iran, exhibits several surface conditions. This playa (kavir in Persian) is one that discharges ground-water; the water table is very close to the surface. The brightest appearing zones on the playa are salt accumulation, and the darker areas are silt and salt admixtures. Figures 9 and 10 are conventional low-altitude air photos showing two areas at each end of the playa. The principal features on the playa are visible on the Gemini photo but detail is lacking. The area shown in Figure 8 is marked on the Nimbus I AVCS (Figure 3), which shows that the zones of salt on the playa can be delineated and that they were free of surface water at the time of imaging.

Figure 4.

Figure 5.

Figure 6.

Figure 4. Willcox Lake (Playa), Arizona, Photographed on the Gemini IV Mission, 5 June 1965, with 70 mm MS Ektachrome. This black and white reproduction is enlarged about eight times and is only a segment of the original transparency, as is Figure 5. Note moist zone (arrow) on this hard silty clay surface.

Figure 5. Willcox Lake, Arizona, Photographed on the Gemini V Mission, Late August 1965, with 70 mm MS Ektachrome. Note disappearance of the moist zone that was present on the June 1965 Gemini photo (Figure 4).

Figure 6. Willcox Lake, Arizona: Reduced Photomosaic of Conventional Airphoto, Scale Same as Figures 4 and 5. Principal features noted here can easily be viewed on the Gemini photos (Figures 4 and 5). (1) hard, dry silty clay (playa); (2) dissected lacustrine sediments of ancient lake; (3) strandlines of former lake level; (4) coarser alluvial slopes; (5) cultivated fields.

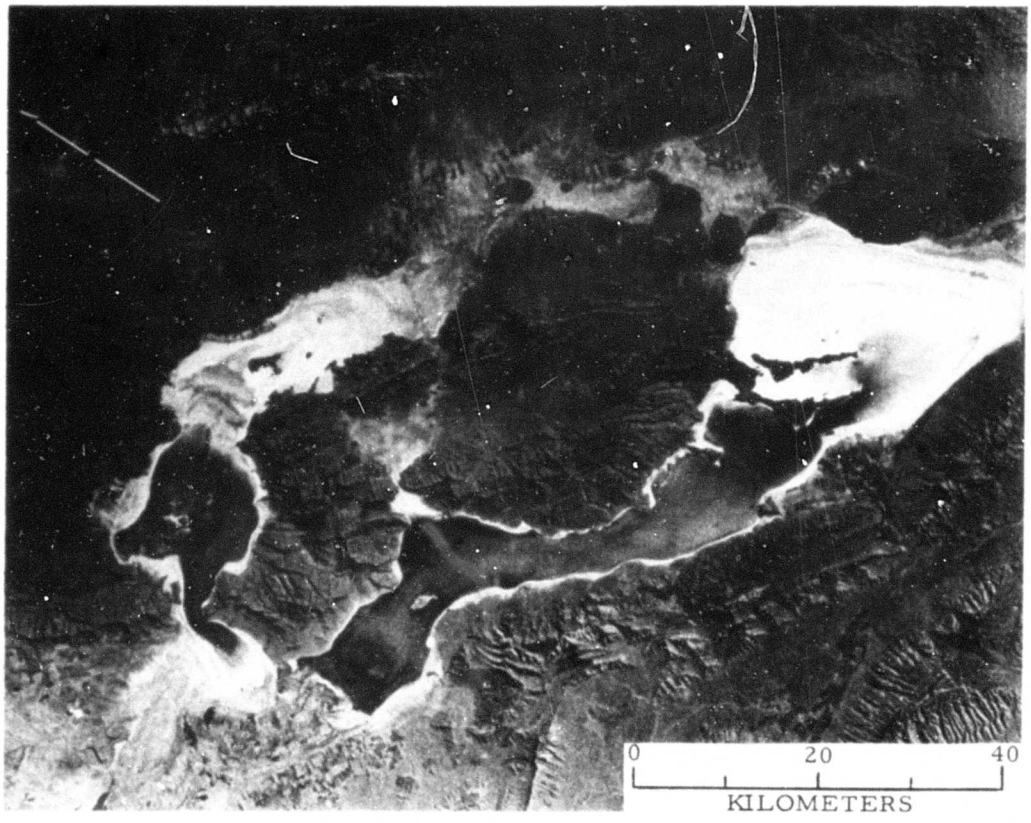

Figure 7. Daryacheh-I-Tasht (Left) and Daryacheh-I-Bakhtigan (Right), Southern Iran, Photographed on the Gemini V Mission with 70 mm MS Ektachrome in Late August, 1965. This black and white reproduction of the original color transparency clearly shows the variation in water depth in these two salt lakes, ranging from water-free salt crust to deeper water (dark gray). Compare this photograph with the smaller scale Nimbus I AVCS image (Figure 3) that was taken eleven months earlier when these lakes were largely free of standing water.

Many other excellent photographs of playas were taken on the Gemini missions. Water, salt, and moisture boundaries are particularly visible. Thus far the principal limiting factor has been scale, but this can be overcome to some extent through the use of longer focal length lenses. A number of photos were taken with a 250 mm lens and the improvement in detail is considerable. On linear features with good contrast separation, it is possible to resolve features as small as 25 meters.

3.4 Nimbus I HRIR (High Resolution Infrared Radiometer)

The imaging radiometer that operated on the Nimbus I meteorological satellite constructs a visual record of radiant energy that is emitted and reflected from the

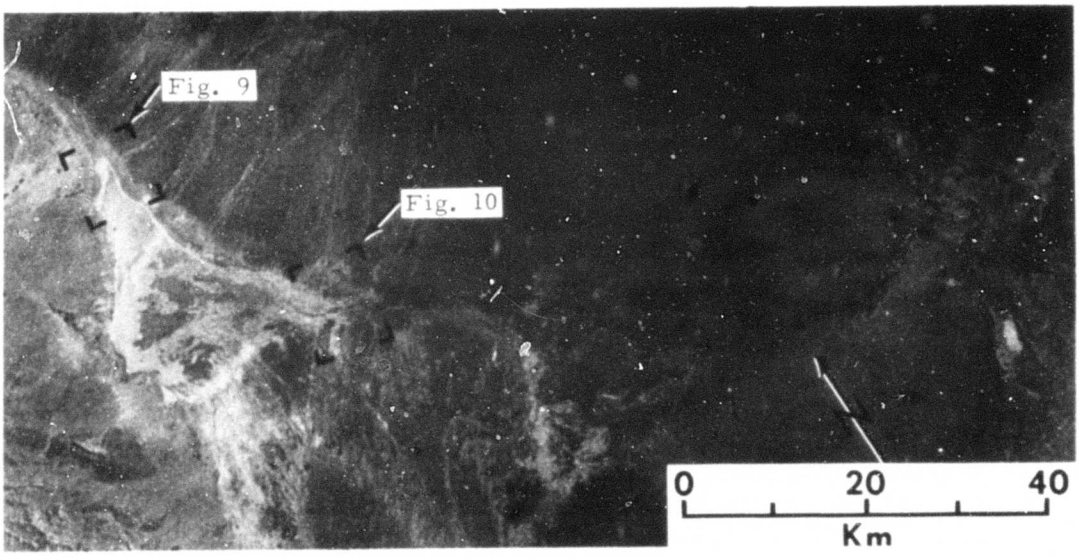

Figure 8. Gemini V Photograph of Lavar Maidan (Left Center), a Large Kavir (Salt Playa) in Southern Iran. This black and white reproduction of the original color transparency taken in late August, 1965 shows little apparent change over the smaller-scale Nimbus I AVCS image taken eleven months earlier (Figure 3). Larger-scale conventional airphotos of parts of the kavir are shown for comparison (Figures 9 and 10).

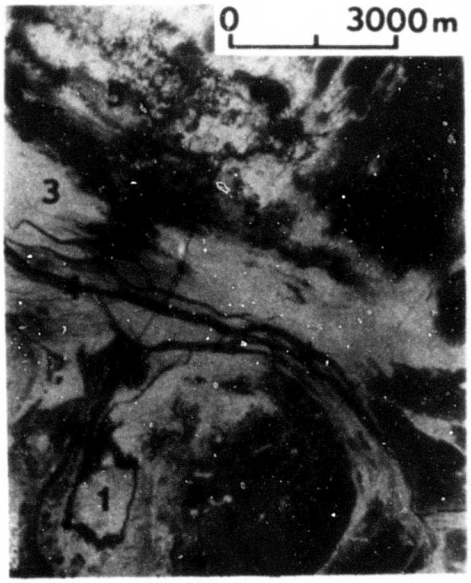

Figures 9 and 10. Conventional Airphotos of Portions of Lavar Maidan for Comparison with Gemini Photograph (Figure 8). Compare the following features: (1) salt crust; (2) alluvial slopes; (3) soft clay-silt with salt admixtures (flat surface); (4) drainage channels; (5) vegetated and dissected lacustrine sediments; (6) water (piezometric surface); (7) moist silt-salt admixture (rough surface).

earth in the 3.4-4.2 μ wavelength region. The system was designed for the primary purpose of observing cloud patterns of the earth during the night. The thermal resolution of the system is about 1-2°K and the subpoint field of view at perigee (423 km) was 3.4 km x 3.4 km, but at apogee (933 km) increased to 7.5 km x 7.5 km. Thus, only very large and relatively homogeneous features may be imaged. Generally the linear resolution of the instrument is no better than 5 km. However, experience has shown that linear features with high contrast may be seen and thus exceed expected resolution. For example, many streams only 1/2 km wide stand out prominently on the imagery (Nordberg, 1965). Similarly, a volcano with an intense thermal point source was observed on the Nimbus II HRIR imagery; it was less than 1/2 km wide (Williams, 1967).

Salar de Atacama, the largest (3225 km^2) salar (salt playa) in Chile was imaged by the HRIR at about midnight on 13 September 1964 (Figure 11). It appears

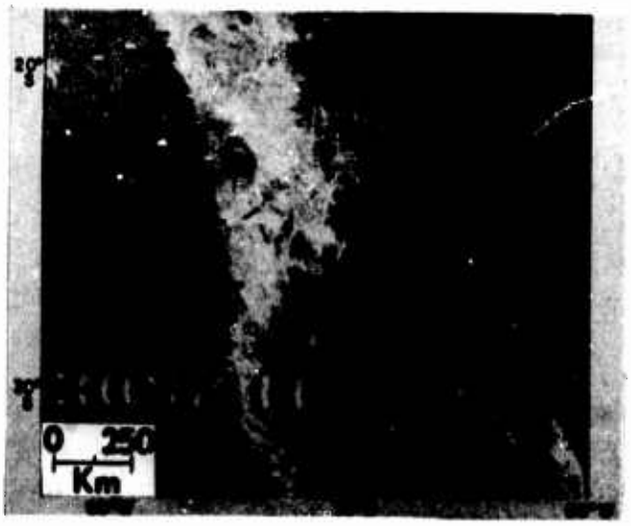

Figure 11. Salar de Atacama, Chile (A), as Imaged on the Nimbus I HRIR System at about Midnight, 13 September 1964. The broad white (cold) band in the center of the picture represents the Andes Mountains. Pie de Palo Mountains (B) appear warmer than the adjacent desert. Photo courtesy of NASA.

as a crescent-shaped form with a discrete band of warmer material (273°K) surrounding a colder (263°K) central portion (Nordberg, 1965). As the salar floor is essentially flat, the measured apparent temperature difference must be explained by actual thermal differences caused by heat-capacity variations in the materials, by differences in emittance, or by a combination of both. Recent on-site studies have suggested that the outer, warmer appearing zone is probably

caused by volcanic debris that covers the alluvial slopes adjacent to the salar, rather than to variations in the salar (Nordberg, 1967). The inner band may surround the central salt core (Conti, 1967). Nonetheless, the system has shown the discrimination capability of gross terrain features.

Infrared imagery of playas taken from low-altitude aircraft shows that surficial soil variations can be readily distinguished; density and moisture differences which influence the heat capacity and emissivity are particularly noticeable. Figures 12 and 13 are night and day infrared images taken at Harper Lake; they demonstrate the soil discrimination capability of infrared imaging radiometers. At night (Figure 12) a pronounced radiometric separation exists between soft, puffy, friable surfaces and hard, dry crusts (see also Chapter 2, Figures 4 and 5, for a view of these surface types). Moist and wet zones are also readily distinguished. During daytime (Figure 13), the infrared radiometric response of these surfaces is reversed from that at night. The soft, puffy surfaces are less dense (and have less heat capacity) and at night appear cooler than the hard, dry crusts. During the day these surfaces appear warmer. The temperature differences between the two contrasting surfaces were measured with a contact thermocouple at the time the imagery was acquired and averaged about 1-2°C. The soft, puffy friable surfaces contain more salt than hard, dry crusts (15% vs 2%) and probably also have different emissivity values. Hovis (1966) has shown that, of many common minerals tested in this spectral region, pure rock salt has the lowest average emissivity. It is uncertain what effect the impure salty clay-silts described here have on emissivity values. In any case, the anomalies are pronounced and are registered on the infrared imagery.

These observations show that at present the limiting factors which preclude utility of satellite-borne imaging IR radiometers for playa studies are a combination of altitude and system resolution which result in low ground resolution. If the ground resolution of future spaceborne infrared imaging systems approaches that of the Nimbus I AVCS imagery (1/2 km), they will be an extremely useful device that will have application to playa studies, and to many other earth science problems concerned with dynamic processes.

4. ADDITIONAL CAPABILITIES

None of the orbital sensing systems previously described were designed for the specific purpose of observing playas. They do, however, possess varying degrees of utility and suggest what types of future systems will have value for viewing playas. Increased capabilities may be gained through the additional use of special purpose photographic emuisions, through direct observation by

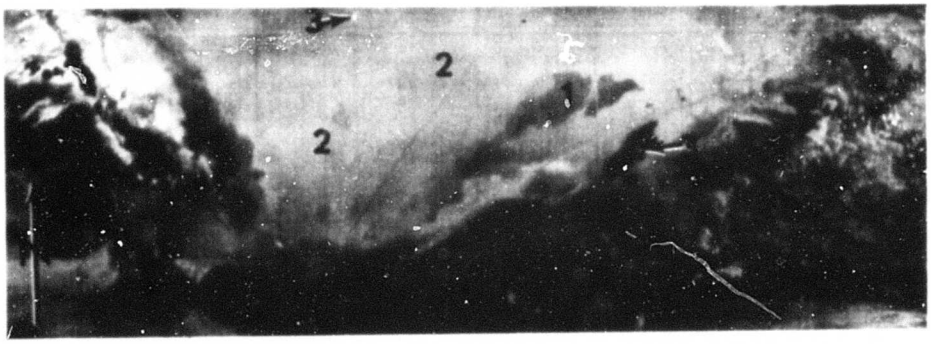

Figure 12. Nighttime Infrared Image (4.5 - 5.5μ), Harper Lake (Playa), 0510 Hours, 12 September 1967. Comparison of surface features on this image with Figure 13 (daytime image) shows thermal discrimination of: (1) soft, dry friable surfaces and (2) hard, dry clay crusts (see Chapter 2, Figures 3, 4, and 8), and contrast (thermal) reversal between day and night images. Other features of interest are; (3) bonfires; (4) alluvial sand and gravel; (5) cultivated fields; (6) standing water; (7) moist playa clays; (8) area of vegetated dunes and channels at east edge of playa.

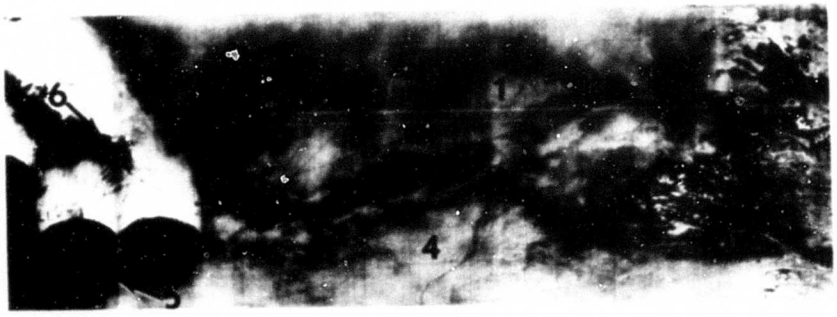

Figure 13. Daytime Infrared Image (4.5 - 5.5μ), Harper Lake, California, 1014 Hours, 14 September 1967. Compare features shown here with those on Figure 12 (nighttime image). Scale is distorted on each image.

scientist-astronauts, and by advanced television imaging systems currently being developed.

4.1 Special Emulsions (Photographic)

Infrared (black and white) and false-color (also known as camouflage detection or CD) films have come into widespread use in recent years for terrain studies. They are both known to possess special capabilities for discriminating moisture variations. A few frames of CD film were exposed during the Gemini VII mission and its superior haze penetration and color discrimination qualities were evident (Lowman, 1966c). On the basis of the Gemini VII experiment and the past excellent results from conventional aircraft, it is thought that CD film would have particular value for photographing playa moisture variations from a satellite.

Infrared films could also be useful, for reasons similar to those cited above. In addition to moisture discrimination properties, the longer wavelength sensitivity reduces adverse visibility effects from the atmosphere. A number of other special photographic methods are possible, such as selective filtration of the visible spectrum (spectrophotography) that can enhance visibility of objects by exploiting maximum spectral contrast between objects (Bliamptis, 1967). For dry clay playas, maximum contrast in the visible spectrum seems to fall from about 6500Å to 8500Å. In this wavelength region, water absorbs greater amounts of radiation, so that water-covered surfaces should be easily discriminated from dry clay.

4.2 Human Observation

A human observer has several important advantages over a camera. He can see almost all that a camera can with a normal focal length lens, but in addition he can track the specific object of interest and look for special effects such as sun glint from wet surfaces or other reflectance variations that a camera could miss. He may be better able to observe dust blown from dry surfaces, or be able to see moist surfaces at the more favorable polarization angles. However, man is unable to remember and reproduce details accurately, so that photography must also be used concurrently with human observation.

4.3 Advanced Telemetering Vidicon Tubes

Several advanced systems are under development that show promise for improving the quality of the best aerial photographs. An RCA "return-beam vidicon tube" has delivered images ten times sharper than images on a conventional TV screen. Already 11,000 lines have been achieved with promises for

future resolution approaching 18,000 lines (Industrial Research, December 1967). Such pronounced improvements are certain to revolutionize future orbital sensing technology.

5. SUMMARY AND CONCLUSIONS

Playas are landforms that generally have high albedo values and good contrast separation from adjacent terrain. They are usually large landform features and are thus comparatively easy to view from space. TIROS and Nimbus TV imagery, Nimbus HRIR infrared imagery, and Gemini color photographs taken over selected playas were examined to determine what features could be seen, with the ultimate aim of determining what types of surface changes could be detected. The features that hold promise for observation from satellites are gross variations in soil moisture, standing water, and salt zone migration. Although none of the systems or the orbital experiments were designed for the specific purpose of viewing playas, the high resolution television imagery (AVCS) and the color photography hold much promise. Principal conclusions reached are:

1) TIROS TV and Nimbus HRIR imagery have too low resolution to provide any useful data, except on the very largest of playas. Infrared imagery does provide data in a different spectral region and yields data which cannot be gained photographically. Future higher resolution infrared imagery systems are therefore apt to be of even greater value.

2) Nimbus I AVCS imagery has provided marginal, yet useful information on large playas and resolved 1/2 km on the ground. Different surface conditions that indicate water, salt, and soil moisture can be seen. These images can best be used over better-known playas, and where higher resolution photography is available for comparison.

3) Color photography, like that used in the Gemini satellites, is the best all-around method for observing playas. Photography using an 80 mm focal length lens is good, but a 250 mm lens is superior. Color provides an added dimension in discriminating subtle variations in composition or surface condition.

4) It is presently feasible to monitor gross changes in playa surface conditions. Standing water, soil moisture, and salt boundaries can be seen. Combinations of sensors are apt to be most useful. Future orbital sensor systems are sure to improve the present capability, even though they may be designed for other purposes.

Acknowledgments

I thank R. Williams, E. Bliamptis, and D. Krinsley for their review of the manuscript, and M. Conti, G. Stoertz, and E. Hasser for their constructive advice on HRIR interpretation. R. Underwood, P. Lowman, J. Lindstrom and W. Nordberg of NASA have encouraged the writer and also provided much of the satellite sensor data.

References

Abdel-Gawad, M. (1967) Geologic Exploration and Mapping from Space, Unpublished Manuscript, North American Aviation, Thousand Oaks, Calif., 19 p.

Bliamptis, E. E. (1967) Remote Sensing of the Geological Environment, AFCRL Report, Bedford, Mass., 23 p.

Conti, M. A. (1967) Evaluation of Nimbus I High Resolution Infrared Radiometer (HRIR) Imagery, Technical Letter NASA-35, U. S. Geol. Surv., Wash. D.C., 14 p.

Cronin, J. F. (1963) Terrestrial Features of the United States as viewed by TIROS, Scientific Report No. 2, Contract AF19(628)-2471, AFCRL-63-664, Aracon Geophysics Co., Concord, Mass., 35 p.

Gettys, R. F. (1965) Evaluation of Color Photos Exposed from the Gemini IV Flight over the Gulf of California, June 1965, Unpublished Manuscript No. T-39-65, U.S. Naval Oceanographic Office, Washington, D.C., 11 p.

Hovis, W. A. Jr. (1966) Infrared spectral reflectance of some common minerals, Applied Optics 5(No. 2):245-248.

Industrial Research (1967) Sharper Space Photos, December 1967, p. 28-29.

International Geophysics Bulletin (1965) U. S. Nat'l. Acad. Sciences, in Transactions Am. Geophys. Union, 46 (No. 1):293-305.

Lowman, P. D., Jr. (1966a) Experiment S-5, Synoptic Terrain Photography; in Manned Space-flight Experiments, Interim Report, Gemini V mission, National Aeronautics and Space Administration, Wash., D.C., p. 9-17.

Lowman, P. D., Jr. (1966b) Synoptic Terrain Photography During Gemini 6 and 7, NASA Goddard Space Flight Center, Unpublished Manuscript, 14 p.

Lowman, P. D., Jr. (1966c) The earth from orbit, National Geographic Magazine, 130(No. 5):644-671.

Lowman, P. D., Jr., McDivitt, J. A., and White, E. H. (1966) Terrain Photography on the Gemini IV Mission, Preliminary Report, Report No. X-641-66-52, Goddard Space Flight Center, Greenbelt, Md., 19 p.

Neal, J. T. (1965) Airphoto Characteristics of Playas, Chapter 6 in Geology, Mineralogy, and Hydrology of U. S. Playas, Environmental Research Paper No. 96, AFCRL-65-166, p. 149-176.

Neal, J. T., and Motts, W. S. (1967) Recent geomorphic changes in playas of western United States, Jour. Geology 75(No. 5):511-525.

Nordberg, W. (1965) Geophysical observations from Nimbus I, Science, Vol. 150 (No. 3696):559-572.

Nordberg, W. (1967) Oral Communication, NASA Goddard Space Flt. Ctr., Greenbolt, Md.

Swanson, L. W. (1962) New Photographic Techniques for Nautical Charting, 1962 Ann. Conference of the Division of Earth Sciences, National Academy of Sciences, Washington, D.C., p. 6.

Tabor, R. (1966) Photogeologic Interpretation of Gemini IV Color Photography, Baja, California, Tech. Letter NASA-24, U.S. Geol. Surv., Wash. D.C., 4 p.

Williams, R. S. Jr., Friedman, J. D., Thorarinsson, S., Sigurgeirsson, Th., and Palmason, G. (1967) Analysis of 1966 Infrared Imagery of Surtsey, Iceland: in Program and Abstracts of Papers, v. VII, IAV, XIVth Gen. Assembly of Int. Union of Geod. and Geophys., p. 61.

Wolfe, E. (1966) Gemini V Color Photography of Salton Sea Area, California, Tech. Letter NASA-34, U.S. Geol. Surv. Wash., D.C., 4 p.

Unclassified

Security Classification

DOCUMENT CONTROL DATA - R&D

(Security classification of title, body of abstract and indexing annotation must be entered when the overall report is classified)

1. ORIGINATING ACTIVITY *(Corporate author)*
Air Force Cambridge Research Laboratories (CRJ)
L. G. Hanscom Field
Bedford, Massachusetts 01730

2a. REPORT SECURITY CLASSIFICATION
Unclassified

2b. GROUP

3. REPORT TITLE

PLAYA SURFACE MORPHOLOGY: MISCELLANEOUS INVESTIGATIONS

4. DESCRIPTIVE NOTES *(Type of report and inclusive dates)*
Scientific. Interim.

5. AUTHOR(S) *(First name, middle initial, last name)*

J. T. Neal, Capt., USAF (Editor)

6. REPORT DATE	7a. TOTAL NO. OF PAGES	7b. NO. OF REFS
March 1968	151	77

8a. CONTRACT OR GRANT NO.

b. PROJECT, TASK, WORK UNIT NOS. 8623-02-

c. DOD ELEMENT 6144501F

d. DOD SUBELEMENT 681309

9a. ORIGINATOR'S REPORT NUMBER(S)
AFCRL-68-0133

9b. OTHER REPORT NO(S) *(Any other numbers that may be assigned this report)*
ERP No. 283

10. DISTRIBUTION STATEMENT

1-Distribution of this document is unlimited. It may be released to the Clearinghouse, Department of Commerce, for sale to the general public.

11. SUPPLEMENTARY NOTES

TECH, OTHER

12. SPONSORING MILITARY ACTIVITY
Air Force Cambridge Research Laboratories (CRJ)
L. G. Hanscom Field
Bedford, Massachusetts 01730

13. ABSTRACT

Numerous environmental processes affect the development and stability of playa (lakebed) surfaces. Of special significance are hydrologic processes that control the amount and flow of both surface and ground water, and climatic variations which in turn influence the hydrology. This report, in six parts, examines some aspects of the playa surface environment. Chapter 1 is an introduction. Chapter 2 describes microrelief changes that developed at Harper Playa, California, following flooding of the playa in 1965-66. Chapter 3 documents a subsurface hydrologic investigation at Rogers Playa, California. The investigation revealed that the piezometric surface has lowered into sand layers beneath the surface, and it may explain why giant desiccation fissures have formed in the surface clays. Chapter 4 describes an investigation of seven Australian playas and suggests that Australia did not undergo a pluvial period like that of the western United States. Chapter 5 describes three kavirs (playas) in northern Iran and indicates that former lakes did exist there, but not to the same extent as in the western United States. Chapter 6 examines the possibilities of observing playa surface changes from satellites, using the present remote sensor technology. It also states that Gemini color photography and high resolution vidicon (TV) imagery are currently useful.

DD FORM 1 NOV 65 1473

Unclassified

Security Classification

Unclassified

Security Classification

14. KEY WORDS	LINK A		LINK B		LINK C	
	ROLE	WT	ROLE	WT	ROLE	WT
Playas Surface Features Arid environment Mineralogy Satellite sensor interpretation						

Unclassified

Security Classification